Automated Manufacture of Fertilizing Agglomerates from Burnt Wood Ash

Thomas Svantesson

LUND UNIVERSITY

Doctoral Dissertation in Industrial Automation
Department of Industrial Electrical Engineering
and Automation

Department of
Industrial Electrical Engineering and Automation
Lund University
Box 118
SE-221 00 LUND
SWEDEN

http://www.iea.lth.se

ISBN 91-88934-24-1
CODEN:LUTEDX/(TEIE-1032)/1-207/(2002)

Printed in Sweden by Media-Tryck
Lund University
Lund, 2002

Gustaf's Law
"Kom ihåg plåten först"

Abstract

In Sweden, extensive research is conducted to find alternative sources of energy that should partly replace the electric power production from nuclear power. With the ambition to create a sustainable system for producing energy, the use of renewable energy is expected to grow further and biofuels are expected to account for a significant part of this increase. However, when biofuels are burned or gasified, ash appears as a by-product. In order to overcome the problems related to deposition in land fills, the idea is to transform the ashes into a product – agglomerates – that easily could be recycled back to the forest grounds; as a fertilizer, or as a tool to reduce the acidification in the forest soil at the spreading area. This work considers the control of a transformation process, which transforms wood ash produced at a district heating plant into fertilizing agglomerates. A robust machine, built to comply with the industrial requirements for continuous operation, has been developed and is controlled by an industrial control system in order to enable an automated manufacture.

Preface

This thesis summarizes my work conducted in Kalmar for the past five years. The work is somewhat special in a numerous of ways; Firstly, I am the first person to have been stationed at the Department of Technology (DoT), University College of Kalmar, but formally accepted as a Ph.D. student at the Department of Industrial Electrical Engineering and Automation, Lund University. Secondly, this is the first joint and interdisciplinary research project between DoT and the Department of Biology and Environmental Science, University College of Kalmar. Therefore, both environmental and technical issues have been targeted.

This thesis presents *our* view on "automated manufacture of fertilizing agglomerates from burnt wood ash". We do not claim that this approach is neither the *only* nor the *best*. Furthermore, one of the messages that this thesis carries is that implementing a novel mechanical solution can heavily reduce the complexity of a specific control problem (kom ihåg plåten först); advanced automatic control should be called upon only when absolutely necessary.

Some time ago, I attended an oral defense of a Ph.D. thesis where the respondent encountered some criticism such as "Why no or few couplings to the physical world?" If I where to guess, the criticism that this thesis will meet may be "Why so many couplings to the physical world?" The work presented in this thesis is only a subspace of all the work that has been conducted within the project. Other tasks that have been accomplished are the selection and purchase of process units, instruments, commissioning, control code programming and testing. This takes a considerable time to achieve practically, but the academical writing about it is minor. As a consequence, the scientific output was poor during the years 1999 and 2001.

Acknowledgements

First of all I would like to thank Tommy Petersson at Graninge - Kalmar Energi AB, for his hard work and support during these five years. Without his efforts, this project would never have been possible. Furthermore, I am grateful to the always positive and enthusiastic Prof. Gustaf Olsson for accepting me as a Ph. D. student at his department. He controlled the evolution of the work and has always given a positive feedback. I also take this opportunity to thank Prof. Alexander Lauber for his guidance and support.

I am indebted to the people at Graninge - Kalmar Energi AB, especially Daniel Jedfelt, Joakim Andersson, Roger Andersson, Tomas Andersson, Mats Petersson, Per Snöberg, Bo Carlsson and Ulf Gunnarsson. They all have been a great support in this work. A special thanks to Bo Lindewald, who helped me to save the situation during the process breakdown, late evening, December 23, 1999.

I would like to thank Anders Hultgren for inviting me to become a Ph.D. student stationed in Kalmar. Furthermore, I would like to express my gratitude to everyone at Lund University and at the University College of Kalmar. I also thank myself, Dr. Christian Rosén, Lic.Eng. Morten Hemmingsson at IEA and Dr. Fredrik Gunnarsson, Division of Automatic Control & Communication Systems, Linköping University for help with problems related to LaTeX.

The second, "green" group working in parallel on the environmental aspects has given me a lot of feedback and many great memories from project meetings. Thanks Dr. Tommy Claesson, for discovering the "new" ash transformation process that utilizes ETEC-dolomite, and Ph.Lic. Sirkku Holmberg for her support, in particular with all the environmental/chemical details.

The material related to an impulse radar system for on-line carbon in fly ash monitoring would not have been presented in this thesis without Bernth Jo-

hansson and Dr. Johan Friborg, Malå GeoScience AB and Kjell Flodberg, Department of Earth Sciences, Geology, Gothenburg. The formalities regarding the patent where neatly handled by Svetlana Jacobsdotter and Göran Borgö. I also would like to thank Carl-Gunnar Nyquist at Atrium 21. Too bad the patent was rejected.

Developing a machine for automated wood ash transformation is a challenging task. In this work I had many valuable discussions and obtained a lot of help from Prof. Anders Axelsson, Centre for Chemistry and Chemical Engineering, Lund University, Ralf Bräunlich and Laszlo Krausler, Amandus Kahl GmbH & Co, Lars-Erik Djupenström and Linnéa Lövgren, Stora Enso, Anders Ericsson and the staff at Thermo Nobel, Christer Flodwall, Roland Carlberg Processystem AB, Liebert Gustavsson, Dectron AB, Håkan Hallmer, University College of Kalmar, Dr. Anders Hallström, APV Pasilac Anhydro AS, Anders Johansson, IP Industri & Projektconsult AB, Dragan Morovic, Vaisala, Lars-Johan Neander (former at Sigma Benima AB), Lars Nestor, Sigma Benima AB, Gert Nordström, AB Nordströms konstruktionsbyrå, Per Sievert, Chemo-Invest AB and Sven Thege, the STG-group HB. I also had fruitful discussions with my father Svante Carlson and his cousin Henry Georgsson.

I would like to thank Prof. Fredrik Gustafsson, Division of Automatic Control & Communication Systems, Linköping University, Prof. Rolf Johansson, Department of Automatic Control, Lund University, Prof. Peter Wide, Department of Technology, Örebro University and Ir. E.J. Quirijns, Systems and Control Group, Wageningen University for the discussions related to the theoretical work presented in this thesis. Furthermore, Prof. Tore Hägglund, reviewed my Licentitate thesis in a very constructive way, and Prof. Gustaf Olsson and Prof. George Fodor proofread this entire manuscript. They have all provided me with valuable comments and suggestions on improvements.

This project has been sponsored by the The Knowledge Foundation whose kind support is gratefully acknowledged.

Finally, I want to thank Josefine and the rest of my immediate family for the love and support they have given me during the completion of this work.

Kalmar, October 24, 2002
Thomas Svantesson

Notation

Common abbreviations, and general notational conventions for mathematical symbols and operands follow. When local differences occur, they are clearly indicated in the text.

Symbols

A, B, C, D, F	Polynomials of order na, nb, nc, nd, nf.
A_m	Gain margin.
α	Parameter used in the GMA-test.
b	Setpoint weight.
$\in$	Belongs to.
C	Field of complex numbers.
c	Concentration of a measured parameter.
$C_{uy}^2(\omega)$	Quadratic coherence spectrum.
$Ca(CO)_3$	Carbonate (calcite).
$Ca(OH)_2$	Slaked lime (portlandite).
CaO	Quicklime.
Cd	Cadmium.
CO_2	Carbon dioxide.
Cu	Copper.
χ	An empirically selected threshold.
$D(0,1)$	Unit disc.
d	Delay of the process.
δ	Difference in phase change of $L(i\omega)$ at two consecutive frequency points.

$\stackrel{\text{def}}{=}$	The left side is defined by the right side.
E^{Feed}	Thermal energy in the feed.
E_{in}^{Air}	Thermal energy from the drying air.
E_{out}^{Air}	Thermal energy in the exhaust air.
E^{Vapor}	Energy required for vaporization of moisture.
e	White noise disturbance.
ε	Predictor residual.
ϵ_r	Relative permittivity (real dielectric constant).
$\eta(t)$	Viscosity.
Δf	Absolute bandwidth.
F	Unspecified distribution of a random variable.
F_r, F_y	Low pass filter of first or second order to filter the reference signal $r(t)$ and measurement signal $y(t)$.
f_c	Carrier (center) frequency.
$\forall$	For all.
Φ	Standard normal distribution function.
Φ_{uu}	Autospectra of the input u.
Φ_{yy}	Autospectra of the output y.
Φ_{vv}	Autospectra of the disturbance v.
Φ_{uy}	Cross spectrum between u and y.
ϕ	Relative humidity.
$\boldsymbol{\varphi}$	Regression vector.
φ_m	Phase margin.
G	Transfer function from u to y.
G_0	True transfer function from u to y.
G_c	Feedback compensator.
G_{ff}	Feedforward compensator.
G_{ry}	Transfer function from r to y.
g	Impulse response of the process.
γ	Parameter varying the influence of the anti-windup scheme in the PID controller.
γ_{CUSUM}	Threshold used in the CUSUM-test.

γ_{GMA}	Threshold used in the GMA-test.
h	Sampling time.
$H(q, \boldsymbol{\theta})$	Transfer function from e to y.
H_2O	Water.
$\mathbf{I}$	Identity matrix of appropriate dimension.
I_i	Intensity of the incident light.
I_r	Intensity of the reflected light.
$k = K$	Proportional gain.
$\mathbf{K}$	Gain matrix in RLS.
k_1	Converts the input voltage into a pulse frequency.
k_2	The applied off-delay.
$k_d = KT_d$	Derivative gain, where T_d is the derivative time.
$k_i = K/T_i$	Integral gain, where T_i is the integration time.
k_p	Uncertainty gain.
κ	Curvature of the loop transfer function $L(i\omega)$.
λ	Forgetting factor in RLS.
$L(q)$	Pre-filter (data-filter).
$L(i\omega)$	Loop transfer function.
M_S	Maximum sensitivity $M_S = \max_\omega \lvert S(i\omega)\rvert$.
M_T	Maximum complementary sensitivity.
M^{Feed}	Moisture in the feed.
M_{in}^{Air}	Inlet drying air moisture.
M_{out}^{Air}	Exhaust air moisture.
$M^{Product}$	Product moisture.
$m_u, \hat{\mu}$	Estimated mean.
μ_i^*	Bootstrap estimate of the mean.
NO_X	Oxides of Nitrogen.
ν	Drift parameter in the CUSUM-test.
O_2	Oxygen.
ω	Frequency in rad/s.
ω_c	Loop gain cross-over frequency.
ω_{fl}, ω_{fh}	Lower/upper break frequencies for the data filter.
$\mathcal{P}$	Structured set.

$\mathbf{P}$	Parameter covariance matrix in RLS.
p_{ij}	Transition probability from state S_i to state S_j.
p_i	Probability that the GMA starts in state i.
$\mathbf{p_0}$	Initial probability vector.
$P_e(t)$	Normalized effective power.
$P_e(k)$	Periodic observations of $P_e(t)$.
P_e^{crit}	Critical effective power (mixture viscosity).
Pb	Lead.
$Q(t)$	Water flow.
Q_{max}	Maximum water flow.
R	Field of real numbers.
r	Setpoint.
$\widehat{\mathbf{R}}_{uu}(n)$	Correlation matrix.
$r_{uu}(\tau)$	Autocorrelation of a stochastic process u.
$\mathcal{S}$	State space of a Markov chain.
$S(i\omega)$	Sensitivity function.
$s(k)$	Distance measure.
S_a	Absorbing state.
S_i	Midpoint of the ith interval.
σ	Conductivity.
σ^*	Estimated standard deviation.
$T(i\omega)$	Complementary sensitivity function.
ΔT	Temperature difference $\Delta T = T_{in} - T_{out}$.
T_{cycle}	Cycle time of the triac (actuator).
$T_{in}(t)$	Temperature of the inlet drying air.
$T_{out}(t)$	Temperature of the exhaust air.
T_r	Filter time constant in the filter F_r.
t_0	Starting time for the detection algorithm.
t_a	Alarm time.
t_k	Sampling times.
$\{\cdot\}$	Sequence of numbers.
$\boldsymbol{\theta}$	Vector of unknown parameters.

$\hat{\boldsymbol{\theta}}$	Estimated parameter vector.
$\boldsymbol{\theta}^*$	Limiting estimate of $\boldsymbol{\theta}$.
u	Process input.
u_f, y_f	Filtered process input and output values.
u_I	Intergal part of the control signal.
u_{lead}	Lead part of the control signal.
v	External variable that represents disturbances.
$v_{\min}$, $v_{\max}$	Minimum and maximum control signal respectively.
W_o	Initial weight of undried product (kg).
W_d	Weight of dry matter in product (kg).
w	Measurement noise.
X	Moisture content.
X_c	Critical moisture content.
X_{db}	Moisture content on the dry basis.
X_e	Equilibrium moisture content.
X_{wb}	Moisture content on the wet basis.
x	Mixing ratio.
$\mathcal{X}$	A sample, i.e., a collection of n numbers drawn at random from a completely unspecified distribution.
$\mathcal{X}^*$	Bootstrap (re)sample.
y	Process output.
y_F	Filtered measurement before A/D conversion.
Zn	Zinc.

Operators and Functions

$\arg\min_x f(x)$	The minimizing argument of $f(x)$.
$\|z\|$	Absolute value of $z \in \mathrm{C}$.
Δ	The operator $1 - q^{-1}$.
$E\{X\}$	The expected value of a stochastic variable X.
$\exp(x)$	The exponential function, e^x.
$F_X(x)$	The probability distribution function.

$f_X(x)$	The probability density function.
`floor(x)`	Rounds the elements of `x` to the nearest integers towards minus infinity.
$\mathcal{N}(m, P)$	The Gaussian (normal) distribution with mean m and covariance matrix (variance) P.
p	Differential operator d/dt.
q, q^{-1}	Forward/backward shift operator, $qy(k) = y(k+1)$.
s	Laplace transform variable.
$\sim$	Distributed according to relation.
$\log(x)$	The natural logarithm of x.
$\Pr[A]$	The probability of event A.
$Var\{X\}$	The variance of a stochastic scalar X.

Acronyms

ACAA	American Coal Ash Association.
AC	Analys Centrum.
A-D	Analog-to-Digital.
ANFIS	Adaptive Neuro-Fuzzy Inference Systems.
ARL	Average Run Length.
ARMA	AutoRegressive MovingAverage.
ARMAX	AutoRegressive MovingAverage with eXternal input.
ARX	AutoRegressive with eXternal input.
BJ	Box-Jenkins.
CCD	Charge Coupled Device.
CFB	Circulated Fluidized Bed.
CHP	Combined Heat and Power production.
CIFA	Carbon In Fly Ash.
COMLI	COMmunication LInk.
CPU	Central Processing Unit.
CUSUM	CUmulative SUM.
D-A	Digital-to-Analog.
ETEC	Environmental TEChnical.

FAR	False Alarm Rate.
FETC	Federal Energy Technology Center.
GF	Grate Fired.
GMA	Geometric Moving Average.
GPR	Ground Penetrating Radar.
HA	Hardware Alarms.
IAE	Integrated Absolute Error.
IE	Integrated Error.
IEC	International Electrotechnical Commission.
LOI	Loss-On-Ignition.
LQG	Linear Quadratic Gaussian.
MC	Moisture Content.
MTFA	Mean Time between False Alarms.
MTD	Mean Time to Detection.
NIR	Near InfraRed.
OE	Output Error.
PC	Personal Computer.
PE	Persistent Excitation.
PM	Program Module.
PID	Proportional Integral Derivative.
PLC	Programmable Logic Controller.
PRBS	Pseudo Random Binary Sequence.
RLS	Recursive Least Square.
RMS	Root Mean Square.
SA	Software Alarms.
SFC	Sequential Function Chart.
SM	Sub Module.
UCK	University College of Kalmar.
UWB	Ultra-Wide Band.
VM	Variable Module.
WA	Water Amount.
WAH	Wood Ash Hydration.
WAS	Wood Ash Stabilization.

Glossary

Absorption	Uptake of moisture by a dry product.
Adiabatic	Changes to the humidity and temperaure of air without loss or gain of heat (in drying).
Bound moisture	Liquid physically or chemically bound to a solid product matrix that exerts a lower vapor pressure than pure liquid at the same temperature.
Constant-rate drying	The drying period in which the rate of moisture loss is constant, since external resistances are limiting the moisture transfer.
Critical MC	The amount of moisture in a product at the end of the constant rate period of drying.
Dry bulb temperature	Temperature measured by a dry thermometer in an air-water vapor mixture.
Equilibrium MC	The MC of a product at which it neither gains nor looses moisture to its surroundings (at a given temperature and pressure, the product is in equilibrium with the air vapor mixture surrounding it).
Falling-rate drying	The drying period in which the rate of moisture loss declines.
Latent heat	Latent heat is the heat (energy) in an air stream due to the *moisture* of the air. An airstream of 80°C/60%RH has more latent heat than an air stream of 80°C/50%RH.
Leaching	Washing out of soluble components from a product.
Sensible heat	Sensible heat is the heat (energy) in an air stream due to the *temperature* of the air. An airstream of 80°C/50%RH has more sensible heat than an air stream of 70°C/50%RH.
Wet bulb temperature	Temperature measured by at wet thermometer in an air-water vapor mixture.

Contents

Chapter 1

Introduction

1.1 Background

Most parts of this section originate from Holmberg (2000).

Sweden supports the resolution concerning the environment and progress, which was taken at the U.N. convention, UNCED, Rio 1992. After this, it is now our obligation to aim for a lasting development. We should encourage an environmentally-sound use of renewable sources of energy, and furthermore the adaptation to the ecological cycle. The today active system for producing energy with biomass fuel is included in the resolution taken at the U.N., but still, the adaptation to the ecological cycle is not fully brought to an end. With the ambition to create a sustainable energy system, the use of renewable energy in Sweden is expected to grow further and biofuels are expected to account for a significant part of this increase.

When biofuels are burned or gasified, the majority of the nutrients, except nitrogen, will retain in the ashes. The ashes are alkaline and the nutrients appear in similar proportions as in the harvested biomass. Thus, wood ash contains a broad spectrum of mineral nutrients, macro and micronutrients as well as heavy metals and organic contaminants. Therefore, to maintain a long-term productivity of the forest soils, particularly in areas affected by acidification, recycling of nutrients back to forest soils in form of wood ash is desirable. Furthermore, an advantage of recycling ash instead of deposition in land fills, which is mostly applied today, will be that problems accompanied with land fills (leaching, space occupation, costs) will be significantly reduced. However, because

there is a great diversity in the types of ash formed in various kinds of biomass derived fuels, it is urgent to characterize the ash materials in order to get suitable dissolution rates, as well as technologies for reducing their content of harmful components – the nutrient recycling system must be environmentally safe.

Today ash recycling is required by the forestry authorities for whole-tree harvesting on the acidified soils of south-western Sweden. Whole-tree harvesting means that not only the kernel wood but also the nutrient-rich parts of trees, such as bark, branches, tops and needles, are removed from the forest during the felling. By recycling wood ash in amounts similar to those withdrawn with the fuel, it is possible to compensate for the nutrient losses. However, the ash cannot be recycled directly without any preprocessing; its volatility would then cause severe spreading problems. Hence, at the combustion an oxidation occurs. Therefore, primarily, the main substances in the wood ash appear as oxides (Windelhed, 1998b). This implies that many components in the wood ash become *alkaline* and *reactive*. Therefore, a direct spreading would cause heavy damage to the vegetation. Other drawbacks of the direct spreading are that the fertilizing substances are emitted too fast, or that the ash could clog up the pores of the surrounding living plants. The idea is therefore to transform the ashes into a product – agglomerates – that more easily could be recycled. This product should be manufactured locally at the heating plant and then distributed to the forests nearby. The aim is thus to implement a closed-loop system as symbolized by Figure 1.1, in which the wood ash is recycled back to the forest grounds.

Wood ashes are difficult to handle because of their volatility. It is therefore necessary to *stabilize* the wood ash before the transportation and spreading. It is also necessary to stabilize the ash in order to control the leaching rate of the nutrients and the wood ash included heavy-metals, as for example cadmium (Cd), copper (Cu), lead (Pb) and zinc (Zn), see Eriksson (1993). In stabilized wood ash, heavy-metals are sparingly soluble. Thus, the heavy-metal emission from recycled (stabilized) wood ashes are comparable with the felling remains left at the felling area. It is also shown that berries and fungus do not obtain any higher concentrations of heavy-metals after spreading of stabilized wood ash (Lundborg, 1997). It is therefore recommended to recycle an amount of wood ash that will add a total heavy-metal concentration comparable to the take out at the felling. Then the forest soils are not supplied with more heavy-metals

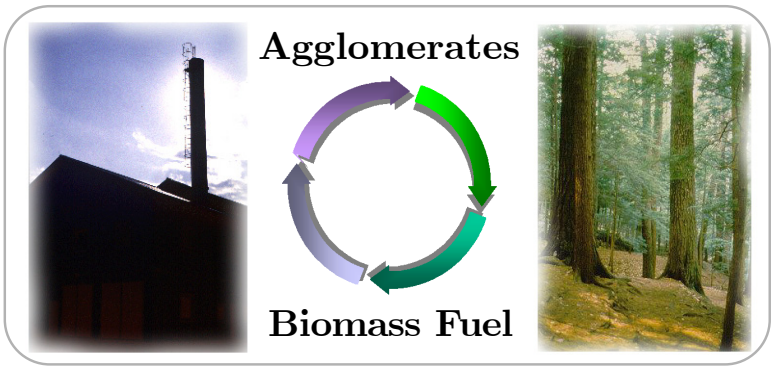

Figure 1.1: The closed-loop system.

compared to the take out, thus resulting in a non-increasing concentration.

Solving the management problems concerning ashes from biofuel combustion are of global interest. In the United States 2.7 million tones of ash is generated annually by power boilers fired with bark, wood and wood wastes, and over 80% of that ash is deposited in land fills (Williams, 1988). In Cameroon, 68% of the country use wood and wood residues to satisfy their energy requirements, and the ash originating from the wood industry is often disposed in large amounts in the neighborhood surrounding the factories, causing serious environmental problems (Voundi et al., 1998). In Austria, the total amount of ash produced in heating plants 1995-96 was about 68 000 tons per year and by 2005 the ash amount is expected to lie between 85 000 and 104 000 tons per year (Holzner, 1998). In 1993 the combustion of wood resulted in an estimated amount of 2400 tons of ash in Switzerland (Wunderli et al., 2000). The most abundant biofuels in Denmark are straw and wood chips (Sander, 1997), and the expected production of ash from straw and wood fired district heating plants and Combined Heat and Power production (CHP) plants is 80 000 tons in 2010 (Bertelsen, 1998). The Finnish wood industry annually produces approximately 150 000 tons of wood ash that could be recycled in forest ecosystems (Fritze et al., 2000). The annual production of wood ash is estimated to be between 100 000 to 150 000 tons in Sweden and approximately 15% of the wood ash is produced at district heating and combined heat and power plants. A major part of the Swedish ashes is however deposited as waste. The disposal cost for ashes is between 30 to 85 USD per ton, including a tax on land filling

Figure 1.2: An aerial view of the central heating plant ”Draken” of Kalmar.

of waste, 25 USD per ton, since January 1, 2000.

During 1992-1997, NUTEK (the Swedish National Board for Industrial and Technical Development; since January 1998 The Swedish National Energy Administration), Sydkraft and Vattenfall co-operated within the R&D programme ”Recycling of wood ash”. The purpose of the programme was to evaluate the ecological effects of recycling wood ash to forests; to characterize ashes from different combustion and gasification processes; and to develope technologies and logistics for wood ash recycling. Main emphasis was on the characterization of Circulated Fluidized Bed (CFB) and Grate Fired (GF) boiler ashes from combustion of bark and forest residues or mixtures of peat or coal and wood (Rosen et al., 1993, Steenari, 1996, Gyllin and Kruuse, 1996, Rühling, 1996, Karlsson, 1997, Nilsson and Eriksson, 1997, Eriksson, 1996, 1998, Nilsson and Eriksson, 1998, Sfiris et al., 1999, Eriksson, 1999).

In this thesis, however, the central heating plant ”Draken” of Kalmar, Sweden, will be used as case study. The main fuel at this heating plant is sawdust produced by a wood-flooring manufacturer. The heating plant execute sawdust combustion in a converted coal-fired boiler and produces 200-300 tons per year of collected wooden fly ash. An aerial view of central heating plant ”Draken” is shown in Figure 1.2.

Figure 1.3: The Anelema quarry, Estonia. Photo: Sirkku Holmberg.

1.2 Proposed Method - The Kalmar Approach

In this thesis, a novel method to automatically transform wood ashes into fertilizing *agglomerates* is presented. These agglomerates are easy to handle and have adequate properties for recycling. The solution is to mix the ash with water and a mineral, called Environmental TEChnical (ETEC) dolomite, which acts as a binding agent. The proposed transformation process consists of four different processing units, which are indicated by Figure 1.4. The ash, ETEC-dolomite and water are first mixed into a material that is used for agglomeration. When the Wood Ash Hydration (WAH) process is completed, the mixture is processed in a *roll-pelletizer* where the actual agglomeration occurs. The agglomerated material is then dried before it is packed. The dolomite originates from the *Anelema quarry*, Estonia – see Figure 1.3 – and since 1999, the dolomite delivered has a particle size less than 4mm. The use of a limestone, such as the ETEC-dolomite, is recommended by the forestry authorities since it reduces the acidification in the forest soil at the spreading area (ash + limestone = vitalizing). Furthermore, due to the mix of ash and dolomite in the produced agglomerates, the heavy-metal load caused by the fertilizers are even more reduced. Other common binders used for wood ashes are cement and lignosulphate, but agglomeration without additives is also applied. However, this approach is based upon the self-hardening capacity of wood ash and requires an ash with low content of unburnt carbon (Steenari and Lindqvist, 1997).

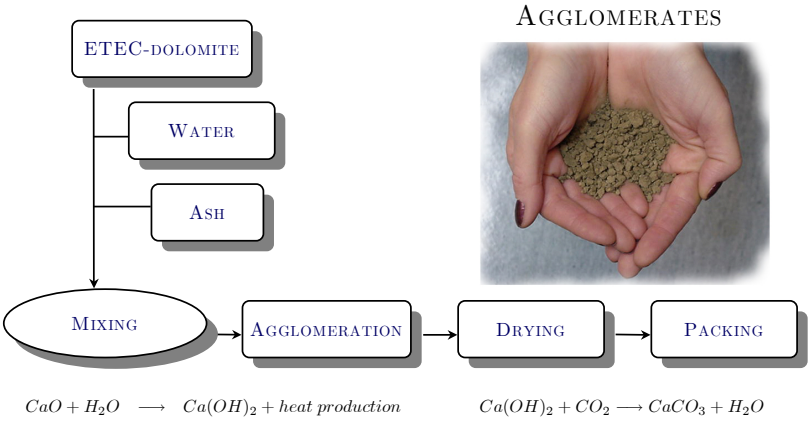

Figure 1.4: The general ash transformation process.

When stabilizing wood ashes that are well burnt (less than 10% of unburnt carbon) two reactions are dominating (Nilsson, 1993). In the first stage of the transformation process – called the WAH process – the first chemical reaction occurs: *slaked lime* is formed by treating *quicklime* with water:

$$CaO + H_2O \longrightarrow Ca(OH)_2 + heat\ production \tag{1.1}$$

The reaction is fast and *exothermic* and the wood ash now becomes less reactive. When slaked lime is formed the stabilization continues through *carbonization* with help from the carbon dioxide available in the air:

$$Ca(OH)_2 + CO_2 \longrightarrow CaCO_3 + H_2O \tag{1.2}$$

This reaction is fast initially but the rate is decreasing after $3-7$ days. The most important transformation is that of $Ca(OH)_2$ to $CaCO_3$, since it reduces the solubility of calcium and the alkalinity of the ash. Thus, a pH shock in the forest soil can be avoided. Therefore, from an environmental point of view the occurrence of carbonization is positive. However, complete carbonization is not desirable before spreading because the agglomerates then get brittle (Holmberg et al., 2001). Handling and spreading of brittle particles would increase the weight fraction of small particles in the particle size distribution and increase the dust problems during spreading. However, when the agglomerates become dryer, the carbonization diminish. Therefore, after the WAH process has taken

place, it is of great importance that the product is dried immediately. Hence, the hardening reactions of wood ashes are similar to reactions that occur in coal ashes as well as in cement and concrete. Therefore, using additives (organic or inorganic binders) and heating are two methods that increase the hardening rate and the mechanical strength of the final product (Holmberg et al., 2001).

1.3 Objective and Scope

The objective is to develop the idea outlined above into a well-proven, professional method for producing ash agglomerates. The agglomerate manufacture should be *automatic* and *batch-wise,* all the way from mixing the ingredients to packing the finished products. Since the heating plant Draken produces 200-300 tons per year of filtered wood ash, the ash transformation process must be capable of handling at least 1 ton of wood ash per day. Furthermore, the control system for the ash transformation process must be integrated with the heating plant computer system so that information easily can be exchanged between the local control system and the system used for supervision. Since there are several stages in this process, which all will run concurrently, it is necessary to use real-time control. Furthermore, because of the industrial environment an industrial control system is suitable as a base. Hence, the local control system should not only be able to interact with the process, it should be able to interact with the *operator* as well. It is very important to emphasize that the *man-machine interface* plays an essential role in these kind of applications. If the operator does not understand the information he/she is receiving, it is impossible to take the correct decision about the next step in the process. Therefore, it is important to also facilitate the exchange of information between the *user* and the equipment to be controlled. A well designed interface not only makes work conditions more pleasant, but also helps considerably to reduce errors and thus limit the extent of possible damage.

Since each stage of the transformation process earlier has been controlled manually (Lindahl and Claesson, 1996), it is important to utilize the knowledge that the original process operators possess. This could help a great deal on the way from *art to science* in the control design and in programming sequences and logic. Furthermore, it is of utmost importance to make sure that the transformation process will work well also during *emergency conditions*.

1.4 Design: An Overview

Real control problems, like the ash transformation process, are often large and poorly defined, while control theory deals with well-defined problems. According to the dictionary, *structuring* can mean to construct a systematic framework for something. In this context, however, structuring is the operation that overcomes the gap between the real problems and the problems that control theory can handle.

The problem of structuring occurs in many disciplines. Formal approaches have also been developed. The terminology used here is borrowed from the fields of computer science, where structuring of large programs has been subject of much work. There are two major approaches, top-down and bottom-up.

The *top-down* approach starts with the problem definition – the ash transformation process. The problem is then divided into successively smaller pieces, adding more and more details. The procedure stops when all pieces correspond to well-known problems. It is a characteristic of the top-down approach that many details are left out in the beginning. More and more details are added as the problem is subdivided.

The *bottom-up* approach starts with the small piece, which represents known solutions for subproblems. These are then combined into larger and larger pieces, until a solution to the large problem is obtained.

Top-Down Approach

The top-down approach involves the selection of control principles, choice of control variables and measured variables.

Control Principles

A control principle gives a broad indication of how a process should be controlled. The control principle thus tells how a process should respond to disturbances and command signals. The establishment of a control principle is the starting point for a top-down design. Several examples of control principles can be found in Åström and Wittenmark (1997).

Choice of Control Variables

After the control principle has been chosen, the next logical step is to choose the control variables. The choice of control variables can often be limited for various practical reasons. Because the selection of control principle tells what physical variables should be controlled, it is natural to choose control variables that have a close relation to the variables given by the control principle. Because mathematical models are needed for the selection of control principles, these models also can be used for controllability studies when choosing control variables.

Choice of Measured Variables

When the control principle is chosen, the primary choice of measured variables is also given. If the variables used to express the control principle cannot be measured, it is natural to choose measured variables that are closely related, such that an estimator can determine the value that cannot be measured. Typical examples are found in chemical-process control, where temperatures – which are easy to measure – are used instead of compositions, which are difficult to measure.

Bottom-Up Approach

In a bottom-up approach to control system design, the choice of control variables and measurements comes first. Control-loops are then designed for the individual process operations of the system – the ash transformation process. At each iteration, different control designs are introduced in the local loops until a system, with the desired properties, is obtained. The controllers used to build up the system are the standard types based on the ideas of *feedback*, *feedforward, prediction* and *estimation, optimization* and *adaptation.* Throughout this thesis, the *bottom-up* approach is used as design method for the ash transformation process.

1.5 Problem Descriptions & Research Approach

This section is closely related to the different stages of the ash transformation process, which are indicated by Figure 1.4. The problem descriptions will be stated in this context and their relations to several of research areas such as

measurement science, *signal processing*, *mathematical & empirical modeling* and *automatic control* will be clarified.

There are always some unburnt remains of carbon in the ash. This is so because the combustion is not always optimal due to varying quality of the fuel, and due to different combustion loads. The amount of unburnt carbon influences the overall properties of the produced agglomerates in a very definable way: this will decelerate the proposed *self-hardening* process for agglomerates produced with no binding agent (Nilsson, 1993, Windelhed, 1998b). It should also be stressed that the produced agglomerates do not benefit from high carbon contents since their fertilizing properties will then deteriorate. Therefore wood ash carbon content analysis may be necessary, which is related to the area of *measurement science*. Hence, it is "fairly easy" to decrease the carbon content in the fly ash and thus improve the burner efficiency by increasing the oxygen ratio during combustion. On the other hand, the burner then produces high NO_X levels at elevated O_2. This is not allowed by the authorities and puts us into a dilemma. To optimize the combustion efficiency without elevated NO_X levels is a challenging control problem – however not within the scope of this thesis. Further details are given in Chapter 2.

Mixing ash/dolomite/water in order to obtain granular material is one method to stabilize wood ashes. The main problem is predicting the quantity of water to be added, since the necessary amount varies with the wood ash quality (Nordenberg, 1996, Sundqvist, 1999, Windelhed, 1998b). In Sundqvist (1999) it is reported that the critical water-to-ash ratio varies between ash types and must therefore be determined for each ash. Hence, if the quantity of water exceeds the necessary amount one will obtain a mixture useless for agglomeration. Therefore, accurate water control is crucial. In this problem it is important that the water is distributed over a wide area, yielding a homogenous mixture; this calls for a novel actuator. Furthermore, what sensor technology that should be used is open. When the actuator(s) and sensor(s) are selected, a model is a useful and compact way to summarize the knowledge about the process. This model can be empirical or mathematical. All these problems must be targeted and these are related to different areas such as *actuator technology*, *measurement science*, *signal processing* and *system identification*. Chapters 3 and 4 are dedicated to these issues.

What method to apply in order to obtain automated wood ash agglomeration is truly a delicate problem. In Nilsson (1993) several techniques used to agglomerate wood ashes are presented. Furthermore, a number of experiments in Sweden to agglomerate wood ashes, on-going or finished, are documented in Nordenberg (1996). The main problem is to find a method that has no maintenance problems, is easy to operate and has large production capabilities. This problem is targeted in Chapter 5.

The *modeling* and *control* of dryers is an issue that has been extensively studied. For example, the problem of measuring the moisture content of the desiccated material has always attracted a special attention. As a result, one has to combine knowledge within the areas of *measurement science*, *signal processing*, *mathematical modeling* and *automatic control* to solve any problem related to automated dehydration. Furthermore, controller tuning and implementation issues have to be targeted as well; these topics are discussed in Chapter 6.

As reported in Windelhed (1998a) and Lövgren et al. (2000), the today applied method for agglomerate dehydration is based on the so called *self-hardening* principle: firstly, the produced agglomerates are ejected into a platform lorry. When this lorry is fully loaded, the agglomerates are transported and dumped in large heaps at an intermediate storing facility; this is where the actual self-hardening occurs. In Lövgren et al. (2000) it is concluded that the time required for the self-hardening process to be successful is about *one month* at a temperature of 0 degree's Celsius. This and several other drawbacks of the method are presented in Chapter 7, and these imply that a new method must be developed; a drying method suitable for automated manufacture. Hence, fast and effective dehydration of the ash agglomerates gives the possibility of immediate packing and distribution.

In Chapter 8, the general philosophy applied during the implementation of the control system is presented. The academical potential of the work presented in this chapter may not be the greatest, but on the other hand, for the operator of any process controlled by computers, a well designed, robust and good structured program/operator interface is of most value. This takes a considerable time to achieve practically, but the academical writing about it is minor.

1.6 Related Works

Measurement of Unburnt Carbon in Wood Ashes

Most of the methods today are developed for coal-fired boilers. Several off/on-line methods are available. The Loss-On-Ignition (LOI) test is the standard off-line method for determination of carbon content in fly ash. However, in Brown and Dykstra (1995) it is shown that this conventional test method is not an accurate measure of unburnt carbon in fly ash. Sometimes, there are significant quantities of slaked lime (portlandite) $Ca(OH)_2$ and carbonate (calcite) $CaCO_3$ in the fly ash. Along with the particulate carbon they lose weight under the high-temperature oxidation conditions of the LOI test. The weight loss from these minerals easily exceeds that due to carbon resulting in gross errors in the LOI tests for fly ashes. The Federal Energy Technology Center (FETC), U.S. Department of Energy is periodically organizing conferences on unburnt carbon in utility fly ash. Recommendable publications from FETC on the topic of on-line Carbon In Fly Ash (CIFA) monitoring are Larrimore and Sorge (1997), Trerice et al. (1998) and Snowdon (1998).

Modeling and Control of Mixing Processes

Mixing is a basic process operation used to blend several ingredients into a new product. The quality of this product is in many cases highly dependent on the mixture characteristics. Therefore there is a need for accurate mixture viscosity control. For example, at the mixing of bread dough various ingredients as water, flour, yest, shortening, sugar, salt, oil and reducing agents are blended into a homogenous mass through physical work. This mixing is an important step in making all kinds of bread because the characteristics of the mixed dough are critical to successful baking. In Fowler (2000) a system for automated bread dough mixing is presented, which measures the input electrical power to the dough mixer and utilizes fuzzy logic to determine the product quality. A similar technique is applied to bread dough mixing in Wide (1999). Here the selected sensor signal is the current from one phase of the mixer motor. This signal is analyzed by time series analysis to detect variations in the measurements. By calculating, for example, the variance it is possible to identify a significant change of the dynamical process, e.g. when the ingredients have changed into dough. Other sensor signals presented by the research community for testing bread dough are the torque required to rotate a sensor paddle at a constant

speed (Babb and Casson, 1970) and the expected moisture content of the dough (Donskoi et al., 1979).

The concrete production industry is another area in which accurate mixture viscosity control is important. A concrete production process is difficult to control, especially in the case of low water-cement ratio, because the property of concrete depends on not only the mix-proportions but also the mixing method. Different solutions are presented in the literature: In Mikulic and Krstic (1995) a proposal for a neural network is given that can solve the water quantity problem in the mix design. Furthermore, the use of fuzzy sensor data fusion for quality monitoring in concrete mixing plants is presented in Boscolo et al. (1993). Here an adaptive fuzzy system is proposed in order to estimate the amount of water in the concrete. In this system the input variables are obtained from measurements of the mixture conductivity, the dielectric constant at low frequency, the temperature, the apparent viscosity and the ratio of the reflectance at two different optical wavelengths.

Often the dynamics of any mixing operation are considered to be highly nonlinear. An alternative interpretation is that it may be considered as a hybrid system modeled by a set of local linear time-varying or time-invariant differential equations with connected logic conditions. These logic conditions often depend on the mixture characteristics. In many applications, as the ones described above, the goal is blending several ingredients and to obtain a mixture with a certain critical viscosity. At this target viscosity, a switch between two local models often occurs. Therefore, the approach of using an on-line adaptive parameter estimator combined with a change detector that detects the abrupt change in the process dynamics may serve as a mixture quality control algorithm.

One of the main contributions of this thesis is a new approach for mixture quality control based on *adaptive filtering and change detection* (Willsky, 1976, Basseville and Nikiforov, 1993, Gustafsson, 2000). The ash stabilization batch mixing process presented in Chapters 3 and 4 will be used as case study. This process blends ash, dolomite and water in order to obtain material suitable for agglomeration. The main problem is predicting the quantity of water to be added, since the required amount of water varies with the wood ash quality. The used sensor signal is the normalized effective power that represents the rate of useful work being performed by the three-phase asynchronous machine used for the stirrer drive.

Equipment	Granule size	Capacity
Fluidized bed granulation	0.1-1 mm	0.5-5 ton/h
Rotating drum	1-5 mm	5-100 ton/h
Rotating pan	1-5 mm	5-100 ton/h
High shear mixer	0.3-0.8 mm	0.5-50 ton/h
Prilling	0.5-1 mm	0.5-50 ton/h
Roll compaction	1.5-10 mm	0.5-5 ton/h
Tabletting	any shape $>$ 2mm	$<$ 2 ton/h
Screw extrusion	1-10 mm	0.5-5 ton/h

Table 1.1: Types of granulation equipment and their characteristics.

Modeling and Control of Agglomerators

Particle size enlargement by agglomeration is often desirable for several reasons: to obtain prevention of dust formation; to increase bulk density and to decrease bulk volume. Furthermore, a defined shape and weight may improve the appearance of the product. Agglomeration is used in various industries, like the *pharmaceutical industry* (Morris et al., 1998, Thies and Kleinebudde, 1999, Harnby, 2000, Leuenberger, 2001b,a), the *agricultural industry* (Adetayo, Litster and Cameron, 1995, Walker et al., 2000, Zhang et al., 2000), in *mineral processing* (Kapur et al., 1973, Abouzeid et al., 1979, Litster and Waters, 1990, Dutta et al., 1997, Ripke and Kawatra, 2000), and in the *food industry* (Tanihara et al., 1996, Knight, 2001). In Wauters (2001), the apparatuses in Table 1.1 are described as suitable granulation equipment.

A comprehensive presentation of the previous and contemporary work within the research field "modeling and mechanisms of granulation" is to be found in Wauters (2001). Furthermore, the fundamentals of the emerging high-shear pelletization technique is outlined in Ramaker (2001). The issue of on-line particle size measurement has been considered in Harayama and Uesugi (1992) where an on-line measurement of agglomerate size with an image processing technique is presented. In Yokoi et al. (1999) a novel phase Doppler method is proposed for sizing of moving spherical particles and the today commercial product OptiSizer PSDA^{TM} inspects and analyzes granule particle size distributions from 40 micrometers to larger than 10 millimeters in diameter using a Charge Coupled Device (CCD) camera for high-speed image capture

(OptiSizer, 2002). The approach of applying a CCD camera combined with *fuzzy logic* for granulation process control have been reported in Watano and Miyanami (1999) and Watano (2001). As an alternative, since the moisture content of the granules during the liquid spraying phase is a central parameter describing the granule growth kinetics (Adetayo et al., 1993, Adetayo, Litster and Cameron, 1995, Adetayo, Litster, Pratsinis and Ennis, 1995), the use of a multi-channel Near InfraRed (NIR) moisture sensor is used in Rantanen et al. (1998, 2000, 2001) for on-line monitoring of moisture content in a fluidized bed granulator. However, new interesting techniques for model based control of granulation systems using crude estimates of the recycle size distribution are presented in Zhang et al. (2000) and Pottmann et al. (2000).

In Nilsson (1993) several techniques used to agglomerate wood ashes are presented thoroughly. A number of experiments in Sweden to agglomerate wood ashes, on going or finished, are documented in Nordenberg (1996). In this thesis, Chapter 5 is dedicated to wood ash agglomeration techniques.

Modeling and Control of Dryers

The *modeling* and *control* of dryers is an issue that has been extensively studied in recent years both from a theoretical and from a practical point of view. The existing literature on this topic can be given a first classification according to the type of dryers, and to the desiccated material. Many types of dryers are used: *drum dryers* (Courtois and Trystram, 1994, Rodriguez et al., 1996a,b), *cross-flow dryers* (Platt et al., 1992, Douglas et al., 1994a,b,c, Quiang and Bakker-Arkema, 2001), *solar dryers* (Farkas, Mészaros and Seres, 1998), *fluidized-bed dryers* (van Boxtel and Knol, 1996), *fixed-bed dryers* (Farkas, Remenyi and Biro, 1998b), *rotary dryers* (Douglas et al., 1993, Savaresi et al., 2001, Hallström, 1985, Shahhosseini et al., 2001) and *belt dryers* (Kiranoudis, 1998, Kiranoudis and Markatos, 2000). The variety of desiccated material is huge: *maize* (Courtois et al., 1991), *rice* (Bonazzi et al., 1994, Toyoda, 1989, 1992), *corn* (Courtois, 1995, Courtois et al., 1995, Trelea et al., 1997), *agricultural products* (Toyoda et al., 1997, Nybrant, 1986) and *tea leaves* (Temple and van Boxtel, 1999, Temple, Tambala and van Boxtel, 2000, Temple and van Boxtel, 2000b,a, Temple, van Boxtel and van Straten, 2000) are just a few examples.

An important feature that can be used to categorize the literature is the modeling approach: *black-box* or *first-principles*. Traditionally, black-box approaches

are rarely used in this since physical insight in the model is important, and a large set of "good" (stationary and characterized by high signal-to-noise ratio) input-output measurements is rarely available. The black-box models typically used are standard AutoRegressive Moving Average (ARMA), Box-Jenkins (BJ) or Output Error (OE) models, if linearity is assumed (Toyoda et al., 1995), or *neural-nets* (or similar non-linear parametric functions) if non-linear phenomena must be captured (Farkas, Remenyi and Biro, 1998a,b, Trelea et al., 1997). On the other hand, traditional first-principles models range from partial differential equations to sophisticated stochastic models (Mészaros et al., 1999). However, there is a large range of models in between black-box or first principles. Like characteristic drying curves, lumped and logarithmic models etc.

The control strategy used to regulate the dryer is another main distinctive feature. A number of control approaches have been tested: from classical, such as Proportional Integral Derivative (PID) or Linear Quadratic Gaussian (LQG) based and recently developed $\mathcal{H}_\infty$ techniques for linear systems, up to "trendy" non-linear control schemes such as exact linearization (Siettos et al., 1999) or neural-networks/fuzzy-logic based approaches; see e.g. (Zhang and Litchfield, 1993). A comprehensive overview of control strategies for dryers operation is to be found in Courtois (1996) or Quirijns et al. (2000).

It is worth mentioning that, in dryer control problems, the issue of measuring the moisture content of the desiccated material has always attracted a special attention (Carr-Brion, 1986). The fast, cheap and accurate measurement of moisture content is a formidable problem, which is still open. This problem is particularly important since it typically imposes strong limitations on the control strategies that can be used in practice. Papers explicitly dealing with this issue are, e.g. Rodriguez et al. (1996b) and Toyoda et al. (1995, 1997).

1.7 Outline and Contributions

The main contributions of this work may be summarized as follows:

- A robust machine has been developed and is controlled by an industrial control system in order to enable automated manufacture of fertilizing agglomerates from burnt wood ash.
- Different approaches for on-line Carbon In Fly Ash (CIFA) monitoring

are surveyed and a new measuring device based on *impulse radar* is presented.

- A new scientific method is developed and implemented in order to predict the necessary amount of added water in the WAH process.
- The novel *roll pelletizing* method presented in Windelhed (2000) and Lövgren et al. (2000) was used at full-scale tests in Kalmar during 2001. This evaluation resulted in some improvements of the method for wood ash agglomeration.
- A new method is developed for automated dehydration of agglomerates. The method enables immediate packing and distribution of the product.

1.8 Academic Work

Some of the results of this thesis have, or will, appear as published material. The work on the transformation process was initially focused on the issue of on-line Carbon In Fly Ash (CIFA) monitoring and the Wood Ash Hydration (WAH) process – former called the Wood Ash Stabilization (WAS) process. This resulted in the Licentiate thesis

- Svantesson, T. (2000). *Automated Manufacture of Fertilizing Granules from Burnt Wood Ash*, Licentiate thesis, Department of Industrial Electrical Engineering and Automation, Lund University, Lund, Sweden.

This Ph.D. thesis addresses the problem of wood ash agglomeration and dehydration as well. Below are all the publications by the author listed.

Journals and Magazines

Most parts of Chapter 4 appear in

- Svantesson, T. and Olsson, G. (2002). A novel method for mixture viscosity control based on change detection. Accepted for publication in *Control Engineering Practice*.

A popular science presentation of the project appears in

- Svantesson, T., Holmberg, S. and Claesson, T. (1999). Granulerad aska ger näring till skogsbruket, *Recycling Scandinavia* **1**: 50–51. In Swedish.

Conference Papers

The ash transformation concept presented in this thesis are filed together in

- Svantesson, T. and Olsson, G. (2003). Taking automatic control into wood ash recycling, *American Control Conference*, The Adams Mark Hotel, Denver, Colorado USA. Submitted.
- Svantesson, T., Lauber, A. and Olsson, G. (1998). Automated manufacture of granules from burnt wood ash, *Proceedings of Fifth National Science - Technical Conference. Macro-Levelling and Reclamation of Areas with use of By Products Combustion*, Swinoujscie, Poland.

The material presented in Chapter 3 is published in

- Svantesson, T., Lauber, A. and Olsson, G. (2000). Viscosity model uncertainties in an ash stabilization batch mixing process, *Proceedings of 17th IEEE Instrumentation and Measurement Technology Conference, IMTC 2000*, Vol. 2, Baltimore Maryland, USA, pp. 909–914.

Certain aspects of Chapter 4 appears in

- Svantesson, T. and Olsson, G. (2000a). Detection of abrupt parameter changes in an ash stabilization batch mixing process, *Preprints of the Swedish National Conference on Automatic Control, Reglermöte 2000*, Uppsala, Sweden, pp. 324–329.
- Svantesson, T. and Olsson, G. (2000b). Optimal adaptive control of an ash stabilization batch mixing process using change detection, *Proceedings of IEEE International Conference on Control Applications, CCA 2000*, Vol. 1, Anchorage, Alaska, USA, pp. 109–114.

Technical Reports

The material presented in Chapter 5 is published in

- Svantesson, T. and Olsson, G. (2002a). Wood ash agglomeration – have we reached an automatic solution yet?, *Technical Report TEIE-7187*, Department of Industrial Electrical Engineering and Automation, Lund University, Sweden.

A shorter and more technical presentation is to be found in

- Svantesson, T., Petersson, T. and Jedfelt, D. (2001). Utvärdering av försök med valspelleteringsmetod, *Technical Report*, Department of Technology, University College of Kalmar, Sweden. In Swedish.

The material presented in Chapter 7 is also the topic of

- Svantesson, T. Quirijns, E. J. and Olsson, G. (2002b). Wood ash agglomerate moisture control − hardware, sensors and control algorithms, *Technical Report TEIE-7188*, Department of Industrial Electrical Engineering and Automation, Lund University, Sweden.

Miscellaneous

- A patent-application has been filed for an impulse radar system for online CIFA monitoring.

Some of the material presented in Chapter 4 has been used in

- Gustafsson, F. (2000). *Adaptive filtering and change detection*. John Wiley & Sons, Ltd.
- Gustafsson, F. (2001). *Adaptive Filtering and Change Detection Toolbox*. Department of Electrical Engineering, Linköping University, Linköping, Sweden.

Work that has not been explicitly included in this thesis, but was performed just before, and during the Ph.D. studies was published in

- Svantesson, T. and Hultgren, A. (2002). Teaching automatic control using the parallel-cart process, *Preprints of the Swedish National Conference on Automatic Control, Reglermöte 2002*, Linköping, Sweden. pp. 19–24.
- Hultgren, A., Kulesza, W., Lenells, M., Svantesson, T. and Lauber, A. (1997). Virtual real-time measurement system with a switched Kalman filter, *Proceedings of IEEE Workshop on Emergent Technologies & Virtual Systems for Instrumentation and Measurement*, Ontario, Canada.

1.9 Co-author Affiliation

Prof. Gustaf Olsson
Industrial Electrical Engineering
and Automation
Lund University
P.O. Box 118
SE-221 00 Lund, Sweden

Dr. Tommy Claesson
Ph.Lic. Sirkku Holmberg
Department of Biology and
Environmental Science
University College of Kalmar
SE-391 82 Kalmar, Sweden

Ir. E.J. Quirijns
Systems and Control Group
Wageningen University
6703 HD Wageningen
The Netherlands

Prof. Alexander Lauber
Department of Technology
University College of Kalmar
SE-391 82 Kalmar, Sweden

M.Sc. Daniel Jedfelt
B.Sc. Tommy Petersson
Graninge - Kalmar Energi AB
P.O. Box 822
SE-391 28 Kalmar, Sweden

Chapter 2

Wood Ash Carbon Content Analysis - A Survey

As already remarked in Section 1.5, the amount of unburnt carbon influences the overall properties of the produced agglomerates in a very definable way: this will decelerate the proposed self-hardening process for agglomerates produced with no binding agent. It should also be stressed that the produced agglomerates do not benefit from high carbon contents since their fertilizing properties will then deteriorate. Therefore wood ash carbon content analysis may be necessary.

2.1 Introduction

There are always some unburnt remains of carbon in the ash. This is so because the combustion is not always optimal. The lack of optimality is due to several reasons. Firstly, in the wintertime much heat must be produced to satisfy the needs of customers. As a result, there is an extraordinary high burner load during this period, which implies high carbon contents. Secondly, the quality of the fuel may change several times a day. This will cause high carbon contents as long as the combustion parameters are not adapted to the new fuel.

The traditional methods to determine the carbon content of wood ashes have been mostly inaccurate and time consuming. This chapter presents a survey of the problems and available methods for off-line and on-line Carbon In Fly Ash (CIFA) monitoring. Good publications from the Federal Energy Technology Center on the topic of on-line CIFA monitoring are Larrimore and Sorge

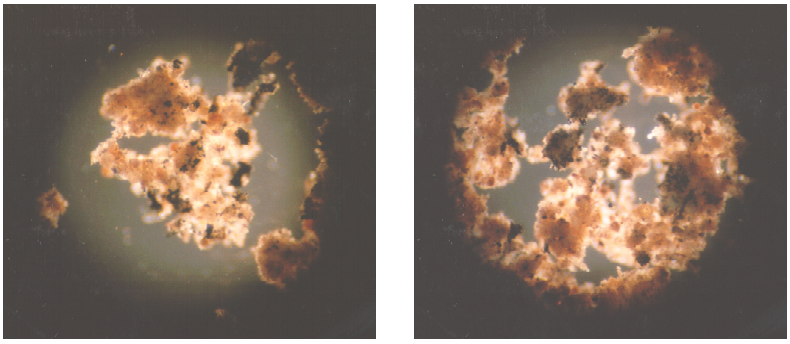

Figure 2.1: Two microscope photographs that show the carbon particles in a wood ash sample

(1997), Trerice et al. (1998) and Snowdon (1998). For a survey of the economical motivations, see Peetz-Schou (1998). One additional method presented in the academia for on-line monitoring is *photoacoustic detection*, which also has the potential for automatic, on-line monitoring (Dykstra and Brown, 1995). Furthermore, a technique based on electrostatic separation for the removal of carbon in wood ash is presented in Ban et al. (1995). This method is interesting, but cannot be classified as an on-line measuring method for CIFA.

Problems in Determining the Carbon Content

In Figure 2.1 two microscope photographs show a close-up of a wood ash sample. As seen in the pictures, dark areas are spotted in the wood ash. These dark areas are clusters of carbon particles. As a result of this observation it is natural to ask if there is a simple correlation between the wood ash carbon content and the color of the ash sample. If this is the case, the rash reader may claim that this problem is simple to solve, and states the following proposition: an ash sample that is properly burnt is *white*, otherwise the color of the sample should change according to the gray-scale and turn *darker* if the ash is not properly burnt. If this is so, the problem would be easy to solve with *Machine Vision*[1]. The more prudent reader (including the author of this thesis) would be a little more cautious. For example, consider the information given in Table 2.1. The

[1] Machine Vision is a form of artificial intelligence in which video images are converted into formats which are recognized by computers.

Carbon Content Analysis					
Nr	wl [%] UCK	wl [%] AC	**Nr**	wl [%] UCK	wl % AC
1	11.5	11.7	**6**	15.5	15.2
2	11.5	10.9	**7**	16	14.7
3	18	14.1	**8**	20.5	16.8
4	17	16.7	**9**	26	24.8
5	49	51.5	**10**	48	47.8

Table 2.1: The weight loss (wl) in percent of each ash sample provided from Graninge - Kalmar Energi. This series of ash samples was sent to Analys Center (AC) for validation, shown in the table as well.

table shows that the carbon content of the different samples analyzed at the University College of Kalmar (UCK) are of the same magnitude as the results obtained at Analys Centrum (AC), which validate the results obtained at UCK. Both utilized the method of LOI *Swedish Standard: SS 02 81 13* (1981) – an off-line procedure where a sample is taken to be dried and reburnt; the weight loss of the sample, after it is reburnt (preceded by drying), is then proportional to the amount of unburnt carbon. When inspecting the samples it is concluded that they all have approximately the same color on the gray scale. In spite of this, as shown in the table, there is an *evident* difference between the carbon contents of the samples. The results in Table 2.1 should however be interpreted with caution. As mentioned earlier, if there are significant quantities of slaked lime (portlandite) $Ca(OH)_2$ and carbonate (calcite) $CaCO_3$ in the fly ash, this may cause problems since these substances, along with the particulate carbon, lose weight under the high-temperature oxidation conditions of the LOI test. Then the weight loss from these minerals easily exceeds that due to carbon, resulting in gross errors in the LOI tests for fly ashes (Brown and Dykstra, 1995). Therefore, a second, more advanced analysis is carried through. Three different samples of wood ash with different qualities and colors are investigated. The more advanced analysis determines the amount of $CaCO_3$ and subtracts this from the weight lost under the high-temperature oxidation in order to obtain the *true* weight loss due to the carbon, see Eriksson (1993). The results are shown in Table 2.2. The conclusion drawn from the results shown in Table 2.2 is that for the three ash samples used in the test, there is no difference between the two compared methods. However, this proves *nothing* for the samples pre-

Carbon Content Analysis				
All measures are weight - %	**Sample 1**	**Sample 2**	**Sample 3**	Inst.
Total Carbon Content	59.6	35.4	8.5	**SP**
$CaCO_3$	0.63	0.86	2.0	**SP**
Unburnt Carbon	59.0	34.5	6.5	**SP**
Unburnt Carbon (wl)	61.4	35	3.5	**UCK**

Table 2.2: The more advanced method used at the Swedish National Testing and Research Institute (SP) in comparision with the results from the LOI test used at the University College of Kalmar (UCK).

sented in Table 2.1, and it cannot be excluded that the portlandite and calcite are the reason for these "strange" results. To continue the investigation, a photograph of the three samples is shown in Figure 2.2. Here a digital camera is used to visualize the working conditions for any system based on machine vision. It is clear that there is a difference between the three samples. However, it is not easy to detect by visual means that the difference between the worst and best ash sample is as great as 53% of unburnt carbon. It should also be stressed that experimental results show that the color of the ash varies with different fuels (an unknown parameter) used at combustion; for example, the ash can sometimes be brown. Referring to Figure 2.1, a heuristic explanation to this observation may be that the color of the residue material (when the carbon particles are excluded) is varying as a result of the fuel composition. Hence, the presence of $Ca(OH)_2$ and $CaCO_3$ do not affect the color since they are not visible to the eye. These facts imply that a measuring method based on machine vision would be poor and that the theory of the rash reader will fail. Therefore, more precise methods are needed.

Motivation

Earlier work (Nilsson, 1993) shows that one could obtain problems to self-harden the wood ash if there is a substantial amount of unburnt carbon present. After the ash is hydrated with water, the presence of organic material (unburnt carbon) disturbs the hardening process. Therefore, the self-hardening approach requires that wood ashes with large amounts of unburnt carbon is sorted out, which calls for a CIFA monitor. A second motivation for on-line analysis is that if the wood ash contains an amount of unburnt carbon, for example greater

Figure 2.2: A photograph of the three samples presented in Table 3.2. The leftmost sample is Sample 1.

than 50%, the fertilizing properties of the produced agglomerates will deteriorate. Today, at Graninge - Kalmar Energi AB, it is only possible to determine the CIFA (with any accuracy) by using the method of Loss-On-Ignition (LOI) presented in *Swedish Standard: SS 02 81 13* (1981). This procedure takes about four hours and is labor-intensive. To avoid this procedure, an on-line measuring device would be convenient.

2.2 Different Approaches of On-line Analysis

Two types of on-line measurements exist for the assessment of unburnt carbon in wood ashes: *direct* and *indirect:*

- *Direct* methodologies use a laboratory-like procedure to weigh the collected ash and oxidize the sample. Determining the amount of unburnt carbon in the collected ash sample requires two quantities: the mass of the collected sample, and the amount of CO_2 released during oxidation. Direct carbon-in-ash measurements offer a high level of accuracy but has a quite long processing time, up to 15 minutes.
- *Indirect* methods include the attenuation of a light beam or microwaves, as well as measurements of ash capacitance. They can be capable of generating a high data rate, but with less accuracy than monitors employing a direct measurement method. This method is undoubtedly the most rapid on-line method.

Two *indirect* methods are considered for the task of CIFA analysis. The Near InfraRed (NIR) approach and the *impulse radar* approach. The latter is a new

method for on-line monitoring of carbon in wood ash. During 1998, the author and *Malå GeoScience AB* applied for a patent of this novel measuring approach. Unfortunately, the patent was rejected. As a result, a prototype of the measuring device was not developed. Nevertheless, in Section 2.2, the philosophy of the measuring device is presented.

The NIR approach

On-line infrared measurement is usually performed with IR wavelengths between 1.0 and $2,5\mu m$. The measurement technique is based on the fact that various molecular groups can selectively absorb NIR light (Benson, 1995). The on-line sensor must be capable of detecting small changes in absorption and in this case of accurately relating these to the carbon content. Since NIR absorption is primarily concerned with absorptions by -OH, -CH, and -NH groups, most organic materials can be analyzed using absorption at different wavelengths. Absorption of NIR light in transmission and reflectance follows an exponential law (Beer-Lambert) and to a first approximation the following equation can be used for reflectance measurement:

$$\log \frac{I_i}{I_r} = Kc \tag{2.1}$$

where I_i is the intensity of the incident light, I_r the intensity of the reflected light, K is the absorption coefficient and c is the concentration of the measured parameter.

It is clear that by measuring the log ratio of incident and reflected intensities at the relevant absorption bands a signal proportional to concentration would be obtained. In on-line analysis it is not possible to measure the incident light intensity and therefore at least one reference wavelength outside the region of absorption is used to approximate this. The reflected intensity at this wavelength is then *rationed* against that of the absorption, thus providing a measure of the amount of absorption irrespective of the level of illumination. A further important practical point in taking a ratio of the reference and measured signals is that factors other than concentration variations of the component under analysis affect both signals equally, and therefore cancel out in the calculation. Important examples of such factors in an industrial measurement are instrument-to-object distance, dust build-up on optical surfaces and atmospheric humidity

variations, all of which cannot be controlled in most on-line applications. This simple two-wavelength model helps to clearly describe the operation of an on-line instrument. In practice additional wavelengths are normally necessary but the principles of operation are similar. But one question remains: is it possible to separate the carbon from other substances in the wood ash when looking at the absorption?

The Impulse Radar approach

Conventional radar sends out short bursts of single-frequency (narrow band) electromagnetic energy in the microwave frequency range. Other radars step through multiple (wide-band) frequencies to obtain more information. An impulse, or a Ultra-Wide Band (UWB) radar sends *individual pulses* that contain energy over a very wide band of frequencies. The shorter the pulse, the wider the band, thereby generating even greater information. Because the pulse is so short, very little power is needed to generate the signal. An UWB radar is one having a very large bandwidth (Taylor, 1995),

$$0 \leq \frac{\Delta f}{f_c} \leq 1 \tag{2.2}$$

where Δf is the *absolute bandwidth* and f_c is the *carrier* (or *center*) *frequency*. An UWB radar is characterized to have $0.25 < \Delta f / f_c \leq 1$.

The number of applications for Ground Penetrating Radar (GPR) is quite large, see Ulriksen (1982). It is mainly used for geological surveying, detecting of pipes and other buried objects (Brunzell, 1998). The proposed on-line CIFA analyzer utilizes the principle that the unburnt carbon found in fly ash affects the transmitted signal more than the ash itself. How an electromagnetic wave travels through a media is mainly determined by two properties; the *relative permittivity* ϵ_r (or dielectric constant) and the *conductivity* σ. The dielectrical properties determine the velocity of the electromagnetic wave through the media. The conductivity of the media determines how much of the input energy that is absorbed. Both these parameters are frequency dependent.

The objective is to utilize the impulse radar system to measure the *relative permittivity* ϵ_r (or dielectric constant) and the *conductivity* σ of an ash sample. The measuring device is depicted in Figure 2.3. The measuring system is installed on the recovery chute of the precipitator where the fly ash is removed.

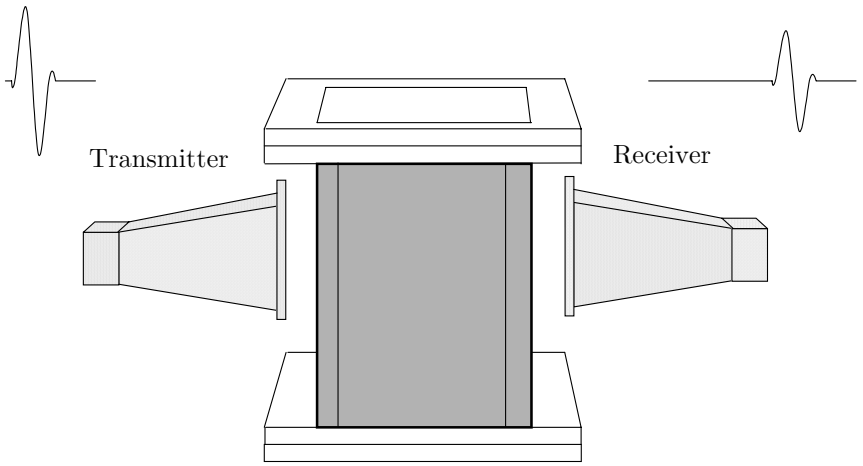

Figure 2.3: The impulse radar system for *indirect* on-line CIFA monitoring.

An impulse is sent from the transmitting horn-antenna through the ash sample and is received by another horn-antenna at the opposite side. The transmitted impulses have a very short duration of $1-10\ ns$ and a bandwidth of $100-800$ MHz.

Equipment for direct sampling at sampling frequencies necessary for this application is still expensive today, and most samplers rely on *repetitive sampling*. The impulse is transmitted several times and from each pulse one or several samples are taken. The trigger point for the sampler is delayed from pulse to pulse, such that after a number of pulses the whole waveform is sampled. The principle is shown in Figure 2.4, where 4 pulses are sampled with a sampling frequency of a fourth of the desired sampling frequency. The recorded measurement is then sent to a computer for further processing.

During one measuring cycle, the delay and attenuation of the received pulse are measured. The delay provides information about the *relative permittivity* ϵ_r of the ash sample, whereas the attenuation of the received pulse provides information about the *conductivity* σ. The ash sample collector is made of a non-conducting material. In order to obtain a representative measurement it is important that the bulk density of the ash sample in the rectangular chute is the

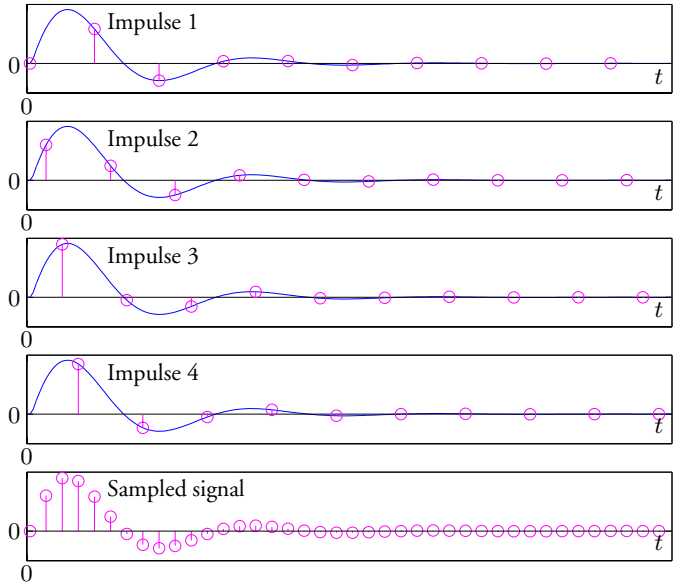

Figure 2.4: The principle of repetitive sampling.

same for each analysis. Finally, the parameters ϵ_r and σ are used to obtain the carbon content of the wood ash sample.

2.3 Summary and Concluding Remarks

There are always some unburnt remains of carbon in the ash. This is so because the combustion is not always optimal due to varying operating conditions. In this chapter two potential methods for on-line CIFA monitoring are presented. However, one disadvantage with the method of NIR spectroscopy is that only the top layer of the sample is analyzed, i.e., this layer must be representative for the whole ash sample. A good reference on instrumentation and calibration for NIR spectroscopy is Osborne et al. (1993). This reference also lists manufacturers of both laboratory and on-line equipment.

It is concluded that the presence of $Ca(OH)_2$ and $CaCO_3$ do not affect the

color of the wood ash, since these are not visible to the eye. On the other hand, this may result in gross errors in the LOI tests for fly ashes (Brown and Dykstra, 1995). It is also concluded that experimental results show that the color of the wood ash varies with different fuels used at combustion. This implies that a measuring method based on machine vision would be poor.

The prices of the today available CIFA analyzers based on microwave methods, for example, the device presented in Berthold (2000), are too expensive for the application of wood ash transformation. Also, equipment using a direct methodology based on oxidation of the ash sample is expensive (≈ 1.5 MSEK). Therefore, at present, no on-line measuring device is installed.

Hence, in Samuelsson (2002) that recently was issued by the Swedish National Board of Forestry, it is stated that there are currently *no requirements* on the wood ash carbon content. This implies that the installation of a CIFA monitoring device is needless. Instead, all wood ash is transformed into agglomerates, i.e., no ash is sorted out to be reburnt. However, an attempt to optimize the burner efficiency by increasing the oxygen ratio during combustion, and at the same time reducing the NO_X emissions by adding ammoniac to the air, has been launched and is ongoing. The usefulness of the approach is presented in Rudling (2000), but due to running-in problems in Kalmar, the benefits of the method is still to be determined.

Earlier work (Nilsson, 1993) shows that one could obtain problems to self-harden the wood ash if there is a substantial amount of unburnt carbon present. After the ash is hydrated with water, the presence of organic material (unburnt carbon) disturbs the hardening process. But hence, the method of self-hardening is not used in the ash transformation process presented in this thesis. Instead a new method is developed for automated dehydration of the produced agglomerates, which enables immediate packing and distribution; the details are given in Chapter 7.

Chapter 3

Wood Ash Hydration - Empirical Modeling

Mixing ash/dolomite/water in order to obtain granular material is one method to stabilize wood ashes. The main problem is predicting the quantity of water to be added, since the necessary amount varies with the wood ash quality (Nordenberg, 1996, Sundqvist, 1999, Windelhed, 1998b). In Sundqvist (1999) it is reported that the critical water-to-ash ratio varies between ash types and must therefore be determined for each ash. However, one possible solution is to measure the mixture viscosity and study whether this parameter can be used to control the amount of added water. In this thesis, a novel method is presented where the viscosity is continuously estimated in the batch mixing process. The viscosity is estimated by measuring the normalized effective power $P_e(t)$, which represents the rate of useful work being performed by the three-phase asynchronous machine used as stirrer drive. In this chapter, an empirical model of the viscosity dynamics is developed.

First, an introduction to the general problems are given, followed by a survey of some topics in *system identification* available for the reader unfamiliar with the topic. Next, the experimental setup and the results from the first and second stage experiments are presented, and the chapter ends with a summary and concluding remarks. The reader is encouraged to go back to Figure 1.4, if a reminder is necessary of the different stages in the ash transformation process.

For the mixing of the ash, ETEC-dolomite and water, a `Fejmert S-500` mixer

is utilized, see Appendix B. The dolomite and ash are mixed in the first step. The ratio between the two dry matters are always the same. The next step is to add water to start the Wood Ash Hydration (WAH). By measuring the normalized effective power $P_e(t)$ a good estimate of the mixture viscosity is obtained; this measurement provides information how to control the variable water flow. After the ash hydration is completed the mixture of ash, dolomite and water is transformed into agglomerates using a roll-pelletizer described in Chapter 5. After this is carried through, the mixer has to be cleaned. Therefore, a *high-pressure cleaning procedure* is provided to prevent any superstructure within the mixer. During this procedure a dust preventing system (see Appendix B) is controlled so that an underpressure is introduced into the mixer. This will seal the mixer so that no water is leaking out. After the cleaning procedure is finished, the mixer is ready to mix a new batch.

3.1 System Identification

The notion of a mathematical model is fundamental to science and engineering. A model is a very useful and compact way to summarize the knowledge about a process. The process models can sometimes be obtained from first principles of physics. It is more difficult to get the model of the disturbances, which is equally important. These models often have to be obtained from experiments. The types of models that are most often used are *state-space models* (internal models) and *input-output models* (external models). The models for the disturbances are in most cases for the internal models given as a dynamic system driven by white noise. For the external models the disturbances are often given in terms of *spectral densities* and *covariance functions*. Models for disturbances can, however, only rarely be determined from the first principles. Thus, experiments are often the only way to get models for the disturbances.

A process cannot be characterized by *one* mathematical model. A process should be represented by a *hierarchy* of models ranging from detailed and complex simulation models to very simple models, which are easy to manipulate analytically. The simple models are used for exploratory purposes and to obtain the gross features of the system behavior. The complicated models are used for a detailed check of the performance of the control system. The complicated models take a long time to develop. Between the two extremes, there may be many different types of models.

There are no general methods that always can be used to get a complete mathematical model. Each process or problem has its own characteristics. Some general guidelines can be given, but under no circumstances can they replace experience. Model building using physical laws requires knowledge and insight about the process.

In most cases it is not possible to make a complete model only from physical knowledge. Some parameters must be determined from experiments. This approach is called *system identification*, and the following discussion is inspired by Åström and Wittenmark (1997), Ljung (1987), Söderström and Stoica (1989) and Johansson (1993).

The System Identification Procedure

The identification process amounts to repeatedly selecting a model structure, computing the best model in the structure, and evaluating the properties of this model to see if they are satisfactory. The cycle run as follows (Ljung, 1987):

1. Design an experiment and collect input and output data from the process to be identified.
2. Examine the data. Some pre-treatment may have to be applied. Use the first half of data for identification, and the second half for validation.
3. Select a model structure.
4. Compute the best model in the model structure according to the input, output and the given criterion of fit.
5. Examine the properties of the model obtained.
6. If the model is good enough then stop, otherwise go back to the third step and try another model set. Other estimation methods can also be performed (fourth step), further pre-treatment can be applied to the data (first and second step).

System identification is thus the experimental approach to process-modeling as indicated by Figure 3.1, and includes *experimental planning*; *selection of model structure*; *parameter estimation* and *model validation* (Ljung, 1987).

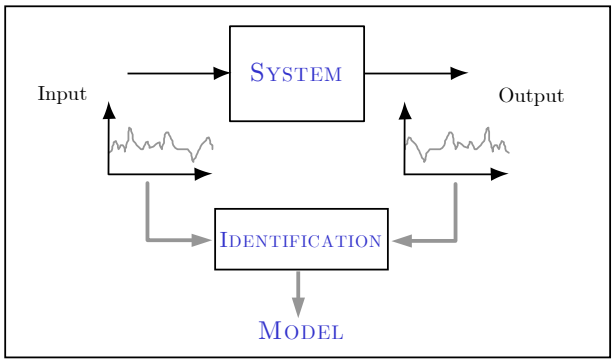

Figure 3.1: The approach of system identification for process-modeling.

When investigating a process where the *a priori* knowledge is poor, it is reasonable to start with transient or frequency-response analysis to get crude estimates of the dynamics and disturbances. The results can then be used to plan further experiments.

Experimental Planning

It is often difficult and costly to experiment with industrial processes. Therefore, it is desirable to have identification methods that do not require special input signals. Many "classic" methods depend strongly on having the input to be of a precise form, e.g., sinusoid or impulse. Other techniques can handle virtually any type of input signals at the expense of increased computations. One requirement of the input signal is that it should excite all process modes of interest sufficiently.

It is sometimes possible to base system identification on data obtained under closed-loop control of the process. This is very useful from the point of view of applications. For instance, adaptive controllers are based mostly on closed-loop identification. The main difficulty with data obtained from a process under feedback is that it may be impossible to determine the parameters in the desired model, i.e., the system is not identifiable, even if the parameters can be determined from an open-loop experiment. Identifiability can be recovered if the feedback is sufficiently complex. It helps to make the feedback nonlinear and time-varying, and to change the set points.

Model Structures

The *model structures* are derived from prior knowledge of the process and the disturbances. In some cases the only priori knowledge is that the process can be approximated by a linear system in a particular operating range. It is then natural to use general representations of linear systems. Such representation are called *black-box models*. An example of a generalized model structure is:

$$A(q)y(k) = \frac{B(q)}{F(q)}u(k) + \frac{C(q)}{D(q)}e(k) \tag{3.1}$$

where u is the input, y is the output, and e is a white noise disturbance and q is the *forward-shift operator.* The parameters, as well as the order of the models, are considered as unknown. Depending on which of the five polynomials A, B, C, D and F are used, different model-structures will arise. The AutoRegressive with eXternal input (ARX) model structure, which uses the polynomials A and B in (3.1), is linear in the unknown parameters, but for example, in the AutoRegressive Moving Average with eXternal input (ARMAX) structure, which utilizes the polynomials A, B and C in (3.1), the output can not be written as a linear regression.

Parameter Estimation Methods

Solving the parameter estimation problem requires *input-output data* from the process*; a class of models* and *a criterion.* Parameter estimation can then be formulated as an optimization problem, where the best model is the one that best fits the data according to the given criterion. The results of the estimation problem depends, of course, on how the problem is formulated. For instance, the obtained model depends on the amplitude and frequency content of the input signal. There are many possibilities for combining experimental conditions, model classes and criteria. There are also many different ways to organize the computations. Consequently, there is a large number of different identification methods available. One broad distinction is between *on-line methods* and *off-line methods.* The on-line method gives estimations *recursively* when the measurements are obtained and is the only alternative if the identification is going to be used in an adaptive controller or if the process is time-varying. In many cases the off-line methods give estimates with higher precision and are more reliable, for instance in terms of convergence. This is due to the fact that an off-line formulation is a simpler problem to solve.

Criteria

When formulating an identification problem, a criterion is introduced to give a measure of how well a model fits the experimental data. The criteria can be postulated. By making statistical assumptions it is also possible to derive criteria from probabilistic arguments. The criteria for discrete-time systems are often expressed as:

$$J(\boldsymbol{\theta}) = \sum_{k=1}^{N} g(\varepsilon(k)) \tag{3.2}$$

where $\boldsymbol{\theta}$ is a vector of unknown parameters, ε is the input error, the output error, or a *generalized error*. The prediction error is a typical example of a generalized error. The function g is frequently chosen to be quadratic, but it is possible for it to be of many other forms.

The first formulation, solution, and application of an identification problem where given by Gauss in his famous determination of the orbit of the asteroid Ceres (Gauss, 1963). Gauss formulated the identification problem as an *optimization* problem and introduced the principle of least squares, a method based on the minimization of the sum of the squares of the error. Since then, the least-squares criterion has been used extensively. The *least-squares method* is simple and easy to understand. Under some circumstances it gives estimates with the wrong mean values (bias). However, this can be overcome by using various extensions. The least-square method is restricted to model structures where the output can be written as a *linear regression*. For a description of identification of other systems, good references are Ljung (1987), Söderström and Stoica (1989) and Johansson (1993).

When the disturbances of a process are described as a stochastic process, the identification problem can be formulated as a statistical parameter-estimation problem. It is then possible to use the *maximum-likelihood method*. This method has many attractive statistical properties. It can be interpreted as a least-square criterion if the quantity to be minimized is taken as the sum of squares of the prediction error. The maximum-likelihood method is a general technique that can be applied to a wide variety of model structures.

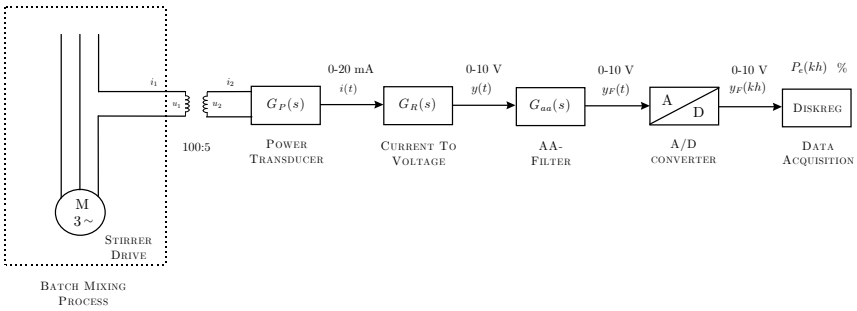

Figure 3.2: The setup used for measurement.

Model Validation

When a model has been obtained from experimental data, it is necessary to check the model in order to reveal its inadequacies. For *model validation*, it is useful to determine such factors as step responses, impulse responses, poles and zeros, model errors, and prediction errors. It is also a good approach to use another set of experimental data to validate the model. If the model does not pass the validation test, it must be revised i.e., we loop in the system identification procedure until a proper model is obtained. Since the purpose of the model validation is to scrutinize the model with respect to inadequacies, it is useful to look for quantities that are sensitive to model changes.

3.2 Experimental Setup

Measurement System

In Svantesson et al. (2000), the viscosity is estimated in the batch mixing process by measuring the normalized effective power $P_e(t)$, which represents the rate of useful work being performed by the three-phase asynchronous machine used for the stirrer drive. The measurement system used in the experimental setup is depicted in Figure 3.2.

One of three phases to the motor is connected to the primary side of a 100:5 current transformer. The secondary side of the transformer is connected to a power transducer, the load measurement EL-FI G3 power meter (ELFI, 1999), that electronically measures the input power to the asynchronous machine and

compensates for the internal losses in the induction motor. Thus, the transducer compensates for variations in the mains voltage and always estimates the actual power applied on the motor shaft. The electrical output from the transducer is a direct current $0 - 20\ mA$ and the dynamics $G_P(s)$ are given by the transfer function

$$G_P(s) = \frac{K}{sT + 1} \tag{3.3}$$

where K and T are user-adjustable parameters. The current from the power transducer is converted into a voltage of $0 - 10\ V$ with $G_R(s) = R = 500$ Ω. The anti-aliasing filter is a third order Butterworth-filter with a cut-off frequency of $3\ Hz$

$$G_{aa}(s) = \frac{1}{(\beta s + 1)\left(\beta^2 s^2 + \beta s + 1\right)} \tag{3.4}$$

where $\beta = (6\pi)^{-1}$. The filtered signal $y_F(t)$ is A/D-converted and stored in `DISKREG`, a software package developed at the Department of Technology for real-time data acquisition and control. During the experiments, the sample time $h = 0.1\ s$ is used, but preceding further processing the input and output signals are resampled to the sample time $h = 1\,s$ by decimation. The power transducer is calibrated so that a voltage of $10\ V$ corresponds to full load, i.e. in `DISKREG` the range $0 - 10\ V$ is interpreted as $0 - 100\%$ of the maximum effective power $P_e(t)$.

Actuator

The objective is to detect when $P_e(t)$ has reached the level P_e^{crit}, which represents the target mixture viscosity; hence, if more water is added in the hydration process after P_e^{crit} has been reached, one will obtain a mixture useless for agglomeration. The process input signal to be controlled is the water flow $Q(t)$. Here it is crucial that the water is distributed over a wide area, yielding a homogenous mixture (Svantesson, Lauber and Olsson, 1998). To achieve this, spray nozzles and an on/off control valve are adopted. An illustration of the actuator in the experimental setup is shown in Figure 3.3.

As previously, `DISKREG` is used but here as an input signal generator. The generated signal $u(kh)$ is D/A-converted and the Voltage/Pulse converter transforms the DC voltage into a proportional pulse frequency. Furthermore, an off-delay

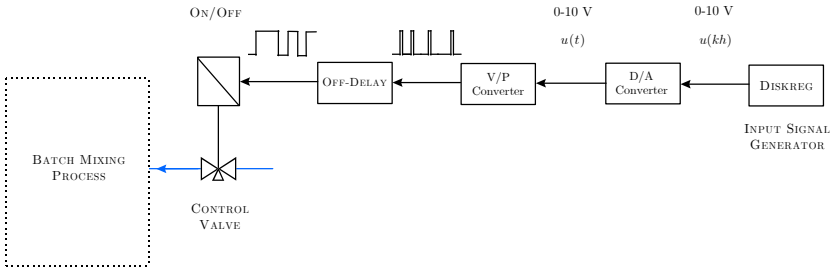

Figure 3.3: The setup used to generate the input signal.

is incorporated in such way that a continuously open valve is obtained if $u(t)$ attains its maximum value. The time between the generated pulses increases with decreasing input voltage $u(t)$. The water flow $Q(t)$ to the WAH process is thus a linear function of the input voltage $u(t)$

$$Q(t) = f(u(t)) = u(t)k_1k_2Q_{\max} \tag{3.5}$$

where $u(t)$ is the input voltage (V), k_1 $(pulse/sV)$ is a constant that converts the input voltage into the corresponding pulse frequency, k_2 $(s/pulse)$ is the applied off-delay and $Q_{\max}$ $(liter/s)$ is the maximal available flow of water. By using this approach, the flow of water is controlled with good precision and we comply with the constraints regarding a fine spray of water as input to the WAH process. A photograph of the experimental setup is shown in Figure 3.4.

3.3 First Stage Experiment

A standard procedure of identification is to start with some *first stage experiments*, which include simple experiments followed by continued experiments (*second stage experiments*). For a first stage experiment some simple input signal could be used. Dominating time constants in the output response and low-frequency noise can be evaluated from, for example, a step/pulse response. The first stage experiments are carried out with different amplitudes in order to determine the operating range of a *linear model*. The experimental conditions for the first stage experiment are selected to be

$$\mathcal{H} : u \text{ is a } \textit{pulse sequence}\text{; each pulse has an amplitude of } \gamma \cdot 10\% \tag{3.6}$$

Figure 3.4: The experimental setup. The software `DISKREG` is used for data acquisition.

where γ is an integer. The measurement of the normalized effective power $P_e(t)$ is only available as periodic observations of $P_e(t)$ sampled with a time interval h (the sampling period). Let the values of $P_e(t)$ be represented by a sequence

$$\{P_e(k)\}_{k=0}^{\infty}; \quad P_e(k) = P_e(kh) \quad \text{for } k = 0, 1, \ldots \tag{3.7}$$

then the measurement of $P_e(k)$ can be expressed as

$$P_e(k) \quad \stackrel{\text{def}}{=} \quad y(k) = x(k) + v(k) = g(k) * u(k) + v(k) \tag{3.8}$$

where $y(k)$ is an observation of a variable $x(k)$, the convolution of the system input $u(k)$ with the systems' impulse response $g(k)$ corrupted by a variable $v(k)$, which is some external input that represents disturbances. The raw input-output data from the first stage experiment is shown in Figure 3.5. Here the sample time $h = 0.1\ s$ is used. In the figure it is seen that the process has "slow dynamics", which implies that the dynamics of the power transducer and anti-aliasing filter can be neglected. Due to the slow dynamics, the input and output are resampled to $h = 1\,s$ by decimation; the decimation is preceded by pre-filtering. By observing the figure and disregarding the initial behavior (caused by gearbox oil heat-up in the stirrer drive, which implies a decreased resistance), it may be inferred that the system has positive gain and no time-delay. This

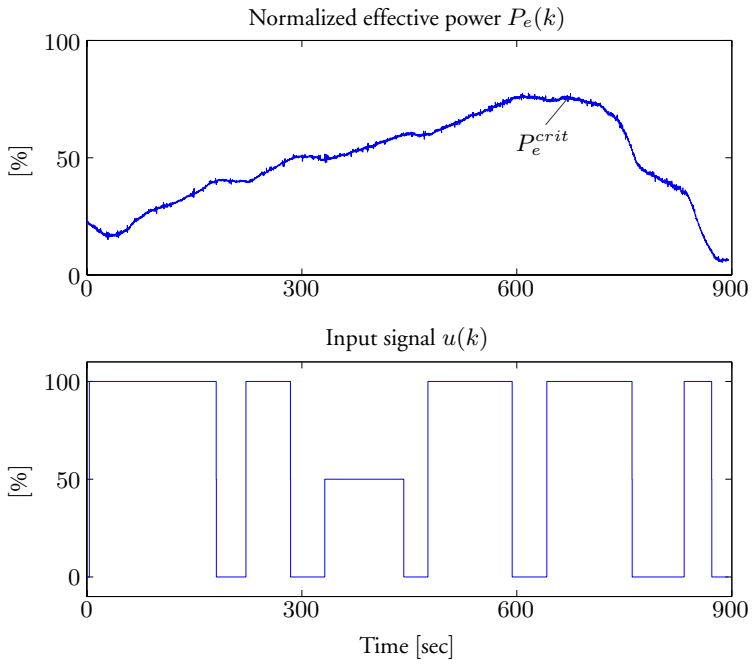

Figure 3.5: Raw input-output data from the first stage experiment.

description of the system is valid up to $t \approx 700\ s$ when the critical effective power P_e^{crit} is reached. Then the mixture viscosity changes and the normalized effective power decreases rapidly giving a mixture useless for granulation.

Test of Linearity

The *coherence spectrum* is particularly interesting as a test of linearity in an input-output relationship. If it is assumed that (3.8) is valid, then the quadratic coherence spectrum between the two signals u and y is defined as the ratio

$$C_{uy}^2(\omega) = \frac{|\Phi_{uy}(i\omega)|^2}{\Phi_{uu}(i\omega)\Phi_{yy}(i\omega)} \tag{3.9}$$

where Φ_{uy} is the *cross-spectrum*, Φ_{uu} and Φ_{yy} are the *autospectra* of the input u and output y respectively. To see that the quadratic coherence always takes

on a value in the interval $0 \leq C_{uy}^2(\omega) \leq 1$, we use that $\Phi_{uu} \in \mathrm{R}$ and rewrite equation (3.9) as

$$\begin{aligned} C_{uy}^2(\omega) &= \frac{\left|\Phi_{uy(i\omega)}\right|^2}{\Phi_{uu}(i\omega)\Phi_{yy}(i\omega)} = \frac{\left|G(i\omega)\right|^2 \Phi_{uu}^2(i\omega)}{\Phi_{uu}(i\omega)\Phi_{yy}(i\omega)} \\ &= \frac{\left|G(i\omega)\right|^2 \Phi_{uu}^2(i\omega)}{\Phi_{uu}(i\omega)\left(\left|G(i\omega)\right|^2 \Phi_{uu}(i\omega) + \Phi_{vv}(i\omega)\right)} \end{aligned} \tag{3.10}$$

which can be rewritten as

$$C_{uy}^2(\omega) = \frac{\left|G(i\omega)\right|^2}{\left|G(i\omega)\right|^2 + \frac{\Phi_{vv}(i\omega)}{\Phi_{uu}(i\omega)}} = \frac{1}{1 + \frac{\Phi_{vv}(i\omega)}{\left|G(i\omega)\right|^2 \Phi_{uu}(i\omega)}} \tag{3.11}$$

From (3.11) it is concluded that the quadratic coherence always takes on a value in the interval $0 \leq C_{uy}^2(\omega) \leq 1$, with a value close to one in the frequency range where the noise level is low ($\Phi_{vv} \ll \Phi_{uu}$) and if the system is linear (Johansson, 1993). The coherence function may thus be viewed as a type of correlation function in the frequency domain. Using the data set $Z^{100-700} = \{y(k), u(k)\}_{k=100}^{700}$, the coherence function estimate $\hat{C}_{uy}^2(\omega)$ is calculated and shown in Figure 3.6. The coherence spectrum with coherence close to 1 for frequencies up to $0.03\,Hz$ verifies that there is a satisfactory coherence between the two signals. This gives promise of successful identification with a linear model. Since a linear input-output relationship is observed in Figure 3.5, it may also be inferred that the noise level is larger, i.e., the magnitude of the input autospectrum Φ_{uu} is smaller for frequencies above $0.03\,Hz$. The results shown in Figure 3.6 should however be interpreted with caution since the viscosity dynamics seem to be time-varying.

The content of unburnt carbon that is present in the wood ash is the main parameter that determines the wood ash quality. For each experimental batch, the wood ash carbon content is determined by using the test of LOI (*Swedish Standard: SS 02 81 13*, 1981). Six repeated samples are taken from the batch used in the first stage experiments and a confidence interval for the asymptotic distribution is calculated using the *Student's t-distribution*

$$\mu^* \pm t_{(n-1)_{\alpha/2}} \frac{\sigma^*}{\sqrt{n}} \tag{3.12}$$

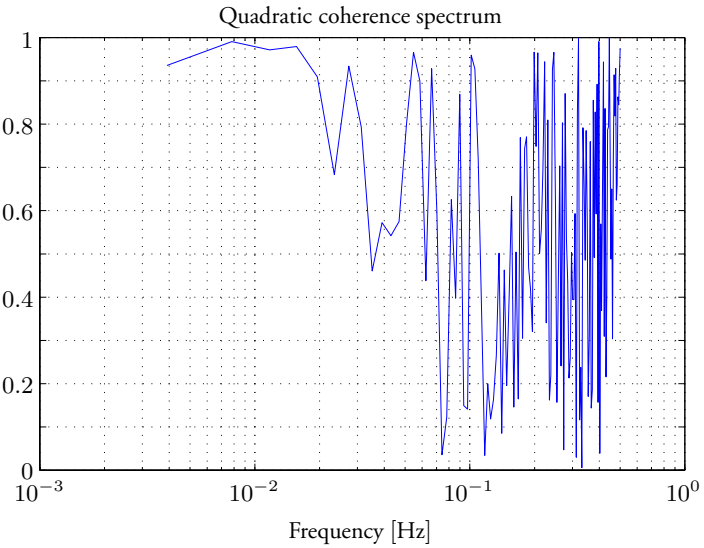

Figure 3.6: Empirical coherence spectrum $\hat{C}^2_{uy}(\omega)$.

where μ^* is the *estimated mean* of the n collected samples from the population, $n-1$ is the *degrees of freedom*, α is the *significance level* and σ^* is the *estimated standard deviation*. For the batch used in the first stage experiment, a 95%-confidence interval for the asymptotic distribution of the wood ash carbon content is 51.4 ± 0.8 % of unburnt carbon.

3.4 Estimating Process Dynamics

There may of course be several reasons why a model of a dynamical systems is sought. A common one is that the model is needed to design a regulator for the system. It is then important that available design variables are chosen so that the resulting model becomes as appropriate as possible for the control design. Originally, the idea was to fit the dynamics of the WAH process to a parametric model and to construct a model of the model errors that are present in the nominal model. This procedure is called *model error modeling* (Ljung, 1999). When the error models are linear, it is preferable to present the nominal model uncertainties in frequency domain. This approach is however not successful due to the fact that the process dynamics of the WAH are time-varying. Therefore, it is necessary to estimate a model on-line at the same time as the input-output

data is received. The measurement of $P_e(k)$ can be expressed as

$$P_e(k) \quad \stackrel{\text{def}}{=} \quad y(k) = \boldsymbol{\varphi}^T(k,d)\boldsymbol{\theta}(k) + e(k) \tag{3.13}$$

where $\boldsymbol{\theta}(k)$ is a parameter vector containing the system parameters, d is the delay of the system, $\boldsymbol{\varphi}^T(k,d)$ is the regression vector and $e(k)$ is additive white noise. The estimated model parameters are expressed as a parameter vector $\hat{\boldsymbol{\theta}}$,

$$\hat{\boldsymbol{\theta}} = \begin{bmatrix} \hat{a}_1 & \cdots & \hat{a}_{na} & \hat{b}_1 & \cdots & \hat{b}_{nb} \end{bmatrix}^T \tag{3.14}$$

where na and nb are the orders of the process denominator/numerator polynomials $A(q)$ and $B(q)$ respectively, c.f. equation (3.1). With a given time delay d, the regression vector $\boldsymbol{\varphi}$ can be written as

$$\boldsymbol{\varphi}(k,d) = [-y_f(k-1) \ \cdots \ -y_f(k-n_a) \ u_f(k-1-d) \ \cdots \ u_f(k-n_b-d)]^T \tag{3.15}$$

where y_f and u_f are the filtered process output and input values

$$y_f(k) = L(q)y(k) \qquad u_f(k) = L(q)u(k) \tag{3.16}$$

Here $L(q)$ is a suitable pre-filter (data-filter); see Section 3.A. The regressor $\boldsymbol{\varphi}$ is used to estimate the parameter vector $\hat{\boldsymbol{\theta}}$, and the required least-square equations are (Ljung, 1987)

$$\begin{aligned} \hat{\boldsymbol{\theta}}(k) &= \hat{\boldsymbol{\theta}}(k-1) + \mathbf{K}(k)\left[y_f(k) - \boldsymbol{\varphi}^T(k,d)\hat{\boldsymbol{\theta}}(k-1)\right] \\ \mathbf{K}(k) &= \mathbf{P}(k)\boldsymbol{\varphi}(k,d) = \frac{\mathbf{P}(k-1)\boldsymbol{\varphi}(k,d)}{\lambda + \boldsymbol{\varphi}^T(k,d)\mathbf{P}(k-1)\boldsymbol{\varphi}(k,d)} \\ \mathbf{P}(k) &= \frac{1}{\lambda}\left[\mathbf{P}(k-1) - \frac{\mathbf{P}(k-1)\boldsymbol{\varphi}(k,d)\boldsymbol{\varphi}^T(k,d)\mathbf{P}(k-1)}{\lambda + \boldsymbol{\varphi}^T(k,d)\mathbf{P}(k-1)\boldsymbol{\varphi}(k,d)}\right] \end{aligned} \tag{3.17}$$

where $\mathbf{P}$ is the parameter covariance matrix, $\mathbf{K}$ the gain matrix, and λ a forgetting factor. The Recursive Least Square (RLS) parameter estimator is implemented in `C-code` and incorporated in `SIMULINK S-functions` (Svantesson, 1997, MathWorks, 1998). The implemented algorithm uses the Bierman UD covariance factorization update, which is well suited for real-time implementation (Bierman, 1977). For more details on the algorithm, see Section

3.B. If the input sequence $u(k)$ of the first stage experiment is regarded to be sufficiently exciting, the RLS could be applied to this input-output data with different orders of an ARX model structure. To determine if the input is of sufficient complexity, the criterion of persistent excitation is used.

Definition 3.1 (Persistency of excitation) (Johansson, 1993, Åström and Wittenmark, 1995).

A signal u fulfils the condition of Persistent Excitation (PE) of order n if the following limits exist

$$m_u = \lim_{N\to\infty} \frac{1}{N} \sum_{k=1}^{N} u(k) \tag{3.18}$$

$$r_{uu}(\tau) = \lim_{N\to\infty} \frac{1}{N} \sum_{k=1}^{N} u(k-\tau)u(k) \tag{3.19}$$

and if the correlation matrix

$$\widehat{\mathbf{R}}_{uu}(n) = \begin{bmatrix} \hat{r}_{uu}(0) & \hat{r}_{uu}(1) & \cdots & \hat{r}_{uu}(n-1) \\ \hat{r}_{uu}(-1) & \hat{r}_{uu}(0) & \cdots & \hat{r}_{uu}(n-2) \\ \vdots & \vdots & \ddots & \vdots \\ \hat{r}_{uu}(1-n) & \hat{r}_{uu}(2-n) & \cdots & \hat{r}_{uu}(0) \end{bmatrix} \tag{3.20}$$

is *positive definite* (See Appendix A). □

Persistent excitation of order n is sufficient to obtain consistent estimates of n parameters with the least-squares method. From the definition it is thus concluded that the input signal of the first stage experiment is PE of at least order 6.

The criteria to decide the best model order was selected as minimization of the mean square of the estimation error (Ljung and Söderström, 1983)

$$V_N(\hat{\boldsymbol{\theta}}) = \frac{1}{N} \sum_{k=1}^{N} \varepsilon^2(k) \tag{3.21}$$

where

$$\varepsilon(k) = L(q)y(k) - \boldsymbol{\varphi}^T(k,d)\hat{\boldsymbol{\theta}}(k-1) \tag{3.22}$$

Model set	na	nb	nk	$V_N(\hat{\boldsymbol{\theta}})$
$Ay = Bu + e$	1	1	1	0.3182
	2	1	1	0.1690
	2	2	1	0.1663
	3	1	1	0.1844
	3	2	1	0.2079
	3	3	1	0.2264

Table 3.1: Numerical values of the loss function $V_N(\hat{\boldsymbol{\theta}})$ for different ARX models when the RLS is applied to the data-set obtained from the first stage experiment. The strange result (increasing loss for increasing model order) may be caused by the abrupt change in the process dynamics since, in general, the convergence of the RLS is slower for a higher model order.

The values of the loss function (3.21) for different model orders are shown in Table 3.1. Notice that $nk = d + 1$. Here, a low-pass data-filter

$$L(q) = \frac{1 - f}{q - f} \tag{3.23}$$

with $f = 0.9$ is used. In the table it is observed that the loss function is minimized for a second order ARX model. However it may be useful to select a structure with $na = 2$, $nb = 1$ and $nk = 1$. When inspecting the input-output data shown in Figure 3.5 it may be inferred that the gain of the system switches sign when the mixture viscosity begins to decrease. If this structure is selected, the model may better capture this property. The reason is that if $nb = 2$, two parameters of small magnitude are identified in the numerator polynomial, whereas if nb is chosen to be one, this yields only one parameter to estimate in the B polynomial. As a result, an abrupt change of the system gain will be easier to track.

3.5 Second Stage Experiment

The second stage of experiments is characterized by a systematic design and execution of suitable experiments. These experiments were carried through at randomly selected occasions during a period of two months, in order to identify models for different wood ash qualities. A Pseudo Random Binary Sequence

(PRBS) was used as an input signal during the identification experiments. This signal is implemented for example as

$$u(k) = 0.5(u_1 + u_2) + 0.5(u_1 - u_2)sign(w(k)) \tag{3.24}$$

where $w(k) \in [-1, 1]$ is a sequence of uniformly distributed random numbers, for example computer generated. The actual shape of the input signal should however be adapted to the application. The viscosity dynamics are typically slow, which implies that (3.24) must be modified so that the normalized effective power $P_e(t)$ is able to change adequately during two amplitude switches of the input sequence $u(k)$. This is achieved by only allowing the input sequence to change amplitude each N^{th} sample interval (called the *basic period*). With $u_1 = a$ and $u_2 = -a$ the correlation function for the PRBS sequence with basic period N can be shown to be (Söderström and Stoica, 1989)

$$r_{uu}(\tau) = \begin{cases} a^2 \frac{N-|\tau|}{N} & , \tau = 0, \pm 1, \ldots \pm N \\ 0 & , \ |\tau| > N \end{cases} \tag{3.25}$$

with the spectral density function

$$\Phi_{uu}(\omega) = \frac{a^2}{2\pi} \frac{1}{N} \frac{1 - \cos N\omega}{1 - \cos \omega} \tag{3.26}$$

As seen in (3.26) an input signal with most of its energy located in the low frequency range is obtained if N is large. This will excite the modes of the system that corresponds to slow dynamics. In the second stage experiments, N is selected to be 600.

An example of process input-output data and the convergence of the estimated parameters are shown in Figure 3.7. The figure clearly shows that the process dynamics are time-varying. For the experiment presented in Figure 3.7, a 95%-confidence interval for the asymptotic distribution of the batch wood ash carbon content is 40.9 ± 0.3 % of unburnt carbon. The second stage experiments yield the following physical interpretation of the viscosity dynamics, which also supports the results obtained in Table 3.1: since the mixture is accumulating water, an integrator is to be found in the process dynamics. Further, a time-constant is present, which depends on how the water is "diffused" into the mixture; in the beginning of the WAH procedure the dry mixture absorbs water fast, whereas at the end the mixture becomes more and more saturated

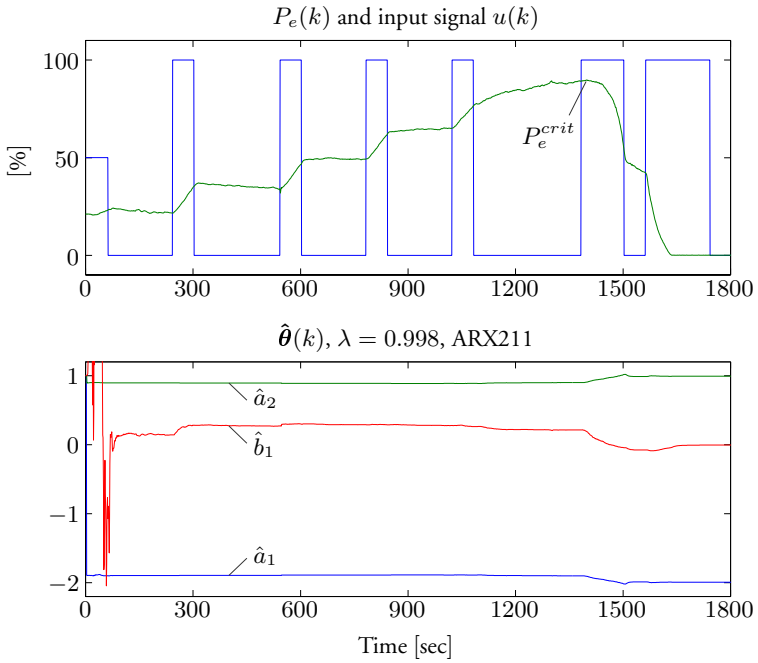

Figure 3.7: A selected second stage experiment. Here a PRBS is used as an input sequence. In the lower plot, the convergence of three parameters in a second order ARX model identified with RLS is shown.

and is not able to absorb water as fast as in the beginning. From a system perspective, the gradual saturation of the mixture is explained as a time-varying time-constant, i.e., the time constant corresponds to a mode that decreases in speed. This implies that the system will, eventually, become a double integrator. Hence, this heuristic discussion is extended in Chapter 4.

For each experiment, it is observed that the estimated process gain $\hat{b}_1$ switches sign (c.f. Figure 3.7) when the mixture viscosity begins to decrease. This property may be used to disable any control action during the WAH procedure. Further, there are strong indications that it is not only the accumulated quantity of water that is related to the instant when the process gain changes. In addition, this instant is also affected by the applied flow of water $Q(t)$ and the wood ash quality (Nordenberg, 1996, Sundqvist, 1999, Windelhed, 1998b).

3.6 Summary and Concluding Remarks

In this chapter, the mixture viscosity of the ash/dolomite/water is estimated by measuring the normalized effective power $P_e(t)$, which represents the rate of useful work being performed by the three-phase asynchronous machine used as stirrer drive. It is shown that this measurement is well suited for control of the amount of added water to the WAH process. A second order ARX model structure has been selected and a RLS parameter estimator is applied to estimate the time-varying dynamics. By using this approach, it is possible to track variations in the process dynamics due to varying wood ash quality.

It should be noticed that the selected ARX model could be exchanged for an identified Output Error (OE) model. The OE model structure is motivated by the interpretation that the random disturbances visible in $P_e(k)$ are caused by the stirrer, which is a part of the sensor (motor + stirrer). The sensor monitors the mixture viscosity, i.e., the random fluctuations are interpreted as measurement noise. However, the models identified with RLS map the true measurement of $P_e(k)$ with good agreement in *deterministic simulations* (Johansson, 1993). This implies that the relation between the process input and output is well defined, i.e., the prediction of the normalized effective power $P_e(k)$ is not built upon old values of $P_e(k)$ only. This make the model most adequate for control of the WAH process.

Furthermore, there are strong indications that it is not only the accumulated quantity of water that is related to the instant when the process gain changes. In addition, this instant is also affected by the applied flow of water $Q(t)$ and the quality of the wood ash. A solution for a fast detection of the abrupt change in the process dynamics is presented in Chapter 4.

Appendix

3.A Choice of Data-filter

The system description is given in the form

$$y(k) = G(q^{-1}, \boldsymbol{\theta})u(k) + H(q^{-1}, \boldsymbol{\theta})e(k) \tag{3.A.1}$$

as the basic description of a linear system subject to additive random disturbances. Here

$$G(q^{-1},\boldsymbol{\theta}) = \frac{B(q^{-1})}{F(q^{-1})} = \frac{b_1 q^{-1-d} + b_2 q^{-2-d} + \cdots + b_{nb} q^{-nb-d}}{1 + f_1 q^{-1} + \cdots + f_{nf} q^{-nf}} \quad (3.A.2)$$

and

$$H(q^{-1},\boldsymbol{\theta}) = \frac{C(q^{-1})}{D(q^{-1})} = \frac{1 + c_1 q^{-1} + \cdots + c_{nc} q^{-nc}}{1 + d_1 q^{-1} + \cdots + d_{nd} q^{-nd}} \quad (3.A.3)$$

and $\{e(k)\}$ is a sequence of independent random variables with zero mean value and variance σ_e^2. For the case of an ARX model $G = B/A$ and $H = 1/A$. In this section we will explain and affect the distribution of the bias

$$G(e^{i\omega},\boldsymbol{\theta}^*) - G_0(e^{i\omega}) \quad (3.A.4)$$

where $G_0(e^{i\omega})$ is the true transfer function and $G(e^{i\omega},\boldsymbol{\theta}^*)$ is the limiting estimate of G. The case of most practical interest is probably to study the fit between $G(e^{i\omega},\boldsymbol{\theta}^*)$ and $G_0(e^{i\omega})$. It is natural to consider the bias distribution of G to be the most important issue, since closed-loop stability of a regulator design will depend on the accuracy of G. The limiting parameter estimate is given by Ljung (1987)

$$\boldsymbol{\theta}^* = \lim_{N\to\infty} \hat{\boldsymbol{\theta}}_N = \arg\min_{\boldsymbol{\theta}} \int_{-\pi}^{\pi} \left|G_0(e^{i\omega}) - G(e^{i\omega},\boldsymbol{\theta})\right|^2 \underbrace{\frac{\Phi_u(\omega)}{\left|H(e^{i\omega},\boldsymbol{\theta})\right|^2}}_{Q(\omega,\boldsymbol{\theta})} d\omega \quad (3.A.5)$$

This means that $Q(\omega,\boldsymbol{\theta})$ will be taken as the weighting function that determines the *bias distribution.* This bias distribution can in turn be affected by properly selecting the

Input spectrum $\Phi_u(\omega)$.	Noise model set.
Prefilter $L(q)$.	Prediction horizon k.

Notice that it is only the ratio $\Phi_u/|H|^2$ that determines the bias distribution; the values of the individual functions Φ_u and H are immaterial. If, for instance the input and output are filtered with the pre-filter

$$y_f(k) = L(q)y(k) \qquad u_f(k) = L(q)u(k) \quad (3.A.6)$$

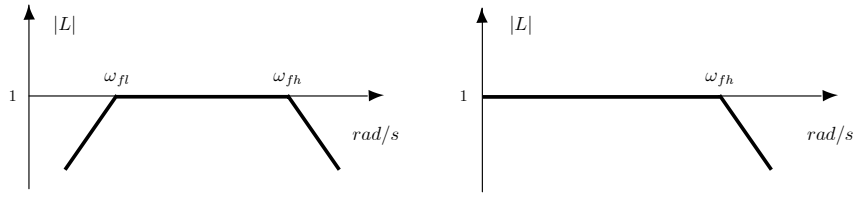

Figure 3.1: The amplitude curve of the bandpass filter (left) and the low pass filter (right).

this will affect the weighting function and the actual weighting function $Q(\omega, \boldsymbol{\theta})$ obtained is

$$\left|L(e^{i\omega})\right|^2 \cdot Q(\omega, \boldsymbol{\theta}) \tag{3.A.7}$$

To identify a system with non-zero mean one can, for example, remove the average value of the signals before they are used in the estimator to obtain a correct model. In recursive methods it is difficult to remove average values. An approach that works for signals with non-zero mean and drifting signals is to differentiate the signals, i.e. to multiply the regressor with $q - 1$. As differentiated signals are quite noisy, it is a good idea to low-pass filter the differentiated signals. Low-pass filtering also removes the undesired high frequency dynamics. A suitable data-filter is then (Åström and Wittenmark, 1995)

$$L(q) = \frac{(q-1)(1-f)}{q-f} \tag{3.A.8}$$

With this filter a disturbance will be removed from the data, except for components in the frequency interval $(\omega_{fl}, \omega_{fh})$ where ω_{fl} is the lower break frequency and ω_{fh} is the upper break frequency for the data-filter, see Figure 3.1. The estimator will thus not be confused by low frequency drift. But hence, if ω_{fh} is too high, the estimator may attempt to fit the model at too high frequencies. Since it is assumed that no low frequency drift is present in the WAH process, a simple low-pass filter

$$L(q) = \frac{1-f}{q-f} \tag{3.A.9}$$

is implemented as data-filter. See Figure 3.1. Using a low pass filter as data-filter gives a good low frequency fit.

3.B Bierman $\mathbf{UDU}^T$ Covariance Update

The three equations given in (3.17) denote one way to mechanize the recursive update of the estimates and the covariance matrix. Although widely accepted both in theory and practice, a straightforward implementation of the RLS algorithm is notorious for its poor numerical property in real application, which can easily destroy the performance of the RLS algorithm (Bierman, 1977, Clarke and Gawthrop, 1979). This can be made clear by taking a look at the covariance updating formula

$$\mathbf{P}(k-1) - \frac{\mathbf{P}(k-1)\boldsymbol{\varphi}(k,d)\boldsymbol{\varphi}^T(k,d)\mathbf{P}(k-1)}{\lambda + \boldsymbol{\varphi}^T(k,d)\mathbf{P}(k-1)\boldsymbol{\varphi}(k,d)} \tag{3.B.10}$$

As time goes on, the covariance matrix converges to a matrix of very small magnitude, which implies that the covariance updating equation (3.B.10) may involve the subtraction of two almost equal matrices with very small magnitudes. This can easily result in poor numerical performance when implemented on digital computers with finite word length and round-of errors (Clarke and Gawthrop, 1979).

Many modified forms of the RLS algorithm exist to improve the numerical performance (Ljung, 1987, e.g., see Chapter 11), among which Bierman's UD factorization method (Bierman, 1977, Thornton and Bierman, 1980) is one of the most successful approaches. Mathematically, Bierman's method is equivalent to the RLS method. However, through a different formulation, namely, the UD factorization, Bierman's algorithm is numerically much more stable than the RLS algorithm (Bierman, 1977, Thornton and Bierman, 1980, Ljung and Ljung, 1985). In Bierman's method, instead of directly updating the covariance matrix $\mathbf{P}(k)$ using equation (3.B.10), a $\mathbf{UDU}^T$ factored form of the $\mathbf{P}(k)$ matrix,

$$\mathbf{P}(k) = \mathbf{U}(k)\mathbf{D}(k)\mathbf{U}(k)^T \tag{3.B.11}$$

is used. That is, at every time interval, $\mathbf{U}(k)$ and $\mathbf{D}(k)$, instead of $\mathbf{P}(k)$, are updated, where $\mathbf{D}(k)$ is diagonal and $\mathbf{U}(k)$ is an unit upper-triangular matrix. The UD factorization preserves the positive-definiteness (see Appendix A, Section 1.1) of the $\mathbf{P}(k)$ matrix and updates the square root of the covariance matrix, thus the numerical condition can be considerably improved. Experiments show that for digital computer implementations, to obtain the same numerical

accuracy, the UD algorithm can use about half the word length required by the conventional RLS algorithm (Hägglund, 1983, Thornton and Bierman, 1980).

A stepwise implementation of Bierman's UD factorization algorithm is summarized in Algorithm 3.B.1. For detailed derivation and discussions, see (Bierman, 1977, Thornton and Bierman, 1980, Ljung and Söderström, 1983).

Algorithm 3.B.1: Bierman $\mathbf{UDU}^T$ Estimate-Covariance Update:

$\mathbf{v} = \mathbf{D}(k-1)\mathbf{f}, \quad \mathbf{f} = \mathbf{U}^T(k-1)\boldsymbol{\varphi}(k,d), \quad \alpha_0 = \lambda$

`for` $j = 1$ `to` n `do` $\quad \%\ n = na + nb$

$\alpha_j = \alpha_{j-1} + \mathbf{v}_j \mathbf{f}_j$

$\mathbf{D}_{jj}(k) = \alpha_{j-1}\mathbf{D}_{jj}(k-1)/\alpha_j\lambda$

$\mathbf{p}_j = -\mathbf{f}_j/\alpha_{j-1}, \quad \bar{\mathbf{K}}_j(k) = \mathbf{v}_j$

`for` $i = 1$ `to` $j-1$ `do`

$\mathbf{U}_{ij}(k) = \mathbf{U}_{ij}(k-1) + \mathbf{p}_j\bar{\mathbf{K}}_i(k)$

$\bar{\mathbf{K}}_i(k) = \bar{\mathbf{K}}_i(k) + \bar{\mathbf{K}}_j(k)\mathbf{U}_{ij}(k-1)$

`end`

`end`

The update gain $\mathbf{K}(k)$ is now given by:

$\mathbf{K}(k) = \bar{\mathbf{K}}(k)/\alpha_n$

Clearly, the UD factorization algorithm is a variant of the RLS algorithm in that the UD factorization technique is used to replace the covariance update (3.B.10) for more stable numerical performance. The UD factorization algorithm was motivated to be, and actually has also been widely regarded as, only a numerical enhancement to the RLS method.

Chapter 4

Wood Ash Hydration - Control

This chapter presents a novel method for detecting abrupt changes in mixture viscosities. This problem arises in numerous industrial applications and different solutions are suggested in the literature, see Section 1.6. An approach of using non-linear filtering for detection – an adaptive filter combined with a change detector – is however outlined here. Furthermore, as a case study we use the Wood Ash Hydration (WAH) process presented in Chapter 3. As stated earlier, the main problem is here to predict the quantity of water to be added, since the required amount of water varies with the wood ash quality. In this chapter, one adaptive filter and two change detectors are applied to this benchmark data and the detectors are evaluated using basic performance measures. It should be stressed that the level P_e^{crit} must be detected as fast as possible, since at the level P_e^{crit} only a small additional amount of water gives a mixture useless for agglomeration. For example, given a saturated batch of 250-300 kg, an additional amount of 2-4 liters of water results in too wet a mixture.

The chapter is organized as follows. A presentation of the adaptive algorithms used for parameter estimation of the mixture dynamics follows this introduction. The structure of a non-linear filter used for change detection is outlined next. To evaluate the two proposed stopping rules different performance measures are introduced and the two stopping rules – the Geometric Moving Average (GMA)-test and the CUmulative SUM (CUSUM)-test – are covered in detail. The chapter finishes with the case study, real-time implementation issues and some concluding remarks.

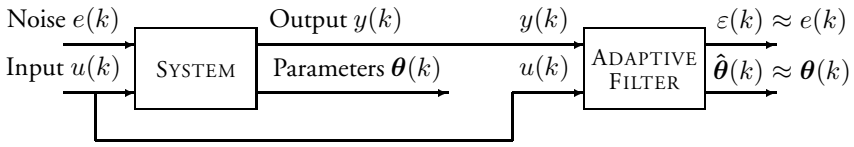

Figure 4.1: The interplay between the adaptive parameter estimator and the system.

4.1 Adaptive Linear Filtering

There are many books covering the area of adaptive filtering. For a literature survey, see e.g. (Gustafsson, 2000, Sec 5.1). Three conceptually different (although algorithmically similar) cases can be distinguished:

1. Signal estimation,

2. Parameter estimation in an unknown model,

3. State estimation in a known model.

In this chapter we will focus on approach number 2. The reason is that faults in actuators and sensors are most easily detected in a state-space context, while system dynamic changes often require a parametric model. However, system changes can be detected by means of state-space descriptions as well; see, e.g., the books Chen and Patton (1999) and Patton et al. (2000). The signal estimation problem arises when the task is to detect an abruptly changing mean level of a noisy signal, which will not be considered. In the context of item 2 the adaptive filter acts as a system inverse, as depicted in Figure 4.1.

Many problems can be recast into estimating the parameters in a linear regression model characterized by a regression vector $\boldsymbol{\varphi}$ and a parameter vector $\boldsymbol{\theta}$. One of the workhorses for adaptive estimation of time-varying parameters in the linear regression framework is the *recursive least squares* (Ljung and Söderström, 1983, Johansson, 1993) presented in Section 3.4.

Figure 4.2: The principle of the one-filter approach for change detection.

4.2 Change Detection

Algorithmically, all proposed change detectors can be put into one of the following three categories:

- Methods using one filter, where a *whiteness test* is applied to the residuals.
- Methods using *two filters*, one slow and one fast, in parallel.
- Methods using *multiple filters* in parallel, each one matched to certain assumption on the abrupt changes.

An adaptive parameter estimator is good at following slow variations in the system parameters. If the system instead changes abruptly it takes quite a long time before the filter adapts to the new system parameters. To improve the performance of the filter a *change detector* (Gustafsson, 2000) can be added. The structure of the selected change detector is shown in Figure 4.2. In the one-filter approach, one adaptive filter is used to determine if there is a change in the system. If the estimated model is correct, the residuals $\varepsilon(k)$ from the filter should be white and Gaussian. Hence, in real applications, due to non-linearity, non-stationary, non-Gaussian noise and disturbance of the process under investigation, sometimes it is difficult to obtain a white and Gaussian residual. The change detector consists of three stages; filter, distance measures and stopping rules:

Filter

The implemented parameter estimator discussed in Section 3.B is here used as a filter. The adaptive filter gives as an output the parameter estimate $\hat{\boldsymbol{\theta}}(k)$ and the residual $\varepsilon(k)$ at time k, c.f. Figure 4.1.

Distance Measures

After a change, either the mean or variance or both will change. This is indicated by the residuals variable $\varepsilon(k)$ from the filter, which become "large" in some sense. The main problem in statistical change detection is to decide what is meant by "large". Therefore a function $s(k)$, called *distance measure* of the residual, $\varepsilon(k)$, at time k is calculated to obtain a measurement of the distance to zero of the residual. Here, the implemented distance measure is the same as the residual, i.e., $s(k) = \varepsilon(k)$, which is useful for detecting a change in the mean of a variable (Gustafsson, 2000).

Stopping Rules

If the residuals are white the expected value $E\{s(k)\}$, of $s(k)$ should be zero. A *hypothesis test* can be used to decide whether the model is correct or not

$$\begin{aligned} \mathcal{H}_0 &: \quad E\{s(k)\} = 0 \\ \mathcal{H}_1 &: \quad E\{s(k)\} \neq 0 \end{aligned} \tag{4.1}$$

This is essentially achieved by low-pass filtering $s(k)$ and comparing this value to a threshold γ. One such method is the Geometric Moving Average (GMA)-test (Roberts, 1959). A one-sided GMA-test is

$$g(k) = \alpha g(k-1) + (1-\alpha)s(k), \qquad \text{alarm if } g(k) > \gamma \tag{4.2}$$

where $0 \leq \alpha < 1$. Here the parameter α is used to tune the low pass effect and the threshold γ is used to tune the performance of the detector. Another method is the CUmulative SUM (CUSUM)-test (de Bruyn, 1968). The one-sided CUSUM-test detects only if $g(k)$ is significantly larger than zero

$$g(k) = \max\left(g(k-1) - s(k) - \nu, 0\right), \qquad \text{alarm if } g(k) > \gamma \tag{4.3}$$

Here the drift parameter ν and the threshold γ are design parameters used to tune the sensitivity of the change detector.

4.3 Basic Performance Measures

In the literature, several basic performance measures are proposed for evaluation of change detectors. Among those defined, *on-line* performance measures are:

Mean Time between False Alarms (MTFA)

$$MTFA = E(t_a - t_0|\text{no change}) \tag{4.4}$$

where t_0 is the starting time for the algorithm and t_a is the alarm time. Related to the MTFA is the *False Alarm Rate (FAR)* defined as $1/MTFA$.

Mean Time to Detection (MTD)

$$MTD = E(t_a - t_k|\text{a change at time } t_k) \tag{4.5}$$

Average Run Length (ARL)

$$ARL(\theta) = E(t_a - t_k|\text{a change of magnitude } \theta \text{ at time } t_k) \tag{4.6}$$

This function generalizes MTFA and MTD. The ARL function can be evaluated from Monte Carlo simulations, or other resampling techniques. In some simple cases, it can also be computed numerically without the need for simulation.

4.4 Review of the GMA-test

This subsection provides an overview of the GMA-test; a more thorough discussion is found in Basseville and Nikiforov (1993) and Wieringa (1999). We assume that the observations of $s(k)$ are independently distributed as

$$s(k) \sim \mathcal{N}(\mu(k), \sigma^2) \tag{4.7}$$

where an abrupt change occurring at an unknown time point T is modelled as

$$\mu(k) = \begin{cases} 0 & , k < T \\ \theta & , k \geq T \end{cases} \tag{4.8}$$

Here we want to detect a significant change in the mean $\mu(k)$. The value of the one-sided GMA statistics at time k, which is denoted by $g(k)$, is computed as follows:

$$\begin{aligned} g(k) &= \alpha g(k-1) + (1-\alpha)s(k) \\ t_a &= \min\{k; g(k) > \gamma\} \end{aligned} \tag{4.9}$$

Here the parameter α is a constant satisfying $\alpha \in [0, 1)$, t_a is the alarm time and γ is a threshold that influences the stochastic properties of the test usually expressed in FAR and MTD defined in Section 4.3. Often $g(0)$ is set equal to a target value, or (an estimation of) the mean θ. Furthermore, all information on previous observations that is needed for computing $g(k)$ is stored in $g(k-1)$.

This stopping rule is called a *geometric moving average* (also known as exponential filter) since the weights of past observations are declining as in a geometric series. For a two-sided GMA-test an alarm is given if $|g(k)| > \gamma$ for some threshold γ. Now define $ARL(\theta/\sigma, g(0))$ as the Average Run Length (ARL) of the GMA-test for the mean of $\{s(k)\}$ given that the shift in the mean is equal to θ and that the GMA starts in $g(0)$. The run length is 1 if $s(1)$ is such that $|g(1)| = |\alpha g(0) + (1-\alpha)s(1)| > \gamma$. Otherwise the run of the GMA continues from $g(1)$. From this point on, we expect an additional run length of $ARL(\theta/\sigma, g(1))$. Using the notation $g(k) = g_k$ and $s(k) = s_k$, this leads to the following integral equation for $ARL(\theta/\sigma, \cdot)$

$$\begin{aligned} ARL(\theta/\sigma, g_0) &= \Pr\left[|g_1| > \gamma\right] + \int\limits_{\{|g_1| \le \gamma\}} \left[1 + ARL(\theta/\sigma, g_1)\right] f(s_1) ds_1 \\ &= 1 + \frac{1}{1-\alpha} \int\limits_{-\gamma}^{\gamma} ARL(\theta/\sigma, s_1) f\left(\frac{s_1 - \alpha g_0}{1-\alpha}\right) ds_1 \end{aligned} \quad (4.10)$$

where $f(\cdot)$ denotes the probability density function of $\{s(k)\}$. Equation (4.10) is a Fredholm integral equation of the second kind. The ARL curve can now be evaluated by approximating the integral numerically as outlined in Crowder (1987). However, Lucas and Saccucci (1990) used a Markov-chain approach to evaluate the ARL of the GMA-test. This approach is discussed in Section 4.A and is applied in Section 4.7.

4.5 Review of the CUSUM-test

This subsection provides an overview of the CUSUM-test; a more thorough discussion is found in Basseville and Nikiforov (1993). As in the previous section we consider the case of an unknown, time-varying constant θ with white

Gaussian noise added:

$$\begin{aligned} s(k) &= \mu(k) + \sigma e(k) \\ e(k) &\sim \mathcal{N}(0,1) \end{aligned} \tag{4.11}$$

We want to detect a significant change in the mean $\mu(k)$:

$$\begin{aligned} \mathcal{H}_0 &: \quad \theta < 2\nu \\ \mathcal{H}_1 &: \quad \theta > 2\nu \end{aligned} \tag{4.12}$$

where ν is the minimum change we want to detect. The one-sided CUSUM-test applies and is given by

$$\begin{aligned} g(k) &= \max\left(g(k-1) - s(k) - \nu, 0\right) \\ t_a &= \min\left\{k; g(k) > \gamma\right\} \end{aligned} \tag{4.13}$$

Here, t_a is the alarm time and γ is a threshold that influences the stochastic properties of the test. It can be shown that the functional form of the ARL function is

$$ARL(\theta, \gamma, \nu) = f\left(\frac{\gamma}{\sigma}, \frac{\theta - \nu}{\sigma}\right) \tag{4.14}$$

that is, it is a function of two arguments. The exact value of the ARL function is also here given by the so called *Fredholm integral equation* of the second kind, which must be solved by a numerical algorithm. See for example Section 5.2.2 in Basseville and Nikiforov (1993). However, a direct approximation suggested in Wald (1947) is

$$ARL(\theta, \gamma, \nu) \approx \frac{e^{-2\frac{\gamma(\theta-\nu)}{\sigma^2}} - 1 + 2\gamma(\theta - \nu)/\sigma^2}{2\frac{\gamma(\theta-\nu)}{\sigma^2}} \tag{4.15}$$

and another novel approximation suggested in (Siegmund, 1985a,b), is

$$ARL(\theta, \gamma, \nu) \approx \frac{e^{-2(\gamma/\sigma + 1.166)(\theta-\nu)/\sigma} - 1 + 2(\gamma/\sigma + 1.166)(\theta - \nu)/\sigma}{2(\theta - \nu)^2/\sigma^2} \tag{4.16}$$

In all these approximations a zero initial condition is assumed. By using these approximations, the False Alarm Rate (FAR) is evaluated as

$$FAR = \frac{1}{ARL(0, \gamma, \nu)} \tag{4.17}$$

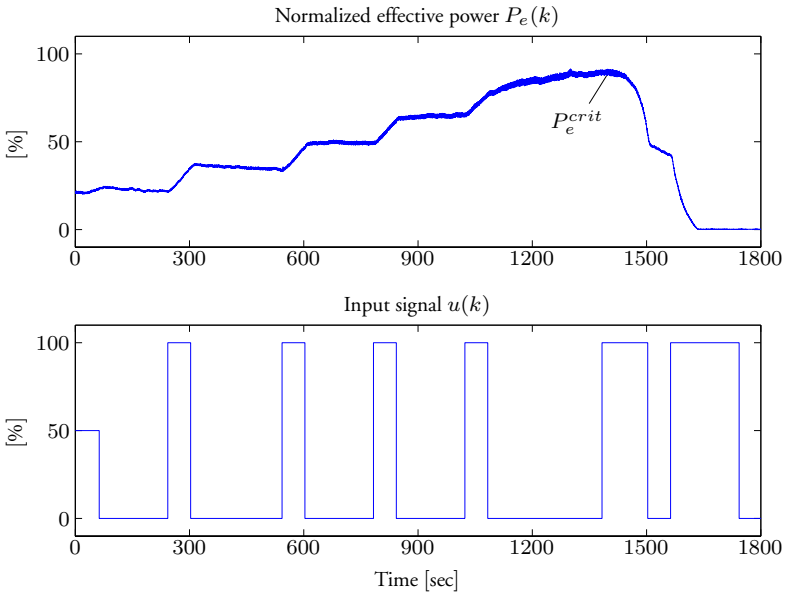

Figure 4.3: Raw input-output data. Here a Pseudo Random Binary Sequence (PRBS) is used as an input (added water) sequence.

and the Mean Time to Detection (MTD) as

$$MTD(\theta) = ARL(\theta, \gamma, \nu) \tag{4.18}$$

using the one-sided CUSUM-test as stopping rule. The same evaluations are valid for the GMA-test.

4.6 Preliminaries

In Chapter 3 it was shown that an ARX model structure of second order is sufficient to describe the time-varying process dynamics of the Wood Ash Hydration (WAH) process. It was also shown that the time delay $d = 0$. An example of raw input-output data collected from the batch mixing process is shown in Figure 4.3. In the figure we see that the mixture becomes saturated, i.e., the point P_e^{crit} is reached at $t \approx 1395\ s$. Nevertheless, more water is added

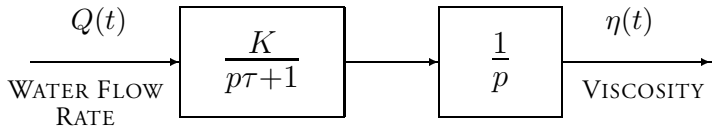

Figure 4.4: Grey box model for the dynamics of the WAH process. Here, p is the differential operator d/dt.

to the stabilization process after P_e^{crit} has been reached and a mixture useless for agglomeration is obtained. The figure clearly shows that the process dynamics are time-varying and we again state the following physical interpretation of the viscosity dynamics presented in Svantesson and Olsson (2000): since the mixture is accumulating water, an integrator is to be found in the process dynamics. Further, a time-constant is present, which depends on how the water is "diffused" into the mixture; in the beginning of the WAH procedure the dry mixture absorbs water fast, whereas at the end the mixture becomes more and more saturated and is not able to absorb water as fast as in the beginning. This implies a *grey box model* shown in Figure 4.4.

From a system perspective, the gradual saturation of the mixture is explained as a time-varying time constant, i.e., the time constant corresponds to a mode that decreases in speed. This implies that the system will, eventually, become a double integrator. To verify this hypothesis, the input-output data shown in Figure 4.3 is used by the parameter estimator presented in Chapter 3. Furthermore, by differentiating the output we remove the integrator and need only to estimate the remaining dynamics

$$G(p) = \frac{K}{p\tau + 1} \tag{4.19}$$

of the grey-box model shown in Figure 4.4. The corresponding discrete-time model $H(q^{-1})$ for sample time h is given by

$$H(q^{-1}) = \frac{K(1 - e^{-\frac{1}{\tau}h})q^{-1}}{1 - q^{-1}e^{-\frac{1}{\tau}h}} \stackrel{\text{def}}{=} \frac{b_1 q^{-1}}{1 + a_1 q^{-1}} \tag{4.20}$$

Using $h = 1$ second and the estimated parameters $\hat{a}_1 < 0$ and $\hat{b}_1$ we can solve

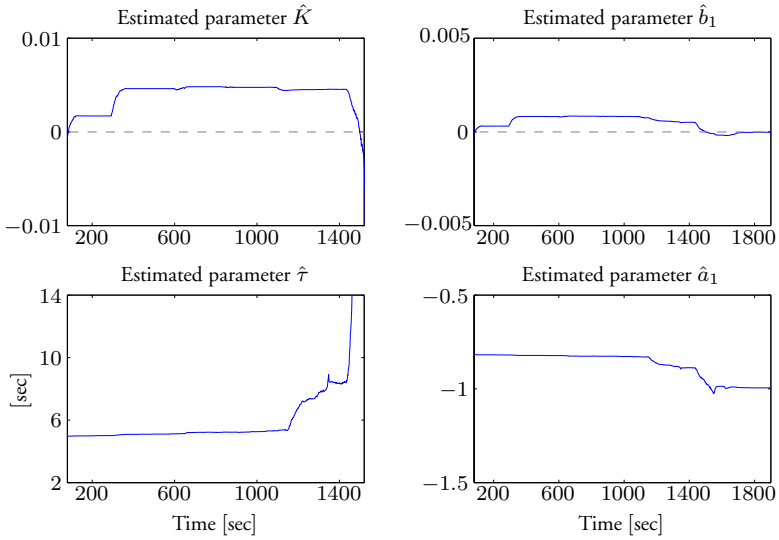

Figure 4.5: The estimated continuous-time parameters $\hat{K}$ and $\hat{\tau}$ of the grey box model. It is observed that the time-constant $\hat{\tau}$ is approximately 5 seconds at the beginning of the WAH process. The estimated parameters $\hat{b}_1$ and $\hat{a}_1$ are also shown for comparison.

for the corresponding continuous-time parameters yielding

$$\hat{K} = \frac{\hat{b}_1}{1 + \hat{a}_1} \qquad \hat{\tau} = \frac{1}{-\ln(-\hat{a}_1)} \tag{4.21}$$

The estimated continuous-time parameters for the data shown in Figure 4.3 are given by Figure 4.5. It is observed that the estimated process gain $\hat{K}$ switches sign when the mixture viscosity begins to decrease. This property may be used to disable any control action during the WAH procedure. However, the time elapsed to obtain $\hat{K} < 0$ is too long for our purposes, therefore a change detector needs to be implemented. To verify that the framework presented in Figure 4.2 fits to our problem we need to:

1. Formulate the estimation problem as a linear regression.
2. Check that the residuals $\varepsilon(k)$ from the adaptive filter before the abrupt change form a white noise sequence.

We start by approaching item 1: the measurement of the normalized effective power $P_e(t)$ is only available as periodic observations of $P_e(t)$ sampled with a time interval h (the sampling period). Let the values of $P_e(t)$ be represented by a sequence

$$\{P_e(k)\}_{k=0}^{\infty}; \quad P_e(k) = P_e(kh) \quad \text{for } k = 0, 1, \ldots \tag{4.22}$$

Then the measurement of $P_e(k)$ can be expressed as

$$P_e(k) \stackrel{\text{def}}{=} y(k) = \boldsymbol{\varphi}^T(k, d)\boldsymbol{\theta}(k) + e(k) \tag{4.23}$$

which is a linear regression.

To check item 2, the RLS parameter estimator using the Bierman UD factorization is implemented in `C-code` and incorporated in `SIMULINK` `S-functions` (Svantesson, 1997). The filter is applied to the input-output data shown in Figure 4.3 for $t \in [100, 1000]$ using the data-filter

$$L(q) = \frac{1 - f}{q - f} \tag{4.24}$$

with $f = 0.9$. The estimated residual autocorrelation and histogram are shown in Figure 4.6. It may be inferred that the sequence $\{\varepsilon(k)\}_{k=100}^{1000}$ indeed form a white noise sequence and that $\{\varepsilon(k)\}_{k=100}^{1000} \sim \mathcal{N}(\hat{\mu}, \hat{\sigma}^2)$. We thus have verified item 2.

4.7 On-line Detection

The change detectors based on the GMA-test and the CUSUM-test are now applied to two data sets that represent a typical behavior of the WAH process. However, since prefiltering with the Δ operator as outlined in Section 4.6 do not yield better detection the full order model is used. In the data sets, random pulses are inserted to the system input and the results are shown in Figures 4.7 and 4.8. When the normalized effective power $P_e(k)$ reaches the level P_e^{crit}, the gain of the WAH process switches sign from positive to negative, which implies that the residuals $\varepsilon(k)$ become negative. Therefore, there is only need for one-sided tests.

From the figures it is concluded that both implemented change detectors are successful in detecting the mixture saturation, i.e., when the level P_e^{crit} is

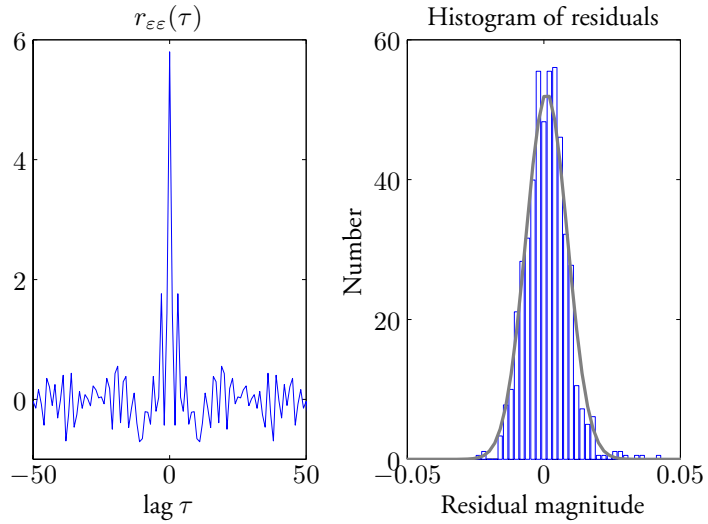

Figure 4.6: Estimated residual autocorrelation $\hat{r}_{\varepsilon\varepsilon}(\tau)$ (left figure) and histogram of residuals (right figure). The normal distribution $\mathcal{N}(\hat{\mu}, \hat{\sigma}^2)$ (solid line) is shown for comparison.

reached. Furthermore, to enable simple evaluation we use the data set shown in Figure 4.8, which contain a distinct change in $P_e(k)$. By visual inspection it may be inferred that the level P_e^{crit} is reached at $t \approx 785s$. Estimated from this data set we also have $\theta \approx 0.035$ and $\sigma \approx 0.0094$. With $\gamma_{GMA} = 0.015$, $\alpha = 0.9$, $\gamma_{CUSUM} = 0.2$ and $\nu = 0.006$ we compute the basic performance measures and the result is given in Table 4.1. In the table, zero initial conditions in the CUSUM-test and GMA-test are assumed. The ARL of the CUSUM-test is evaluated using the Adaptive Filtering and Change Detection Toolbox (Gustafsson, 2001), and the ARL of the GMA-test is evaluated using the tech-

CUSUM	$ARL(\theta, \gamma, \nu)$	**GMA**	$ARL(\theta, \gamma, \alpha)$
Numeric	8.00	Numeric	5.89
Wald	6.84	—	—
Siegmund	7.22	—	—
MC	7.45	MC	5.86

Table 4.1: Basic performance measures.

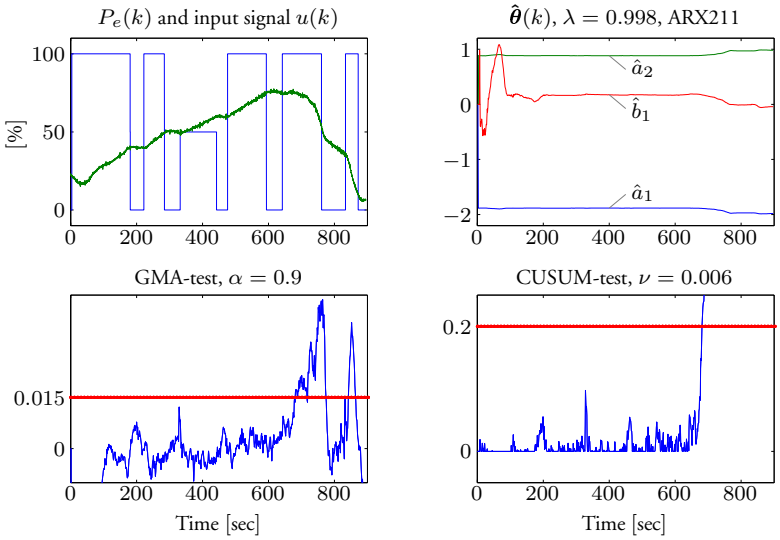

Figure 4.7: The change detector applied to the first data set. The plot to the upper left shows the applied input $u(k)$ and the system response $-P_e(k)$. In the upper right plot the parameter convergence for the RLS is shown using $\lambda = 0.998$. The thresholds $\gamma_{GMA} = 0.015$ and $\gamma_{CUSUM} = 0.2$ are used, which are plotted in the two lower figures as dotted lines. The input data have been rescaled.

nique presented in Section 4.A. By visual inspection it may be inferred that the run length is approximately 8 seconds both for the GMA-test and the CUSUM-test. However, the mean times do not say anything about the distribution of the run length, which can be quite unsymmetrical. Monte Carlo simulations can be used for further analysis of the run length function (Gustafsson, 2001). As an example, the distribution of 500 Monte Carlo simulations using the CUSUM-test is shown in Figure 4.9. It is clear from the figure that the False Alarm Rate is a non-issue. This statement is also verified by evaluating the FAR according to Siegmund's approximation, $FAR = 1/ARL(0, \gamma, \nu) \approx 3 \cdot 10^{-13}$.

By using basic performance measures we have thus verified that both the change detectors are successful in detecting when the mixture becomes saturated, i.e., when the level P_e^{crit} is reached. The GMA-test seems to be slightly faster but

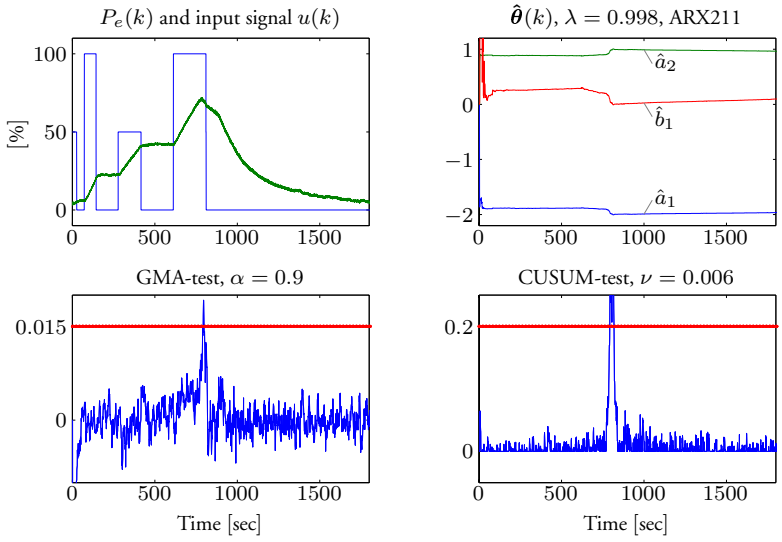

Figure 4.8: The change detector applied to the second data set. The plot to the upper left shows the applied input $u(k)$ and the system response $-P_e(k)$. In the upper right plot the parameter convergence for the RLS is shown using $\lambda = 0.998$. The thresholds $\gamma_{GMA} = 0.015$ and $\gamma_{CUSUM} = 0.2$ are used, which are plotted in the two lower figures as dotted lines. The input data have been rescaled.

the CUSUM-test has a major advantage due to a more distinct detection, c.f. Figures 4.7 and 4.8. Another advantage of the CUSUM-test is that it is easy to affect the final moisture content of the mixture by varying the threshold. For example, the threshold $\gamma_{CUSUM} = 0.1$ gives $ARL(\theta, \gamma, \nu) = 4.15$, which implies faster detection and thus a less moistened mixture, whereas the threshold $\gamma_{CUSUM} = 0.3$ gives $ARL(\theta, \gamma, \nu) = 12.16$ and thus a more moistened mixture, in fact too moistened for practical use in ash recycling applications.

Based on these remarks, the final real-time implementation for the WAH process is summarized as follows: at each batch produced, a PRBS of the water injection is generated in order to obtain a good estimate of the process dynamics. This is to ensure an adequate performance of the CUSUM-test. However, sometimes in real processes it is impossible to apply a PRBS as input to the

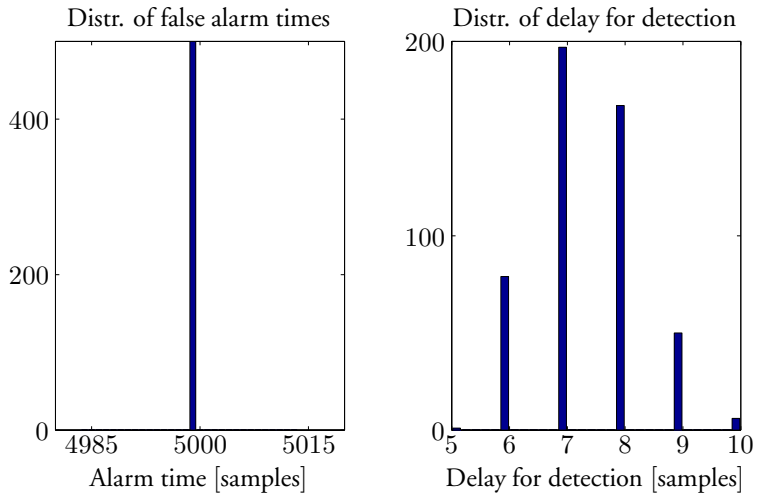

Figure 4.9: Distribution of false alarm times (left) and delay for detection (right), respectively from 500 Monte Carlo simulations. The false alarm times are evaluated using 5000 data in each simulation.

actual system for identification purposes. Then one has to rely on some initial model parameters obtained by other means. After the eventual PRBS is completed, the control signal attains the level $u_{\max}$ until a suitable mixture viscosity is obtained. This control strategy is, despite its simplicity, optimal in the sense that the level P_e^{crit} is reached in minimum time. As a result, this implementation gives a small number of floating point calculations which is positive since most of the available time at the Programmable Logic Controller (PLC) normally has to be used for purposes other than the control algorithm itself, such as communications and alarms.

Practical Considerations of Detector Tuning for Viscosity Control

In the CUSUM-test, the test statistics $g(k)$ sums up its input $s(k)$ with the idea to give an alarm when the sum exceeds the threshold γ_{CUSUM}. With a white noise input, i.e., $s(k) = \varepsilon(k)$, the test statistics will drift away similar to a random walk. There are two mechanisms to prevent this natural fluctuation: to prevent *positive drifts*, eventually yielding a false alarm, a small drift term ν is subtracted at each time instant. To prevent a *negative drifts*, which would

increase the time to detection after a change, the test statistics is reset to zero each time it becomes less than zero. As a rule of thumb, the drift parameter ν can be chosen as one half of the expected change magnitude. Hence, even though the input to the CUSUM-test is not perfectly white, the basic behavior of the algorithm will not change.

Like the CUSUM algorithm, the GMA utilizes all previous observations but the weight attached to data is exponentially declining as the observations get older and older. By varying the parameter α of the GMA statistic the "memory" of the GMA can be influenced. If $\alpha \rightarrow 0$ then $g(k) \rightarrow s(k)$, and the GMA places all of its weight on the most recent observation. If $\alpha \rightarrow 1$, then the most recent observation receives a small weight, whereas the weight attached to previous observations only slightly declines with the age of the observations. Hence, the GMA then takes on the appearance of the CUSUM. For both the CUSUM and the GMA statistics the threshold γ affects the ARL in such way that the MTD is increased and the FAR is decreased if the threshold is slightly increased and vice versa. Furthermore, it is also important to remember that both the forgetting factor in the RLS parameter estimator and the choice of pre-filter $L(q)$ affect the residual $\varepsilon(k)$ and thus the ARL function.

4.8 Real-Time Implementation

The result of identification is dependent upon a careful choice of input to the system under investigation. During the auto-tuning, a Pseudo Random Binary Sequence (PRBS) is used as process input. This input signal shifts between two levels in a certain pattern such that its mean value and covariance function are quite similar to those of a white noise process (Söderström and Stoica, 1989). This signal is therefore adequate for identification purposes since a white noise sequence is PE of any order, see Åström and Wittenmark (1995).

PRBS Signal Generator

In order to generate a PRBS with an auto-correlation function as given in equation (3.25), it is necessary to generate random numbers, *uniformly distributed* between, for example, zero and one. Numerous methods for generating uniformly distributed random numbers have been devised, see e.g. Banks and Carson (1984). The sequence of numbers generated is determined by the initial seed of the PRBS signal generator. Since the generator resets the initial seed at

start-up, the sequence of numbers generated will be the same unless the initial seed is changed.

Definition 4.1 (Uniform distribution) A random variable X is *uniformly* distributed on the interval $[a, b]$ if its *probability density function* is given by

$$f_X(x) = \begin{cases} \frac{1}{b-a} & , a \leq x \leq b \\ 0 & , \textit{otherwise} \end{cases} \tag{4.25}$$

The *probability distribution function* is given by

$$F_X(x) = \begin{cases} 0 & , x < a \\ \frac{x-a}{b-a} & , a \leq x \leq b \\ 1 & , x > b \end{cases} \tag{4.26}$$

The *mean* and *variance* of the distribution are given by

$$E\{X\} = \frac{a+b}{2} \tag{4.27}$$

and

$$\mathit{Var}\{X\} = \frac{(b-a)^2}{12} \tag{4.28}$$

□

In order to generate random numbers uniformly distributed in the interval $[0, 1]$ we put $a = 0$ and $b = 1$. The PRBS signal generator is implemented in the `CALC-IDE` environment described in Section 8.4. The result of a `MATLAB` simulation using the PRBS signal generator for $N = 5$, $h = 1$ and 10000 generated samples is shown in Figure 4.10. See Appendix A, Section 1.2, for the definition of the auto-correlation function and the auto-spectrum. The result of the simulation confirms equation (3.25) and the number of dips in the estimated auto-spectrum is equal $(N-1)/2$. Note that (3.25) is an asymptotic result, which means that it is valid for an infinite sequence.

Anti-Aliasing Filter

Filtering reduces noise errors in the signal. For most applications a low-pass filter is used. This allows through the lower frequency components but attenuates the higher frequencies. The cut-off frequency must be compatible with the

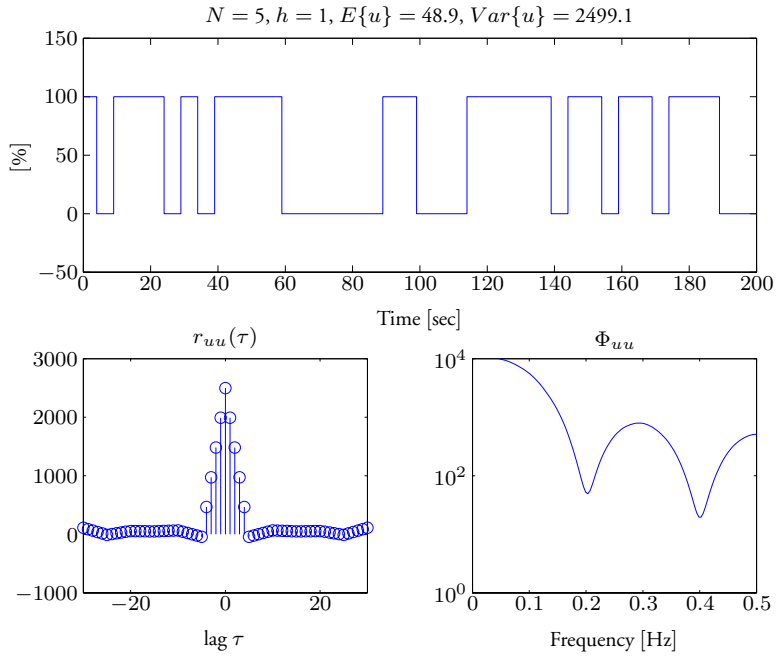

Figure 4.10: The upper plot shows the first 200 samples of the PRBS sequence. The two lower plots show the estimated auto-correlation function and the estimated auto-spectrum.

frequencies present in the actual signal (as opposed to possible contamination by noise) and the sampling rate used for the Analog-to-Digital (A-D) conversion. A low-pass filter that is used to prevent higher frequencies, in either the signal or noise, from introducing distortion into the digitized signal is known as an *anti-aliasing filter* (Åström and Wittenmark, 1997, Franklin et al., 1998). These generally have a sharper cut-off than the normal low-pass filter used to condition a signal. Anti-aliasing filters are specified according to the sampling rate of the system and there must be one filter per input signal.

Very little is lost by sampling a continuous-time signal if the sampling instants are sufficiently close, but much of the information about a signal can be lost if the sampling points are too far apart. It is, of course, essential to know pre-

cisely when a continuous-time signal is uniquely given by its sampled version. Shannons sampling theorem (Shannon, 1949) gives the conditions for the case of periodic sampling. Note that Shannon gives conditions only for an infinite time signal. Also note that in practice we have to be more conservative, i.e., sample a little more frequently.

Practically all analog sensors have some kind of filter, but the filter is seldom chosen for a particular control problem. It is therefore often necessary to modify the filter so that the signals obtained do not have frequencies above the *Nyquist frequency*. The simplest solution is to introduce an analog filter in front of the sampler. The analog inputs of the used control system `SattCon 200`, presented in Section 8.3, all have prefilters. However, for the selected sampling time $h = 1\ s$, the available filter has only a gain of about $-0.4\ dB$ at the Nyquist frequency $\omega_N = \omega_s/2 = \pi$, which is not sufficient. Therefore, a first order filter is designed that serves as an extra anti-aliasing filter. The filter has the transfer function

$$G_{aa}(s) = \frac{1}{s+1} \tag{4.29}$$

and has a gain of about $-10.4\ dB$ at the Nyquist frequency. Due to the slow process dynamics, the dynamics of the anti-aliasing filter are neglected.

4.9 Summary and Concluding Remarks

This chapter presents a novel method for mixture viscosity control; the approach of using non-linear filtering − an adaptive filter combined with a change detector − for detection. Furthermore, the approach is successfully applied to the WAH process. The used sensor signal is the effective power representing the rate of useful work being performed by the stirrer drive. One adaptive filter and two change detectors were applied to benchmark data and the detectors were evaluated using basic performance measures. Two stopping rules were presented and tested; the GMA-test and the CUSUM-test. Both change detectors are successful in detecting when the mixture becomes saturated, i.e., when the level P_e^{crit} is reached. However, the detector based on the CUSUM-test has a more distinct detection. Another advantage of the CUSUM-test is that it is easy to affect the final moisture content of the mixture by varying the threshold γ_{CUSUM}. Furthermore, the modest number of floating point calculations makes the method tractable for most PLCs available on the market today.

Appendix

4.A Computing the ARL using the Markov-Chain Approach

As indicated in Section 4.4, the Markov-chain approach can be used for computing the ARL of the GMA-test, or any other stopping rule. It is an alternative to the Fredholm-integral approach. In Champ and Rigdon (1991) it is shown that if the midpoint rule is used to approximate the integral in the Fredholm-integral approach, the same approximation is reached as when the Markov-chain approach is used. In this Appendix, the method will be explained for a specific case, viz., for determining the ARL of the GMA-test for the mean of independent Gaussian observations.

Lucas and Saccucci (1990) approximate the ARL of the two-sided GMA-test by dividing the interval $[-\gamma_{GMA}, \gamma_{GMA}]$ into $2m+1$ subintervals of width 2δ. The process generating the successive GMA values is then viewed as a (discretized) Markov chain, c.f. Appendix A. The GMA statistics $g(k)$ is said to be in state i at time k if $S_i - \delta < g(k) < S_i + \delta$ for $i = -m, -m+1, \ldots, m$, where S_i represents the midpoint of the ith interval. The states in which no alarm is assumed are transient states. An alarm state is modeled by an absorbing state S_a. Hence, no alarm is assumed whenever $g(k)$ is in a transient state and an alarm is assumed whenever $g(k)$ is in the absorbing state.

If we let p_i denote the probability that the discretized GMA starts in state i, then the initial probability vector $\mathbf{p}_0$ can be written as follows:

$$\begin{aligned} \mathbf{p}_0^T &= \left[\begin{array}{ccccccccc} p_{-m} & p_{-m+1} & \cdots & p_{-1} & p_0 & p_1 & \cdots & p_m & p_a \end{array}\right] \\ &= \left[\begin{array}{cc} \mathbf{p}^T & p_a \end{array}\right] \end{aligned} \tag{4.A.1}$$

where $\mathbf{p}^T = \left[\begin{array}{ccccccccc} p_{-m} & p_{-m+1} & \cdots & p_{-1} & p_0 & p_1 & \cdots & p_m \end{array}\right]$. Since we assume that the GMA-test starts with no alarm, p_a is set to 0. The transition probability matrix is given by

$$\mathbf{P} = \left[\begin{array}{cc} \mathbf{R} & (\mathbf{I}_{2m+1} - \mathbf{R})\,\mathbf{1} \\ \mathbf{0}^T & 1 \end{array}\right] \tag{4.A.2}$$

where the submatrix $\mathbf{R}$ is a $(2m+1) \times (2m+1)$ matrix containing the probabilities of going from one transient state to another, $\mathbf{I}_{2m+1}$ is the identity matrix

of order $2m+1$, and $\mathbf{1}$ and $\mathbf{0}$ are column vectors of ones and zeros, respectively. A typical element of $\mathbf{R}$ is denoted by p_{ij} and represents the probability that $g(k)$ goes from state i to state j in one step. Lucas and Saccucci (1990) approximate the entries of $\mathbf{R}$ by assuming that the GMA equals S_i whenever it is in state i. This yields:

$$\begin{aligned} p_{ij} &= \Pr\left[\text{going to } S_j \mid \text{in } S_i\right] \\ &\approx \Pr\left[S_j - \delta < \alpha S_i + (1-\alpha)s(k) < S_j + \delta\right] \end{aligned} \tag{4.A.3}$$

where $i,\ j = -m, -m+1, \ldots, m$. For the special case of identically independent normal observations $s(k)$ with mean μ and standard deviation σ, the elements of $\mathbf{R}$ are given by

$$p_{ij} = \Phi\left(\frac{(S_j+\delta) - \alpha S_i - (1-\alpha)\mu}{(1-\alpha)\sigma}\right) - \Phi\left(\frac{(S_j-\delta) - \alpha S_i - (1-\alpha)\mu}{(1-\alpha)\sigma}\right) \tag{4.A.4}$$

where Φ represents the standard normal distribution function. The ith stage transition probability matrix $\mathbf{P}^i$ contains the probabilities that the GMA jumps from one state to another in i steps. That is:

$$\mathbf{P}^i = \begin{bmatrix} \mathbf{R}^i & \left(\mathbf{I}_{2m+1} - \mathbf{R}^i\right)\mathbf{1} \\ \mathbf{0}^T & 1 \end{bmatrix} \tag{4.A.5}$$

From $\mathbf{P}^i$, the probability $\Pr\left[\text{Run length} \leq i\right]$ can be computed as:

$$\Pr\left[\text{Run length} \leq i\right] = \mathbf{p}^T\left(\mathbf{I}_{2m+1} - \mathbf{R}^i\right)\mathbf{1} \tag{4.A.6}$$

thus

$$\Pr\left[\text{Run length} = i\right] = \mathbf{p}^T\left(\mathbf{R}^{i-1} - \mathbf{R}^i\right)\mathbf{1} \tag{4.A.7}$$

Using this expression, ARL values based on $2m+1$ states can be computed as

follows:

$$
\begin{aligned}
ARL(2m+1) &= \sum_{i=1}^{\infty} i \Pr\left[\text{Run length} = i\right] \qquad (4.A.8)\\
&= \sum_{i=1}^{\infty} i \mathbf{p}^T \left(\mathbf{R}^{i-1} - \mathbf{R}^i\right) \mathbf{1}\\
&= \mathbf{p}^T \left(\sum_{i=1}^{\infty} i \mathbf{R}^{i-1}\right) \left(\mathbf{I}_{2m+1} - \mathbf{R}\right) \mathbf{1}\\
&= \mathbf{p}^T \left(\mathbf{I}_{2m+1} - \mathbf{R}\right)^{-2} \left(\mathbf{I}_{2m+1} - \mathbf{R}\right) \mathbf{1}\\
&= \mathbf{p}^T \left(\mathbf{I}_{2m+1} - \mathbf{R}\right)^{-1} \mathbf{1}
\end{aligned}
$$

As $2m+1$ goes to infinity, the discretized Markov chain approaches a continuous state Markov chain, and the approximation for the ARL of the GMA-test will get better. Higher order moments of the run length can also be obtained using this Markov-chain approach.

Chapter 5

Wood Ash Agglomeration

5.1 Introduction

After the ash hydration is completed, the mixture of ash, dolomite and water needs to be transformed into a product suitable for recycling. The admissible agglomerate size distribution is that no more than 30% should have a diameter range *less* that 0.25mm. Furthermore, no more than 5% should have a diameter range *greater* than 8mm. Here, different approaches apply for agglomeration – the art of reshaping fine powder into larger particles – and this chapter presents an overview of some of these methods and their applicability in wood ash recycling processes.

In Kalmar, the *drum granulation* technique has been used extensively (Svantesson, 2000). However, due to maintenance problems, the research group initiated during the Fall of 2000 a search for a more robust agglomeration method. This chapter presents the result of that investigation and the experiences gained at the evaluation of the superior method at Graninge – Kalmar Energi.

5.2 Methods Suitable for Automated Agglomeration

In Nilsson (1993) several techniques used to agglomerate wood ashes are presented. Furthermore, a number of experiments in Sweden to agglomerate wood ashes, on-going or finished, are documented in Nordenberg (1996). This section presents an overview of the methods that have been considered as candidates for automated wood ash agglomeration. The evaluation provides information regarding the capacity of each method, but no operating costs are

presented. This is so because in the literature the evaluation of these may differ, thus resulting in a non-objective assessment.

High-Shear Mixer Granulators

Granulation processes in a high-shear equipment have often been considered as black-boxes in which the starting material is converted to granules (Keningley et al., 1997). Changes of the process variables are mainly based on trial and error. A real understanding of what is going on is still missing but some attempts to obtain a deeper understanding are presented in Ramaker (2001) and Hoornaert et al. (1998). The agglomeration process in a high-shear mixer can be divided into several stages:

1. Premixing of the solids,
2. Liquid addition stage,
3. Wet massing stage,
4. Drying stage.

In the wood ash agglomeration procedure presented in Nordenberg (1996), the first three stages take place inside the high shear mixer. For the drying stage, Nordenberg outlines a solution where a microwave furnace is used. However, small scale experiments show that the microwave method is too expensive for practical use. Nordenberg used a Lödige mixer (granulator) to transform the wood ash into granules and a schematic representation of such a device is shown in Figure 5.1. Roughly, it can be stated that the ploughshares ensure mixing while the chopper provides impact forces on the granules. Furthermore, the position of the chopper and the speed of the ploughshares and the chopper affect the granule size distribution. It is reported that the high shear mixer produces granules that are approved by the Swedish National Environment Protection Board and the Swedish National Board of Forestry (Nordenberg, 1996). However, the control of the granulation process is difficult, e.g., the amount of water to be added is very critical and overwetting occurs easily.

The method has a capacity that is highly dependent on the size of the mixer. Furthermore, it may be inferred that the method is expensive assuming that the results presented in Nordenberg (1996) are correct. However, since a `Fejmert`

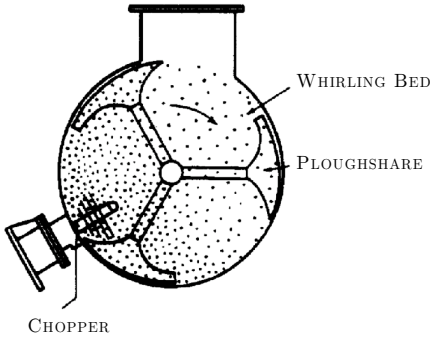

Figure 5.1: A schematic representation of a Lödige mixer granulator.

S-500 mixer has already been installed in Kalmar (Svantesson, 2000), the method using a high shear mixer granulator is not considered.

Dish Granulators

In many granulation processes, size enlargement is achieved by the collision of moist particles undergoing a rolling motion. The inclined *dish granulator* is a suitable device consisting of a shallow cylindrical dish rotating about its cylindrical axis, this being inclined to the horizontal. A typical dish granulator is shown in Figure 5.2. The classifying effect within the dish often causes the product size distribution to be narrow thereby avoiding downstream screening (Chadwick and Bridgwater, 1997). The principles of dish granulation can be summarized in the following steps:

- The fine raw material is continuously added to the pan and wetted by a fine water spray,
- Due to the rotating action of the pan the moistened material forms small seed type particles,
- The seed particles then ”snowball” into larger particles until they discharge from the pan.

The company *Tecwill Granulators Oy* in Finland designs and manufactures ash handling plants based on the dish granulator technique with a capacity of $4 - 7$

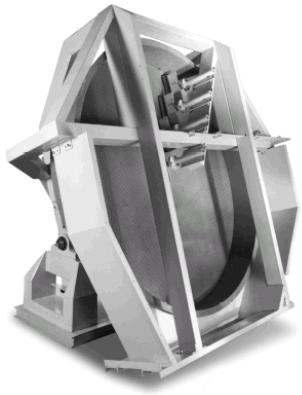

Figure 5.2: A dish granulator for wood ash agglomeration.

tons per hour. Furthermore, Sundqvist (1999) also presents a small experimental setup for manual dish granulation of wood ash. However, maintenance problems have been reported.

Drum Granulators

Drum granulators like dish granulators make agglomerates from fine material. The major difference is the method of controlling agglomerate size. While a dish granulator discharges required agglomerate sizes with little recycle, the agglomerate size produced by a drum is hard to control and requires a closed-loop screening and recycle system back to the feed end of the drum. The previously used *drum granulation* prototype presented in Lindahl and Claesson (1996) and Svantesson (2000) is depicted in Figure 5.3. The drum granulator consists of two rotating parallel cylinders. The fines enter the drum granulator at one end and passes through the cylinders from that end to the other. The time required for the material to pass the cylinders is the variable that controls the *granule size distribution.* This time can be controlled using two parameters (Lindahl and Claesson, 1996): the first is the angular velocity of the rotating cylinders; the second is the inclination. However, the length and diameter of the rotating cylinders are two variables that cannot be manipulated during operation. Still they have an impact on the size distribution. In the literature, mathematical modeling of a drum granulator using *population balance modeling* is presented in Adetayo, Litster and Cameron (1995) and Adetayo, Litster, Pratsinis and En-

Figure 5.3: The drum granulator previously used to granulate the ETEC-dolomite, ash and water in Kalmar (Svantesson, 2000).

nis (1995). Furthermore, the use of machine vision and Adaptive Neuro-Fuzzy Inference Systems (ANFIS) for modeling of a drum granulator unit is reported in Blomqvist and Forsberg (1998). Various control strategies are presented in Crowley et al. (2000), Pottmann et al. (2000) and Zhang et al. (2000).

In Lindahl and Claesson (1996) it is claimed that the drum granulator unit has a capacity of $100 - 200$ kg/hour. However, the capacity of a drum granulator is highly dependent on the size of the drums. In Svantesson (2000) it is stated that if this prototype is to be used in a framework of automated manufacture, the drum granulator unit needs to be rebuilt extensively in order to comply with the industrial requirements for continuous operation. The outcome of such a redesign is however quite uncertain; therefore the method was abandoned.

Roll-Pelletizers

During the Spring of 2001, the author became aware of a new method for wood ash agglomeration. The method is called *roll pelletizing* and its operation is well documented in Windelhed (2000) and Lövgren et al. (2000). A prototype for full-scale experiments has been developed and the prototype, which is depicted in Figure 5.4, was tested at AssiDomän and Stora Enso during 1999. When the ash hydration procedure is finished the mixture of ash, dolomite and water ends up in a large bin. From this bin the mixture is transported to the three rollers shown in Figure 5.4. The first roll presses the mixture onto the conveyor belt yielding a homogenous bed plate; the second one forms strings of the bed plate and the third roll cuts these strings forming agglomerates. The results of the conducted trials at AssiDomän and Stora Enso are documented

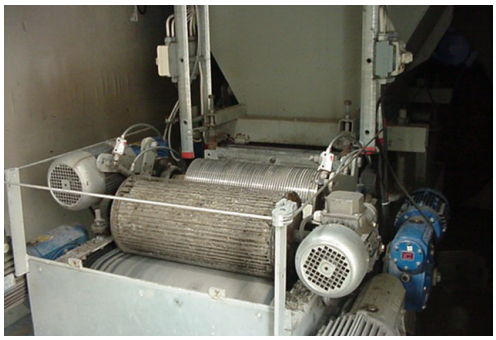

Figure 5.4: The roll pelletizer prototype, VAP-500, presented in Windelhed (2000).

in Windelhed (2000) and Lövgren et al. (2000). Both reports indicate good results; the method is claimed to be robust and the agglomerates produced fulfil the requirements from the Swedish National Environment Protection Board and the Swedish National Board of Forestry. The roll-pelletizing equipment has a capacity of 10 tons per hour (Lövgren et al., 2000), but the capacity can easily be lowered by changing the gearing of the electrical motors.

5.3 Selected Method

Based on the survey presented in Section 5.2, the roll-pelletizing technique is selected as the agglomeration method suitable for automated manufacture. To validate the assessment of the literature study, the prototype has been transported to Kalmar for initial experiments. At the same time, a possible correlation between the wood ash carbon content and the required water amount for each batch produced in the WAH procedure has been explored.

Conducted Experiments

For each batch produced, wood ash, dolomite and water is blended in the mixer and the change detection algorithm presented in Chapter 4 controls the water flow $Q(t)$. Some trials are also conducted to find out if the mixer needs to be thoroughly washed between each batch. The results of the initial experiments are presented in Table 5.1. During the experiments it has been verified that the change detection method works as expected. It is also noticed that the

Date	1/6	5/6	6/6	7/6	8/6
Required water amount [kg]	55.9	36.9	61.7	64.7	61.3
Ash carbon content [%]	[7.0, 7.3]	[14.3, 14.7]	[19.1, 19.5]	[22.3, 22.8]	[20.2, 20.6]
Threshold γ	0.2	0.2	0.2	0.2	0.2
ETEC-dolomite [kg]	100	100	100	100	100
Wood ash [kg]	100	100	100	100	100
Agglomerates accepted	–	Yes^a	Yes^b	Yes^b	Yes^b

Table 5.1: Results of initial experiments. Here the Bootstrap method discussed in the Appendix has been used to give a 95% confidence interval of the carbon content. A 'Yes' indicate that the agglomerates fulfill the quality requirements stated for a product suitable for recycling. The symbol – indicates that the sample is not analyzed due to human error. The superscript a indicates that the content of Phosphorus (P) is above the limit value. The superscript b indicates that the contents of Phosphorus (P) and Zinc (Z_n) are a little low (Holmberg, 2002).

water weight is approximately $20 - 30\%$ of the total weight of the dry mixture. This result is similar to the ones presented in Lindahl and Claesson (1996) and Lövgren et al. (2000). A sample of produced agglomerates is shown in Figure 5.5:

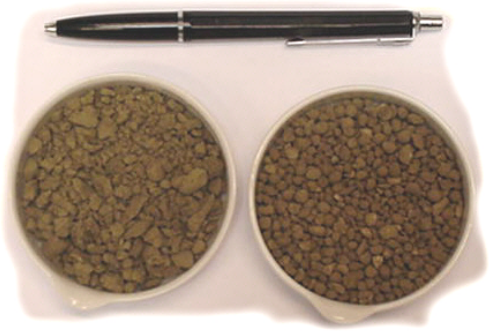

Figure 5.5: Agglomerates produced by the roll-pelletizing equipment are shown to the left. Reference granules to the right produced by the drum granulation method presented in Svantesson (2000).

The somewhat strange amount of water the 5^{th} of June may be explained by the fact that the mixing procedure is sometimes quite erratic. It may happen that some lumps may stick onto the mixer wall causing the normalized effective power $P_e(t)$ to make an abrupt jump that does not originate from a change in the mixture viscosity. To overcome this problem, it is of utmost importance that the mixer is properly washed before each batch produced. Furthermore, to aid proper detection of the change in the mixture viscosity dynamics, a safety net around the detection algorithm may be implemented that only enables the algorithm at a region where a change in the mixture viscosity dynamics is expected. This topic is further discussed in Section 5.4.

Despite the fact that a less amount of water than the optimum was used the 5^{th} of June, a batch of accepted agglomerates was produced. However, it could be inferred by visual inspection that the amount of small agglomerates was larger for this specific batch. Nevertheless, the method here proves its stated robustness; using a blend with a less amount of water than the optimum would not be possible when using a drum granulator. However, an amount of water *greater*

than the optimum is still as devastating as for a drum granulator; the mix will then stick onto the final roll and the conveyor belt shown in Figure 5.4 resulting in an inevitable process breakdown. Therefore, it is concluded that a mix using a smaller amount of water than the optimum is less problematic than using a mix where a larger amount is utilized.

Other experiments conducted during the test period are: to vary the amount of ETEC-dolomite in the recipe; to replace the ETEC-dolomite by two other limes that may be suitable, and to vary the threshold γ in the CUSUM-algorithm. The results of these experiments are shown in Table 5.2. As indicated in the previous chapter, using a threshold $\gamma_{CUSUM} = 0.3$ gives $ARL(\theta, \gamma, \nu) = 12.16$ and thus a more moistened mixture. This is validated in the experiment conducted June 12. Then the total amount of water is 66.3 kg, which gives a too moistened mixture for practical use. Furthermore, when comparing the obtained water amount June 8 in Table 5.1 to the similar information given in Table 5.2 at June 14, one concluding remark may be that it is the wood ash only, not the blend of ash and ETEC-dolomite that determines the viscosity dynamics. However, using only wood ash gives a mixture that is too wet when the change detection algorithm is terminated. On the other hand, this is intuitive since the blend used the 14^{th} of June has a solid/water ratio of 0.62 compared to 0.31 for the blend given in Table 5.2; to be able to use this specific batch in the roll–pelletizing equipment an additional amount of wood ash was added. It is also noticed that overwetting occurred using the lime "Nordkalk". Probably this was caused by the physical properties of this lime. Furthermore, this lime does not contain as much clay as the two others resulting in agglomerates less durable for physical stress.

It may also be inferred from the information given in the tables that there is no evident correlation between the wood ash carbon content and the used water amount.

Sieve Analysis

As stated earlier, the admissible agglomerate size distribution is that no more than 30% should have a diameter range *less* that 0.25mm and no more than 5% should have a diameter range *greater* than 8mm. To verify that the method based on roll-pelletization produces approved agglomerates, a sieve analysis is applied to each sample presented in Tables 5.1 and 5.2. The result is shown in

Date	11/6	12/6	13/6	14/6	15/6	18/6	20/6
Required water amount [kg]	47.4	66.3	58.5	61.3	33.2	53.6	69.0
Ash carbon content [%]	[12.6, 12.9]	–	[4.7, 4.9]	[5.7, 6.0]	[10.2, 11.0]	[8.7, 8.9]	[12.8, 13.3]
Threshold γ	0.2	0.3	0.2	0.2	0.2	0.2	0.2
ETEC-dolomite [kg]	50	50	50	0	50		
Trädgårdskalk [kg]						100	
Nordkalk [kg]							100
Wood ash [kg]	100	100	100	100	100	100	100
Agglomerates accepted	Yes^c	–	Yes	Yes	Yes	Yes^d	Yes^d

Table 5.2: Results of experiments varying the lime and threshold. Here the Bootstrap method discussed in the Appendix has been used to give a 95% confidence interval of the carbon content. A 'Yes' indicates that the agglomerates fulfill the quality requirements stated for a product suitable for recycling. The symbol – indicates that the sample is not analyzed due to human error. The superscript c indicates that the content of Phosphorus (P) is above the limit value and the superscript d indicates that the contents of Phosphorus and Zinc (Z_n) are low (Holmberg, 2002).

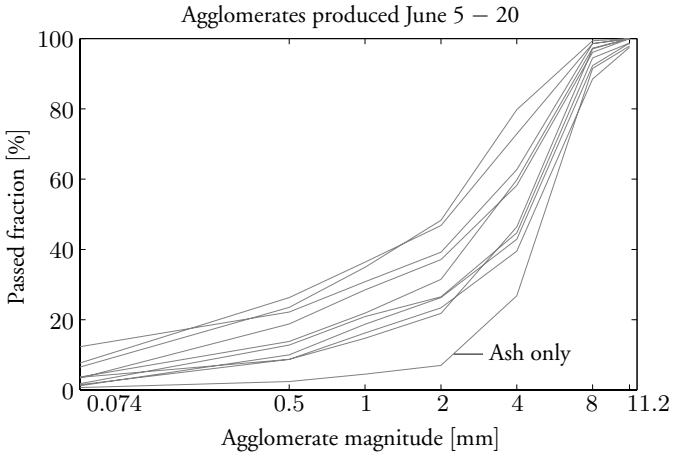

Figure 5.6: The result of a sieve analysis applied to the samples presented in Table 5.1 and 5.2.

Figure 5.6. It is clear from the figure that all samples comply with the demands of an admissable product. The obtained result is similar to other agglomeration techniques presented in for example (Nordenberg, 1996, p.27).

Conclusions

The roll-pelletization method is robust and well suited for automated manufacture. This agrees to what is reported in Windelhed (2000) and Lövgren et al. (2000). However:

- The mixture of ash dolomite and water does tend to stick onto the final roll of the roll-pelletizer and onto the conveyor belt,
- The capacity and size of the roll-pelletizer needs to be smaller,
- The agglomerates are quite brittle immediately after leaving the roll-pelletizer. This implies that the drying method to be selected must be lenient to the product.

However, during the Fall of 2001 the ”state of the art” roll-pelletizing equipment was modified to remove the problems outlined in the first two items. The modifications were conducted by Gert Nordström, AB Nordströms Konstruktionsbyrå; see Svantesson and Olsson (2002).

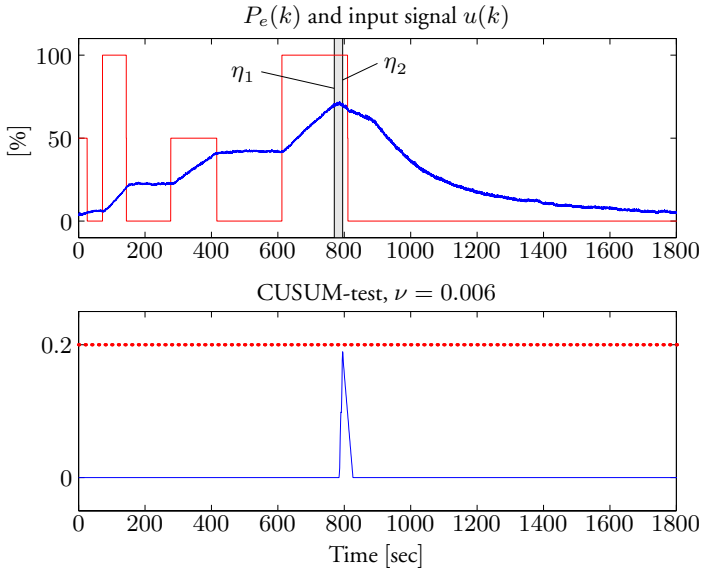

Figure 5.7: The strategy of triggering the change detection when $P_e(k) > 70\%$. It is clear that the shaded region (where the algorithm is enabled) is increasing if the threshold is decreased and vice versa. When using the threshold 70% the CUSUM $g(k)$ does not increase above the threshold $\gamma_{CUSUM} = 0.2$ and the hydration procedure fails.

5.4 Robust Change Detection

As indicated in Section 5.3, a safety net may be implemented that only enables the detection algorithm at a region where a change in the mixture viscosity dynamics is expected. Here different approaches applies and the most straightforward method is to only trigger the CUSUM-algorithm whenever, for example, $P_e(k) > 40\%$. The region when the change detection algorithm is enabled may be decreased by increasing this value. However, the drawback using this method is that when using a too high value, the change detection algorithm may produce inaccurate results. To illustrate this, the strategy is applied on one data set presented in the previous section; the result is shown in Figure 5.7. It is thus clear that it is necessary to implement a more sophisticated method in order to obtain a robust detector. An alternative, and better method to alter the lines η_1 and η_2 in Figure 5.7, is to use a timer and an upper bound for the

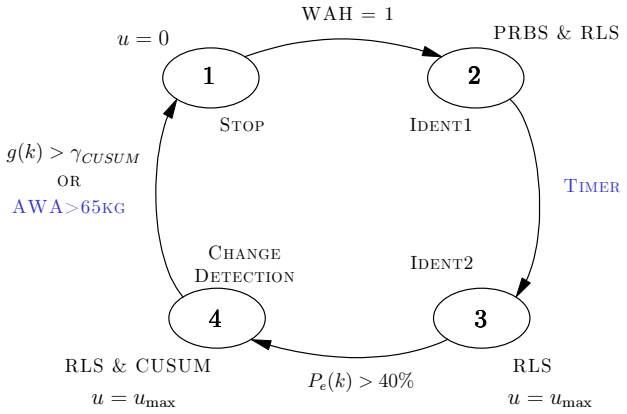

Figure 5.8: A robust implementation of the detection algorithm. An immediate transition to state 1 occurs if the WAH procedure takes too long time or if any vital hardware fails. This is not indicated in the figure.

Accumulated Water Amount (AWA) in the hydration procedure. The scheme of such an implementation is shown in Figure 5.8. In this approach, the control scheme starts in state 1 and moves to state 2 when a batch is to be produced. In state 2, the initial system identification procedure is carried through using the PRBS and RLS; a timer is used to adjust the length of this initial identification. It should also be noticed that the detection algorithm is triggered when $P_e(k) > 40\%$. This value seems to guarantee an adequate performance of the detector. Furthermore, if this timer-value is high enough, the control algorithm will immediately make a transition to state 4. Hence, these two parameters affect the line η_1. Furthermore, the line η_2 is affected by the upper bound on the AWA. Obviously it is possible to create an interval $[\eta_1, \eta_2]$ that includes the critical effective power P_e^{crit} by varying either the timer, the trigger value on $P_e(k)$ or the upper bound AWA.

5.5 Summary and Concluding Remarks

In this chapter, we conclude that the roll-pelletizing method for wood ash agglomeration is found to be the superior method in all categories. The process unit is simple, robust and no advanced automatic control is necessary for its operation. It is also verified that the produced agglomerates fulfil the quality

requirements stated for a product suitable for recycling. However, some parts of the roll-pelletizing equipment must be redesigned in order to be fully adapted to automated manufacture:

- The last of the three rolls needs to be modified. For example, in Lövgren et al. (2000) this roll was not used at all due to lack of functionality.
- The conveyor belt material needs to be replaced by another one with a smoother surface to prevent the agglomerate from sticking onto the belt.

During the Fall of 2001 the "state of the art" roll-pelletizing equipment was modified to eliminate these problems. More details are given in Svantesson et al. (2001) and Svantesson and Olsson (2002). Furthermore, regarding the change detection we conclude the following:

- Between each batch the mixer must be washed. This is crucial due to several reasons: Firstly, if the mixer is not properly washed between each batch a superstructure will occur. Sooner or later this residue must be removed manually, which is a cumbersome task for the operators. Secondly, if the mixer is not washed the normalized effective power $P_e(t)$ for the mixer may be as high as 100% at the beginning of the WAH procedure. Then no useful information will be available for the detection algorithm.
- It is noticed that overwetting occurred only three times during the series of experiments: when the threshold $\gamma_{CUSUM} = 0.3$ was used; when no dolomite was used; and when the lime "Nordkalk" was used. Hence, these conditions are not present during normal operating conditions. A safety network around the detection algorithm has been implemented. This ensures that the algorithm is enabled only in a region where there is an expected change in the mixture viscosity dynamics. Thus, there is a guarantee that no apparent overwetting or underwetting occurs, as described in Section 5.4.
- Hence, if the water-to-ash ratio does not show any apparent changes over a year, which is the case at the central heating plant "Draken" of Kalmar, a foolproof approach is to use the detection algorithm only once to determine a proper ratio. The WAH procedure may then be controlled by a simple weighing-in of water.

- The dolomite is important from two perspectives. Firstly, if no dolomite is used, a product with insufficient nutrient content and inadequate pH is formed (Holmberg, 2000). Secondly, due to the dolomite (or possibly any other suitable solid) the mixture moisture content is adequate for agglomeration when the abrupt change in the mixture viscosity dynamics is detected.

It is also inferred that there is no evident correlation between the wood ash carbon content and the used water amount. Furthermore, the water used to wash the mixer may be recycled in the WAH procedure of the following batch. See Appendix B for a practical solution of such an approach.

Appendix

5.A The Bootstrap Method

The bootstrap is a powerful technique for assessing the accuracy of a parameter estimator in situations where conventional techniques are not valid. This section contains a brief introduction to the basic ideas. More profound material on this topic is to be found in for example Efron and Tibshirani (1993), Hall (1988), Zoubir and Boashash (1988) and Zoubir (1993). Furthermore, the *Bootstrap Matlab Toolbox* (Zoubir and Iskander, 1998) is here used to illustrate the use of Bootstrap techniques for the estimation of wood ash carbon content.

Basic Principle

Let $\mathcal{X} = \{X_1, \ldots, X_n\}$ be a sample, i.e., a collection of n numbers drawn at random from a completely unspecified distribution F. By "at random" it is meant that the samples X_i are *independent* and *identically distributed* random variables, each having distribution F. Let μ denote the mean of the samples X_i. The problem considered in this section is to find the distribution of μ, an estimator of μ, derived from the sample $\mathcal{X}$. A way to obtain the distribution of μ or its characteristics is to repeat the experiment a sufficient number of times and approximate the distribution of μ by the so obtained empirical distribution. In many practical applications this method is inapplicable for cost reasons or because the experimental conditions are not reproducible.

Algorithm 5.A.1: The Bootstrap Principle

1. Conduct the experiment to obtain the random sample $\mathcal{X} = \{X_1, .., X_n\}$ and calculate the estimate $\hat{\mu}$ from the sample $\mathcal{X}$.
2. Construct the empirical distribution, $\widehat{F}$, which puts equal weight $1/n$, at each observation, $X_1 = x_1$, $X_2 = x_2, \ldots, X_n = x_n$.
3. From the selected $\widehat{F}$, draw sample, $\mathcal{X}^* = \{X_1^*, \ldots, X_n^*\}$, called the bootstrap (re)sample.
4. Approximate the distribution of $\hat{\mu}$ by the distribution of $\hat{\mu}^*$ derived from $\mathcal{X}^*$.

The bootstrap paradigm suggests that we resample from a distribution chosen to be close to F in some sense, for example, the sample (or empirical) distribution $\widehat{F}$ that approaches F as $n \to \infty$. Note that the choice of $\widehat{F}$ is not unique; any distribution that approaches F as $n \to \infty$ can be used.

Confidence interval of the mean

Let $X_1, \ldots, X_n$ be n independent and identically distributed random variables from some unknown distribution, and suppose we wish to find an estimator and a $(1-\alpha)100\%$ interval for the mean μ. Usually, we estimate μ by the sample mean

$$\hat{\mu} = \frac{X_1 + \cdots + X_n}{n} \tag{5.A.1}$$

A *confidence interval* for μ can be found by determining the distribution of $\hat{\mu}$ (over repeated samples of size n from the underlying distribution), and finding values $\hat{\mu}_L$ and $\hat{\mu}_U$ such that

$$\Pr[\hat{\mu}_L \leq \mu \leq \hat{\mu}_U] = 1 - \alpha \tag{5.A.2}$$

However, the distribution of $\hat{\mu}$ depends on the distribution of the random variables X_i, which is unknown. In the case where n is large the distribution of $\hat{\mu}$ could be approximated by the normal distribution with the *central limit theorem* (Kendall and Stuart, 1967, Manoukian, 1986). The bootstrap paradigm

suggests that we assume that the sample $\mathcal{X} = \{X_1, \ldots, X_n\}$ itself constitutes the underlying distribution; then by resampling from $\mathcal{X}$ many times and computing $\hat{\mu}$ for each of these resamples, we get a *bootstrap distribution* for $\hat{\mu}$ that approximates the actual distribution of $\hat{\mu}$, and from which a confidence interval for μ is derived. This procedure is described in Algorithm 5.A.1. We now illustrate the basic idea by an example, which was originally given in Zoubir and Boashash (1988).

Example 5.A.1 $-$ ***Bootstrap for calculating a confidence interval for the mean***

Step 0 $-$ Conduct the experiment: Suppose our sample is

$$\mathcal{X} = \{-2.41, 4.86, 6.06, 9.11, 10.20, 12.81, 13.17, 14.10, 15.77, 15.79\}$$

of size 10, with $\hat{\mu} = 9.946$ being the mean of all values in $\mathcal{X}$.

Step1 $-$ Resampling: Using a pseudo-random number generator, draw a random sample of 10 values, with replacement, from $\mathcal{X}$. Thus, one might obtain the bootstrap resample

$$\mathcal{X}^* = \{9.11, 9.11, 6.06, 13.17, 10.20, -2.41, 4.86, 12.81, -2.41, 4.86\}$$

Note that some of the original sample values appear more than once, and others not at all.

Step2 $-$ Calculation of the *bootstrap estimate:* Calculate the mean of all values in $\mathcal{X}^*$. The mean of all values in $\mathcal{X}^*$ is $\hat{\mu}_1^* = 6.54$.

Step3 $-$ Repetition: Repeat Steps 1 and 2 a large number of times to obtain a total of N bootstrap estimates $\hat{\mu}_1^*, \ldots, \hat{\mu}_N^*$. For example, let $N = 1000$.

Step4 $-$ Approximation of the distribution of $\hat{\mu}$: Sort the bootstrap estimates into increasing order to obtain $\hat{\mu}_{(1)}^* \leq \hat{\mu}_{(2)}^* \leq \cdots \leq \hat{\mu}_{(N)}^*$, where $\hat{\mu}_{(k)}^*$ is the kth smallest of $\hat{\mu}_1^*, \ldots, \hat{\mu}_N^*$. For example, we might get $3.39, 3.48, 4.46, \ldots, 8.86$, $8.88, 8.89, \ldots, 10.07, 10.08, \ldots, 14.46, 14.53, 14.66$. A histogram of the obtained bootstrap estimates $\hat{\mu}_1^*, \ldots, \hat{\mu}_N^*$ will thus be obtained.

Step5 $-$ Confidence interval: The desired $(1-\alpha)100\%$ bootstrap confidence interval is $(\hat{\mu}_{(q_1)}^*, \hat{\mu}_{(q_2)}^*)$, where q_1 is the integer part of $N\alpha/2$ and $q_2 = N - q_1 + 1$. For $\alpha = 0.05$ and $N = 1000$, we get $q_1 = 25$ and $q_2 = 976$ and the 95% confidence interval is found to be $[6.27, 13.19]$.

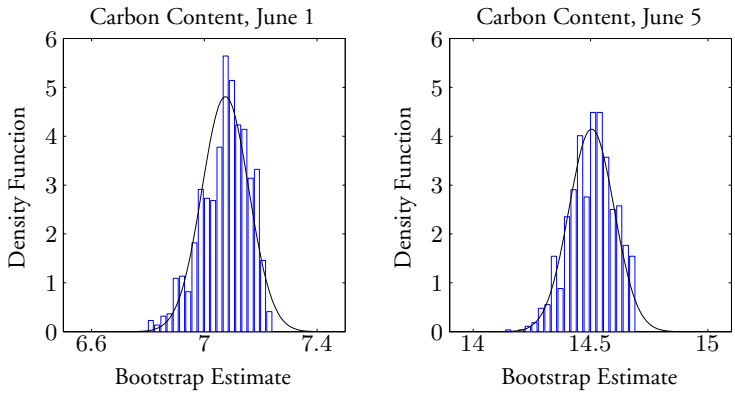

Figure 5.1: Histogram of $\hat{\mu}_1^*, \ldots, \hat{\mu}_{1000}^*$ based on the random sample $\mathcal{X}$. The solid line indicates the normal distribution $\mathcal{N}(\hat{\mu}, \hat{\sigma}^2)$.

The example of confidence interval estimation presented above can simply be evaluated using the following bootstrap command in the Bootstrap Matlab Toolbox (Zoubir and Iskander, 1998)

$$[\texttt{muL}, \texttt{muU}] = \texttt{confinth}(\texttt{X},\texttt{'mean'}, 0.05, 1000)$$

This approach is applied when estimating the wood ash carbon content given in Tables 5.1 and 5.2. At each batch produced five independent wood ash samples were taken. For example, the procedure applied to the wood ash sample

$$\mathcal{X} = \{7.15,\ 7.26,\ 7.06,\ 7.18,\ 6.73\}$$

collected June 1 gives a 95% confidence interval of $[7.0, 7.3]$ $\%$ of unburnt carbon. The same procedure applied to the wood ash sample collected June 5 gives a 95% confidence interval of $[14.3, 14.7]$ $\%$ of unburnt carbon as given in Table 5.1. A histogram of $\hat{\mu}_1^*, \ldots, \hat{\mu}_N^*$ is shown in Figure 5.1, where $N = 1000$ is used. However, it is important to remember that the bootstrap cannot create more information than is contained in the measurements, but it can compute variability measures numerically, which are as good as analytically derived point estimates. In simple words, the bootstrap does with a computer what the experimenter would do in practice if it were possible: he or she would repeat the experiment.

Chapter 6

Controller Design, Analysis and Implementation

As always, it is the total effort of process & control system design and cost that is the final goal. In the previous chapter it was concluded that the recently developed *roll-pelletizing* method for wood ash agglomeration is the superior method in all categories. This process unit is simple, robust and, hence, no advanced automatic control is necessary for its operation. This demonstrates the kind of compromise between process design and control system design that ought to take place more often in process control; a complex control problem can often be simplified by a change in process design. However, in numerous of process designs there is a need for several of control problems to be solved. Then controller design, analysis and implementation have to be targeted, and this chapter is dedicated to these issues.

6.1 Introduction

Some control loops have to be applied to make the ash transformation process automatic. In all implementations of these, a computer is used to control the process; see Chapter 8. However, the design and analysis of a controller may be conducted in continuous time. A straightforward approach is then to use a short enough sampling interval and to make some discrete-time approximations of the continuous-time controller. Therefore, to implement a continuous-time control law – such as, for example, a PID-controller – in a digital computer, it is necessary to approximate the derivatives and the integral that appears in

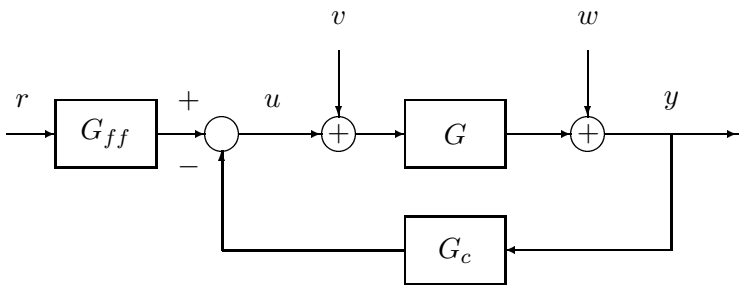

Figure 6.1: Block diagram describing the design problem.

the control law. Different ways to do so are presented in Åström and Wittenmark (1997), Svantesson, Hultgren and Johansson (1998) and Åström and Hägglund (1995). In this thesis, mainly PID type controllers are proposed to control the transformation process. This controller is todays most commonly used control algorithm, see Yamamoto and Hashimoto (1991), and has proven to be sufficiently versatile for the control tasks in this process. For this reason, the evaluation and tuning of such controllers are treated in this chapter as well. Tuning issues are more thoroughly discussed in, Lennartson (2001), Panagopoulos (2000) and Kristiansson (2000). In this thesis the PID-control design presented in Panagopoulos (2000) is exclusively used.

6.2 PID-Controller Design

The design problem is illustrated in Figure 6.1. A process with a transfer function G is controlled with a PID-controller with *two degrees of freedom*, see (Horowitz, 1963). The transfer function G_c describes the feedback from process output y to control signal u, and G_{ff} describes the feedforward from setpoint r to u. The external signals act on the control loop, namely setpoint r, load disturbance v and measurement noise w. The design objective is to determine the controller parameters in G_c and G_{ff} so that the system behaves well with respect to changes in the three external signals as well as in the process model G. Thus, the specification will express requirements on: load disturbance response, measurement noise response, set point response and the robustness with respect to model uncertainties.

The formulation of this design problem can loosely be divided into two categories: specifications on *performance* and *robustness*. The first specification takes care of the rejection of load disturbances, measurement noises, at the same time as a good set point following is obtained. The second specification takes care of the sensitivity to model uncertainties. Initially, the controller is described by

$$u(t) = k\left(br(t) - y(t)\right) + k_i \int_0^t \left(r(\tau) - y(\tau)\right) d\tau - k_d \frac{dy(t)}{dt} \tag{6.1}$$

where k, k_i, k_d, and b are controller parameters. To be more specific, the notation is $k = K$, $k_i = K/T_i$ and $k_d = KT_d$, where K is a proportional gain, T_i is the integration time, T_d is the derivative time and the parameter b is a set point weight. In this context, the feedforward transfer function is formulated as a PI controller

$$G_{ff}(s) = K\left(b + \frac{1}{sT_i}\right) \tag{6.2}$$

and the transfer function from the process variable y to the control variable u is given by

$$G_c(s) = K\left(1 + \frac{1}{sT_i} + sT_d\right) \tag{6.3}$$

If it is needed, the signals y and r can be replaced by their filtered values y^f and r^f, see Panagopoulos (2000). The filtered signals are then generated by

$$Y^f(s) = F_y(s)Y(s) \tag{6.4}$$
$$R^f(s) = F_r(s)R(s) \tag{6.5}$$

where the filters are low pass filters of first or second order. The controller can thus be characterized by either the three or four parameters k, k_i, (k_d), b and the two filters F_y, F_r.

Load Disturbance Rejection

This can be conveniently expressed in terms of the Integrated Absolute Error (IAE) due to a load disturbance in the form of a unit step at the process input, i.e.

$$IAE = \lim_{t\to\infty} \int_0^t |e(\tau)|\, d\tau = \lim_{t\to\infty} \int_0^t |r(\tau) - y(\tau)|\, d\tau \tag{6.6}$$

This criterion is difficult to deal with analytically because the evaluation requires significant computations. The Integrated Error (IE) defined by

$$IE = \lim_{t\to\infty} \int_0^t e(\tau)d\tau = \lim_{t\to\infty} \int_0^t \left(r(\tau) - y(\tau)\right) d\tau \tag{6.7}$$

is much more convenient. In Åström and Hägglund (1995) it is shown that $IE = 1/k_i$. Thus the criterion IE is directly given by the integrating gain of the controller. Hence, $IAE = IE$ if the error is positive. Furthermore, if the system is well damped the criteria will be close to each other which, in our case, will be ensured by the sensitivity constraints presented in the next subsection.

Sensitivity to Modeling Errors

This can be expressed in terms of the largest value of the so called *sensitivity function*. Let the loop transfer function be $L(s) = G_c(s)G(s)$, and define the sensitivity function as

$$S(s) = \frac{1}{1 + L(s)} = \frac{1}{1 + G_c(s)G(s)} \tag{6.8}$$

The *maximum sensitivity* is then given by

$$M_S = \max_{\omega} |S(i\omega)| = \frac{1}{\min_{\omega} |1 + L(i\omega)|} \tag{6.9}$$

It is thus clear that the quantity M_S is the inverse of the shortest distance from the *Nyquist curve* of the loop transfer function to the critical point $(-1, 0)$. Typical values of M_S are in the range of $1.2 - 2.0$ (Lennartson, 2001). Furthermore, with this constraint on M_S it follows from the *circle criterion* (Khalil, 1992, Section 10.1.1) that the closed loop system will also remain stable even if a static nonlinearity $f(x)$ characterized by

$$M_S/(M_S + 1) < \frac{f(x)}{x} < M_S/(M_S - 1) \tag{6.10}$$

is inserted in the loop. A small value of M_S thus ensures that the closed loop system will remain stable in spite of nonlinear actuator characteristics. There is a close relationship between the maximum peak M_S and the gain and phase

margins as well. Specifically, for a given M_S, we are guaranteed (Skogestad and Postlethwaite, 1996)

$$A_m \geq \frac{M_S}{M_S - 1}; \qquad \varphi_m \geq 2 \arcsin\left(\frac{1}{2M_S}\right) \tag{6.11}$$

Typical values of φ_m range from 30° to 60°. Gain margins could typically vary from 2 to 5. Hence, a geometrical interpretation of the criterion given by equation (6.9) is that the Nyquist curve of the loop transfer function is always outside a circle around the critical point $(-1, 0)$ with the radius $1/M_S$. The sensitivity can also be expressed as the largest value of the *complementary sensitivity function* $T(s) = 1 - S(s)$, i.e.

$$M_T = \max_\omega |T(i\omega)| = \max_\omega \left|\frac{L(i\omega)}{1 + L(i\omega)}\right| \tag{6.12}$$

Typical values of M_T are suggested in the literature to be in the range $1.0 - 1.5$.

Measurement Noise

In traditional PID-controllers the filters are often only applied on the derivative term. A common choice is to use a derivative term

$$-\frac{KT_d s}{1 + s\frac{T_d}{N}} Y(s) = -\frac{k_d s}{1 + s\frac{k_d}{kN}} Y(s) \tag{6.13}$$

in the controller, where N is a number in the range $2 - 10$. The modification can be interpreted as the ideal derivative filtered by a first-order system with the time constant T_d/N. The modification acts as a derivative for low-frequency signal components and will reduce the high frequency gain of the controller to be $k(1 + N)$. When, however, there is substantial measurement noise, it is useful to filter the measurement signal even more with a filter, for example, given by

$$F_y(s) = \frac{1}{1 + sT_f} \tag{6.14}$$

The choice of filter time constant T_f in equation (6.14) is a trade-off between filtering capacity and loss of performance. A large value of T_f provides an effective noise filtering, but deteriorates the control performance. On the contrary, a small value of T_f keeps the control performance, but with less efficient noise

filtering. Inserting a filter modifies the loop transfer function, which gives minor changes in control loop performance. Consequently, adjusted controller parameters are obtained simply by repeating the design with the process G replaced by the transfer function $F_y G$. Simulation examples and more details on this filtering approach are given in Panagopoulos (2000).

Set Point Response

The design has so far focused on the response to load disturbances, which is of primary concern. However, it may also be important to have a good response to set point changes. One way to give specifications on the set point response is to consider the transfer function from set point r to process output y given by

$$\begin{aligned} G_{ry}(s) &= \frac{G(s)G_{ff}(s)}{1+G(s)G_c(s)} \\ &= \frac{bks+k_i}{k_d s^2+ks+k_i}\frac{G(s)G_c(s)}{1+G(s)G_c(s)}\frac{F_r(s)}{F_y(s)} \end{aligned} \tag{6.15}$$

where the filter F_r is given by

$$F_r(s) = \frac{1}{1+sT_r} \tag{6.16}$$

Generally, in order to have a small overshoot, the set point weight b and filter F_r must be determined such that the resonance peak of the transfer function G_{ry},

$$M_{ry} = \max_{\omega} |G_{ry}(i\omega)| \tag{6.17}$$

is close to one. Further details are given in Panagopoulos (2000).

PID Design

The method for designing PID-controllers will now be presented. It is given by

$$\begin{array}{ll} \max & k_i \\ \text{such that} & f \geq R^2, \quad \kappa < 0, \quad \delta < 0 \end{array} \tag{6.18}$$

where the function $f(k, k_i, k_d, \omega) \geq R^2$ with $R = 1/M_S$ expresses the robustness constraint that the Nyquist curve of the loop transfer function $L(i\omega)$ must

lie outside a circle with center -1 and radius R. Furthermore, κ is the curvature of the loop transfer frequency function $L(i\omega)$, and δ is the difference in phase change of $L(i\omega)$ at two consecutive frequency points. Consequently, the first constraint in equation (6.18) expresses the sensitivity condition, the second constraint specifies that a negative curvature of $L(i\omega)$ should be obtained and the third constraint prevents $L(i\omega)$ to have undesirable phase leads.

For systems with integral action or close to integral action, i.e. a pole relatively close to zero, the second constraint in equation (6.18) is, however, too severe. It is appropriate to omit the constraint in these cases. Consequently, the design of PID-controllers is separated into two cases depending on the considered system. This separation between integrating and non-integrating processes is done in several previous design methods as well, see Åström and Hägglund (1995).

6.3 Implementation Methods

Practically all control systems that are implemented today are based on digital computers. In order to implement the PID-controller outlined in the previous section, the control algorithm must be discretized. In continuous controller design, the controller itself is discretized. Given a sufficiently short *sampling time*, the time derivatives can be approximated by a finite difference and the integral by a summation. This approach will be used here. Other approaches for computer control, which base the control directly on *discrete-time models*, are presented in for example Åström and Wittenmark (1997) or Franklin et al. (1998).

Computer-Control

A computer controlled system can be described schematically as in Figure 6.2. The output from the process $y(t)$ is usually a continuous-time signal. The output is converted into digital form by the A-D converter. The A-D converter can be included in the computer or regarded as a separate unit, according to one's preference. The conversion is made at the sampling times, t_k. The computer interprets the converted signal, $\{y(t_k)\}$ as a sequence of numbers, processes the measurements using an algorithm, and produces another sequence of "decision" or "control-variables", $\{u(t_k)\}$. This sequence is converted to an analog signal by a Digital-to-Analog (D-A) converter. The events are synchronized by the

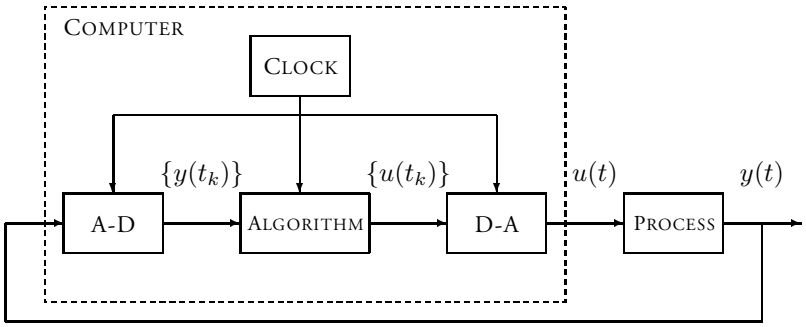

Figure 6.2: Schematic diagram of a computer controlled system.

real-time clock in the computer and the digital computer operates sequentially in time and each operation takes a certain amount of time. The D-A converter must, however, produce a continuous-time signal. This is normally done by keeping the control signal constant between the conversions. In this case the systems runs open loop in the time interval between the sampling instants, because the control signal is constant irrespective of the values of the output. However, if the time interval between the sampling instants is short compared to the process dynamics, this will not deteriorate the performance of the control system (Åström and Wittenmark, 1997).

The Selection of Sampling Interval

The choice of sampling time depends on many factors. One way to determine the sampling period is to use continuous-time arguments (Åström and Wittenmark, 1997): the sampled system can be approximated by the hold circuit, followed by the continuous-time system. For small sampling intervals, the transfer function of the hold circuit can be approximated as

$$\frac{1-e^{-sh}}{sh} \approx \frac{1-1+sh-\frac{s^2h^2}{2}+\cdots}{sh} = 1-\frac{sh}{2}+\cdots \tag{6.19}$$

The first two terms correspond to the series expansion of $\exp(-sh/2)$. That is, for small h, the hold can be approximated by a time delay of half a sampling interval. If we assume that the phase margin can be decreased 5° to 15°, this

then gives the following rule of thumb

$$h\omega_c \approx 0.15 - 0.5 \tag{6.20}$$

where ω_c is the loop gain cross-over frequency (in radians per seconds), see Åström and Wittenmark (1997). For example $h\omega_c = 0.35$ gives a sample rate that is in the order of 20 times the bandwidth of the closed loop system.

Integrator Windup

Although many aspects of a control system can be understood based on linear theory, some nonlinear effects must be accounted for. For example, all actuators have limitations: a motor has limited speed, a valve cannot be more than fully opened or fully closed, etc. However, for a control system with a wide range of operating conditions, it may happen that the control variable reaches the actuator limits. When this happens the feedback loop is broken and the system runs as in open loop because the actuator will remain at its limit independently of the process output. If a controller with integrating action is used, such as a PID-controller, the error will continue to be integrated. This means that the integral term may become very large, or colloquially, it "winds up". It is then required that the error has opposite sign for a long period of time before things turn to normal. The consequence is that any controller with integral action may give large transients when the actuator saturates.

Many solutions are presented in the literature to overcome this problem, see for example Åström and Hägglund (1995), Olsson and Piani (1992), Åström and Wittenmark (1997), Elmqvist et al. (1981) and Svantesson, Hultgren and Johansson (1998). However, in this thesis the implemented control algorithm is the one presented in Svantesson, Hultgren and Johansson (1998). Successful use of this control code implementation, which is outlined in Algorithm 6.1, has been reported in Svantesson and Hultgren (2002).

Algorithm 6.1: PID-Control with Anti-Windup

1. Read the analog input from the A-D converter. Evaluate the control error $e(k) = r(k) - y(k)$.

2. $x(k) = x(k-1) - \frac{hN}{T_d+hN}\left(x(k-1) + y(k)\right)$
3. $u_{lead}(k) = -KN\left(x(k) + y(k)\right)$
4. $u(k) = K\left(br(k) - y(k)\right) + u_I(k-1) + u_{lead}(k)$
5. $v(k) = \min\left(\max\left(u(k), v_{\min}\right), v_{\max}\right)$
6. Set the output value $v(k)$ to the D-A converter.
7. $u_I(k) = u_I(k-1) + \frac{Kh}{T_i}e(k) + \gamma\left(v(k) - u(k)\right)$

Here $x(k)$ is the value of x, which is an internal variable, at t_k, h is the sample interval $t_{k+1} - t_k$, $y(k)$ is the measurement signal, u_I is the integral part of the control signal (using backward approximation), u_{lead} is the lead part of the control signal, $v_{\min}$, $v_{\max}$ are the minimum and maximum control signal respectively, $v(k)$ is the control signal written to the D-A converter and $\gamma \in [0, 1]$ is a parameter varying the influence of the anti-windup scheme; $\gamma = 1$ gives the fastest windup protection and thus $\gamma = 0$ gives none. The algorithm uses the previous value of the integral part, $u_I(k-1)$, in the control signal computations. However, since the sample time is selected to be relatively small, no serious deterioration in the performance is obtained.

6.4 Summary and Concluding Remark

This chapter deals with the issue of design, evaluation and implementation of PID-controllers; the todays most commonly used control algorithm. A survey of the new design method presented in Panagopoulos (2000) is outlined since this tuning method is used in the temperature control problem given in Chapter 7. Furthermore, since practically all control systems that are implemented today are based on computers, the control algorithm must be discretized. Given a sufficiently short sampling time, the time derivatives can be approximated by a finite difference and the integral by a summation. Using these approaches, a discretized PID-controller is developed. The issue of integrator windup and the selection of sampling interval have been discussed as well.

Chapter 7

Agglomerate Dehydration

7.1 Introduction

Drying is simply the process of moisture removal from a product. It can be performed by various methods for a variety of different substances from solids to gases and even liquids (Hall, 1980). Water is often removed from gases by absorption, as in the removal of water vapor from solids by capillary action. Drying can also be achieved mechanically by compression, centrifugal forces or gravity. However, *thermal drying* is the form most commonly used for the drying of for example agricultural products. It involves vaporization of moisture within the product by heat and its subsequent evaporation from the product. Thus, thermal drying involves simultaneous heat and mass transfer. The sensible heat of the drying air is reduced as it is utilized for moisture evaporation. However, the total heat content remains constant, since this loss of sensible heat is regained as latent heat of vaporization of the moisture now present in the air.

In this chapter, a new method for thermal drying of wood ash agglomerates is presented. First, the today adopted method based on self-hardening is discussed followed by an introduction to basic drying concepts. Next, the drying assumptions are presented and the delicate issue of dryer selection is dealt with. Further, temperature and moisture control are discussed and the results from the conducted full-scale tests are presented. The chapter finishes with a summary and concluding remark.

7.2 The Existing Method based on Self-Hardening

As reported in Windelhed (1998a) and Lövgren et al. (2000), the method for agglomerate dehydration mostly applied today is based on the so called *self-hardening* principle: the produced agglomerates are ejected into a platform lorry. When this lorry is fully loaded, the agglomerates are transported and dumped in large heaps at an intermediate storing facility; this is where the actual self-hardening occurs. However, in Lövgren et al. (2000) it is concluded that the time required for the self-hardening process to be successful is approximately *one month* at a temperature of 0 deg C. Furthermore, the method has several other drawbacks:

- To prevent that large lumps will be formed in the platform lorry, it is of utmost importance to empty this lorry some hours after the first agglomerates have entered (Lövgren et al., 2000). For example, this may imply that the lorry has to be transported and evacuated $5 - 10$ times a day, depending on the capacity of the transformation process.
- If the wood ash contains a large amount of unburnt carbon, this will decelerate the self-hardening process for agglomerates with no binding agent (Nilsson, 1993, Windelhed, 1998b).
- One has to be very careful not to re-hydrate the agglomerates at the storing facility, since this may cause leaching of the fertilizing substances. Therefore, the agglomerates must not be hydrated by rain, which implies that some kind of roof has to be used. This roof must, however, enable the water to evaporate freely and not re-hydrate the agglomerates through dropping caused by condensation at the roof.
- The floor at the storing facility must be properly drained. If not, the agglomerates are re-hydrated from underneath.

These drawbacks imply that a new method is desired; a drying method suitable for automated manufacture. Hence, fast and effective dehydration of the ash agglomerates gives the possibility of immediate packing and distribution.

To the best of the authors knowledge, prototype dryers for dehydration of wood ash agglomerates are only presented in Nordenberg (1996) and Svantesson (2000), where the solution to be found in Nordenberg (1996) is a batch

dryer based on microwave heating and the solution presented in Svantesson (2000) is based on a belt dryer heated by hot air. However, Nordenberg concludes that microwave heating is too expensive to be a tractable choice in an ash recycling process. Furthermore, operating problems such as ineffective drying has been reported in Svantesson (2000). The delicate issue of dryer selection is thoroughly treated in Section 7.5.

Originally, the idea was to use the flue gas produced during combustion to dehydrate the agglomerates. This approach is quite attractive, since then there is no need to produce any extra energy at the drying procedure. Further advantages of using flue gases are documented in Holmberg et al. (2001). The flue gas at the central heating plant Draken, which has a temperature of 140-190 deg C, is today not used for anything and is therefore discharged immediately. In Holmberg et al. (2001) it is inferred that no negative effects are obtained using flue gases as drying agent compared to using hot air only. The main obstacle is that a dryer to be used with flue gases becomes quite expensive compared to one that operates with hot air; the reason for this is that the dryer then has to be made out of stainless steel to prevent corrosion. The importance of this drawback is however dependent on the size of the installation. But for the small scale setup in Kalmar the problem becomes apparent. Another obstacle is that it is not trivial to implement an interface to the flue gas channel. Therefore, a decision was made to continue using hot air as drying agent. However, the hot air generator presented in Svantesson (2000), which used diesel to produce the necessary heat, is to be replaced by an industrial electric heater.

Initial Drying Tests in the Lab

To investigate what operating conditions that might be suitable for the dryer, a small laboratory experiment was conducted. The aim was to verify that a drying temperature of 70 deg C is adequate, and to investigate what drying time is necessary to obtain physically hardened agglomerates. A mix of 0.1 kg of lime and 0.1 kg of wood ash was blended and 0.05 kg of water was added to that mix. This means that $X_{wb} = 20\%$ and $X_{db} = 25\%$; see Section 7.3. A small laboratory drum granulator was used and the granules were dehydrated in a furnace using a drying air temperature of 70 deg C; the airflow was unknown.

The granule sample to be dried had an initial weight of 160 g. Periodically, each five minute the sample was removed from the furnace and its weight was

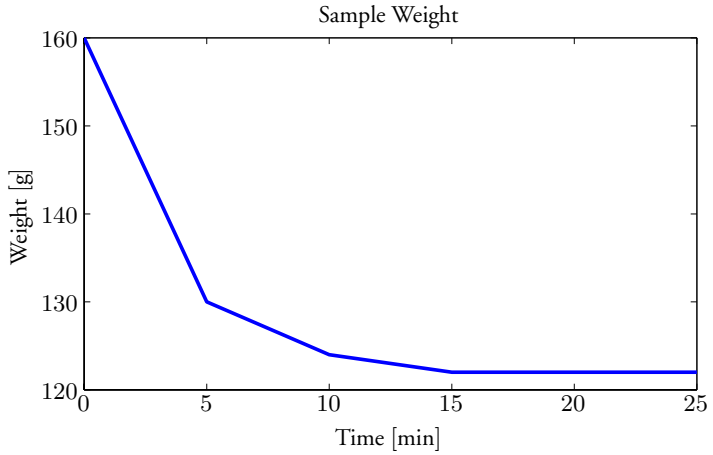

Figure 7.1: The result of an initial drying test in the lab.

measured. Furthermore, the granule hardness was estimated by using physical stress. The obtained weight vs. time is shown in Figure 7.1: at five minutes the smallest agglomerates were hard and looked gray. The larger ones were still moistened and thus brittle and had a somewhat darker color; at ten minutes the agglomerates with a size distribution similar to the ones produced with the agglomeration method presented in Chapter 5 were hard and looked gray as well; at fifteen minutes the largest agglomerates were harder and at 25 minutes all agglomerates were physically hardened. However, some remarks: Firstly, it is important that the blend of ash and dolomite is properly wetted; if too small an amount of water is used the finished product is unnecessary brittle. Secondly, since the agglomerates produced in this setup were more porous, the drying rate may be slower using the agglomerates produced with the roll-pelletizer method. From the figure it may be inferred that, for the used granule sample, the main part of drying occurs within the first ten minutes and that all water is evaporated after $15 - 20$ minutes, which seems to be a proper drying time.

7.3 Basic Drying Concepts

Moisture Content

The quantity of moisture present in a material can be expressed either on the *wet basis* or *dry basis* and expressed either as decimal or percentage. According

to Lewis (1990), the Moisture Content (MC) on the wet basis is the weight of moisture present in a product per unit weight of the undried material, represented as

$$X_{wb} = \frac{W_o - W_d}{W_o} = \frac{\text{mass of water}}{\text{mass of sample}} = \frac{\text{mass of water}}{\text{mass of water } + \text{ solids}} \tag{7.1}$$

where W_o is the initial weight of undried product (kg) and W_d is the weight of dry matter in product (kg). The moisture content on the dry basis is the weight of moisture present in the product per unit weight of dry matter in the product and represented as

$$X_{db} = \frac{W_o - W_d}{W_d} = \frac{\text{mass of water}}{\text{mass of solids}} \tag{7.2}$$

Thus, X_{db} varies linearly and X_{wb} varies nonlinearly with moisture. Furthermore, the moisture contents on the wet and dry bases are inter-related according to the following equations

$$X_{wb} = \frac{X_{db}}{1 + X_{db}} \qquad X_{db} = \frac{X_{wb}}{1 - X_{wb}} \tag{7.3}$$

The moisture content on the wet basis is used normally for commercial purposes, while the moisture content on the dry basis has tended to be employed for engineering research designation.

Mechanism of Drying

The decrease in the MC of the product in the dryer is primarily determined by: the amount of water vapor already carried by the air (relative humidity); the product residence time in the dryer; the dry bulb temperature and the air flow rate. Theoretically any of these variables can be used to control the drying process. Furthermore, other variables that can be used to control the drying process are: amount of material, thickness of material etc.

When hot air is blown over a wet product, water vapor diffuses through a boundary film of air surrounding the product and is carried away by the moving air. A water vapor pressure gradient is established from the moist interior of the product to the dry air. This gradient provide the ”driving force” for the water removal from the product. The boundary film acts as a barrier to both heat

transfer and water vapor removal during drying. The thickness of the film is determined primarily by the air velocity (Fellows, 2000), but is also dependent on material characteristics such as: dimension, shape and moisture content. If the air velocity is low, the boundary film is thicker and this reduces both the heat transfer coefficient and the rate of removal of the water vapor. Water vapor leaves the surface of the product and increases the humidity of the surrounding air, to cause a reduction in the water vapor pressure gradient and hence the rate of drying. Therefore the faster the air, the thinner the boundary film and hence the faster the rate of drying. However, whether the surrounding air influences the drying rate is dependent on the dryer equipment as well. In summary, the three characteristics of the air that are necessary for successful drying when the product is moist are: a moderately high dry-bulb temperature; a low relative humidity and a high air velocity. This of course depends on one's definition of successful drying. For example: when quality or certain nutrients need to be retained or when cracking has to be prevented, these are not the three necessary characteristics of the air. We now continue to analyze the mechanism of drying by considering the batch dryer experiment shown in Figure 7.2.

Constant-rate Period

When a product is put into a dryer, there is a short initial settling down period, shown as A-B in Figure 7.2, as the surface heats up to the *wet-bulb temperature*; since the surface of the material is wet the air in the layer is saturated, which causes the temperature to be wet bulb temperature. Drying then commences and, provided water moves from the interior of the product at the rate as it evaporates from the surface, the surface remains wet. This is known as the *constant-rate period*, shown as B-C, and continues until a certain *critical moisture content,* indicated by X_c, is reached. The surface temperature of the product remains close to the wet-bulb temperature of the drying air until the end of the constant-rate period, due to the cooling effect of the evaporating water. In practice, different areas of the product surface dry out at different rates and, overall, the rate of drying declines gradually towards the end of the constant-rate period.

Falling-rate Period

When the moisture content of the product falls below the critical moisture content X_c, the rate of drying slowly decreases until it approaches zero at the so

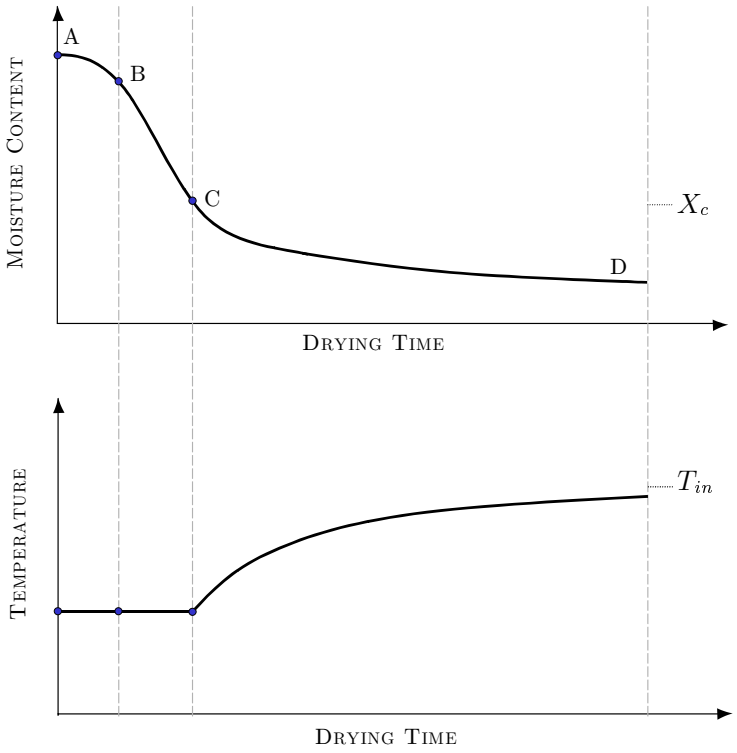

Figure 7.2: The top figure shows the "text-book" version of a typical drying curve in a batch dryer when the humidity, temperature and air flow of the drying air are constant. The lower shows the exhaust air temperature.

called *equilibrium moisture content*, X_e. At this moisture content the product comes into equilibrium with the drying air. This period of drying is called the falling-rate period and, for example, *non-hygroscopic* foods have a single falling-rate period, whereas *hygroscopic* foods have two or more periods (Fellows, 2000).

During the falling-rate period(s), the rate of water movement from the interior to the surface falls below the rate at which water evaporates to the surrounding air, and the surface therefore dries out, assuming that the temperature, humidity and air velocity are unchanged. If the same amount of heat is supplied by the air, the surface temperature rises until it reaches the dry-bulb temperature of the drying air. Most heat damage to products may therefore occur in the falling-rate

period and the air temperature may thus have to be controlled to balance the rate of drying and extent of heat damage.

The falling-rate period is usually the longest part of drying operation and, for example, in grain drying, the initial moisture content is below the critical moisture content and the falling-rate period is the only part of the drying curve to be observed. During the falling-rate period(s), the factors that control the rate of drying change. Gradually the rate of water movement (mass transfer) becomes the controlling factor and during the falling rate period only material characteristics plays a role in the moisture transfer. The air properties do not play a role anymore; the material temperature equals the air temperature, but it is the material temperature that influences the rate of drying and not the air property. Water moves from the interior of the product to the surface by, for example, the following mechanisms (Fellows, 2000):

- water vapor diffusion in air spaces within the product caused by vapor pressure gradients,
- liquid movement by capillary forces, particularly in porous products,
- diffusion of liquids, caused by differences in the concentration of solutes at the surface and in the interior of the product,
- diffusion of liquids which are absorbed in layers at the surfaces of solid components of the product.

During drying, one or more of the above mechanisms may be taking place and their relative importance can change as drying proceeds. It is therefore sometimes difficult to predict drying times in the falling-rate period. The mechanisms that operate depend mostly on the temperature of the air and the size of the product pieces; they are unaffected by the relative humidity of the air and the velocity of the air. This is however an indirect influence, since the material has the same temperature. The material temperature determines the rate of drying controlled by diffusion. Furthermore, the size of the product particles has an important effect on the drying rate in both the constant-rate and falling-rate periods. In the constant-rate period, larger pieces have a larger surface area available for evaporation, whereas in the falling-rate period, smaller pieces have a shorter distance for moisture to travel through the product. Calculation of drying rates is further complicated if the product shrinks during the falling-rate

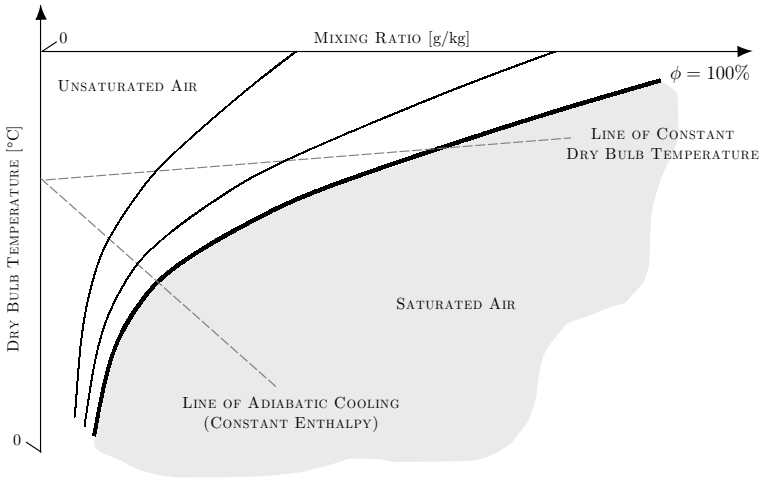

Figure 7.3: A mollier chart for atmospheric pressure.

period. Other factors that influence the rate of drying include the composition and structure of the product, and the product amount placed into a dryer in relation to its capacity.

Mollier Analysis of Drying

The drying process depends largely on the changes that occur in the properties of moist air, i.e., dry air and water vapor, which constitutes the drying air. The *Mollier chart* is an organized presentation of these properties. Consider the simple mollier chart in Figure 7.3. The abscissa represents the mixing ratio (absolute humidity) with the dry bulb temperature as the ordinate. The dew point temperatures are located on the lower curve, which is the saturation line corresponding to $\phi = 100\%$ relative humidity. The constant relative humidity curves are the subsequent curves above the saturation line. The constant wet bulb lines are the straight lines sloping gently downward to the right. The process of heating or cooling at constant absolute humidity are thus along *vertical* lines. Relative humidity decreases with heating along this line and increases with cooling. The wet bulb lines correspond to adiabatic cooling lines − lines of constant enthalpy − resulting from evaporative cooling of air flowing over a wet surface and gaining latent heat of vaporization.

A drying process may employ unheated or preheated air. As the air flows past the product, heat is transferred to the product from the air. This results in vaporization of moisture from the product to the air (simultaneous *heat* and *mass transfer* process) and subsequent increase in the air relative humidity, since the process occurs with a decrease in the dry bulb temperature at constant wet bulb temperature. The benefit of using preheated air is illustrated in the subsequent example. The example also gives the power P that is necessary to heat an airstream of 3000 m^3/hour from a temperature of 0 deg C to a temperature of 70 deg C.

Example 7.1 – *Preheating of air*

Consider the figure below. An airflow of 3000 m^3/hour with air having a rela-

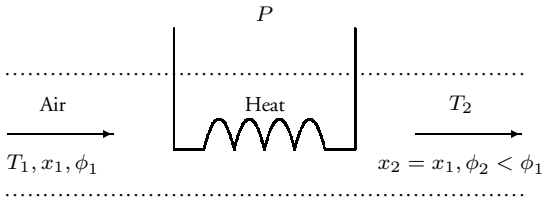

tive humidity $\phi_1 = 100\%$, a mixing ratio x_1 and a temperature $T_1 = 0$ deg C is to be conditioned to have a temperature $T_2 = 70$ deg C. Since no moisture is added in the process, we thus have $x_2 = x_1$. When applying a more detailed Mollier chart than the one previously presented, it is concluded that the relative humidity of the outgoing air, ϕ_2 decreases to 20%. Furthermore, the Mollier chart gives that the required heat quantity for this process is 70 kJ/kg of *dry* air. An approximate value of the necessary power P is thus 65 kW. Hence, when the air is preheated into 70 deg C, the moisture holding capacity of the air is increased by 18 g moisture/kg air.

7.4 Drying Prerequisites

The prerequisites of the agglomerate dehydration problem are as follows:

- The product to be dried consists of agglomerated where no more than 30% have a diameter range *less* that 0.25mm and no more than 5% have a diameter range *greater* than 8mm.
- Hot air with an approximate temperature of 70 deg C is used as drying agent. The air temperature is controlled using an industrial electric heater.
- The agglomerates have an initial moisture content of 25-30% (dry basis). The initial moisture content is approximately known, since the amount of added water to the dry mixture of ash and dolomite is controlled. Furthermore, the moisture content is not expected to decrease during the agglomeration process that precedes the drying stage.
- The control objective is to dehydrate the agglomerates to a MC at which the product is dry (hard) enough to be packed immediately. In this context, for example, this means that the agglomerates can be transported using a spiral-feeder conveying system without being damaged. That implies that the control set point is always the same, which simplifies the control problem.
- The dryer throughput should be approximately 250 kg/h of total mass flowrate.

With these prerequisites the issue of dryer selection is approached.

7.5 Dryer Selection

In many cases, it is still true to say that the selection of equipment for the drying of products remains predominately an art, in which knowledge, experience and science all play important roles. Often, there is no ”right” answer in the absolute sense as more than one solution is both technically and economically viable. However, a careful evaluation at the outset of as many as possible of the factors influencing the choice will help to narrow down the options. The selection of a dryer for new products is always risky, and once the choice is made, it is very

difficult, if not impossible, to alter that decision. In this section, three types of dryers are presented as the possible solution to the outlined drying problem: a vibro-fluid bed dryer, a belt dryer and a bin dyer. The techniques are briefly presented and some advantages and disadvantages of each drying method are given.

Vibro-Fluid Bed Dryers

In vibro-fluid bed dryers (Baker, 1997), the feed is introduced continuously to one end of the fluid bed and fluidized by an air stream from below. In the fluidized state the particles behave like a liquid thereby ensuring a good heat transfer between the air and the particles. As the product moves from one end of the fluid bed to the other, the smaller particles, "the fines", are blown off in the top of the fluid bed together with the air thus ensuring a dustless product to leave the dryer. In order to overcome the fluidization problem, designs are available in which the distributor is vibrated. Material handled in these type of dryers include those having a wide size distribution with a significant number of oversize particles and those which are cohesive, sticky or fragile. Furthermore, with a vibro-fluidized bed, the air velocity can be set low enough to avoid excessive elutration, while the larger particles are kept moving by the vibrations.

The company Jöst GmbH, in Sweden represented by Chemoinvest AB, offers a vibro-fluid bed dryer suitable for agglomerate dehydration. The cost for such an equipment is approximately $30 000; more details are given in Svantesson et al. (2002). However, even though the vibro-fluidized bed dryer seems to have many advantages, the mechanical stress on the agglomerates pose an immediate threat to the applicability of the method.

Belt Dryers

Most belt dryers used in the industry are of the single-pass type (Baker, 1997). The wet feed is deposited onto the belt at the entrance to the dryer. It then passes through a single drying enclosure in which it is contacted with flue gas or hot air. The air flow can be either upwards or downwards through the drying layer and the dried product eventually emerges at the opposite end of the dryer. Compared to a vibro-fluid bed dryer the belt dryer is less efficient during operation. But since the produced agglomerates tend to be fragile when entering the drying stage a belt dryer seems to be a good choice. This statement is verified

in Svantesson (2000), where a belt dryer prototype is used for ash agglomerate dehydration. However, if the material tends to clump together when wet it may be necessary to use a lump-breaker at the end of the dryer.

The company Amandus Kahl GmbH & Co, represented in Sweden by Roland Carlberg Processystem AB, offers a belt dryer suitable for agglomerate dehydration. The cost for such an equipment is $30 000; more details are given in Svantesson et al. (2002).

Bin Dryers

Bin dryers are large, cylindrical or rectangular containers fitted with a mesh base. Hot air passes up through a bed of the product at relatively low velocities. They have a high capacity and low capital and running costs, which make the method feasible in an ash recycling process. Therefore, during late 2001, the research group in Kalmar was joint with Gert Nordström, Nordströms konstruktionsbyrå AB, and together they developed a design for a prototype bin dryer. The dryer, which operates in semi-batch mode, can simultaneously handle two batches of agglomerates; the almost dry at the bottom and the recently pelletized at the top. Hot air is used as drying medium and the cost for such a dryer is approximately $30 000; more details are given in Svantesson et al. (2002). However, the Achilles heal of the method is whether the agglomerates are sufficiently strong to withstand the compression at the bottom and thus retain spaces between the agglomerates to permit the passage of hot air through the bed.

Selected Drying Method

After have filtered out some possible techniques for agglomerate dehydration, the next phase is thus to investigate the applicability of each design. The outcome of these efforts were that a belt dryer from Amandus Kahl GmbH & Co, represented in Sweden by Roland Carlberg Processystem AB, was selected as drying method to dehydrate the ash agglomerates. The conclusive arguments for this choice of dryer were that the belt dryer is the only dryer that enables a thin layer drying combined with a lenient processing of the agglomerates. Technical details regarding the belt dryer is to be found in Svantesson et al. (2002).

Several components can be added or attached to a conveyor dryer. Probably the most important is the *feeder* or *spreader*. Many types of feeders and spreaders

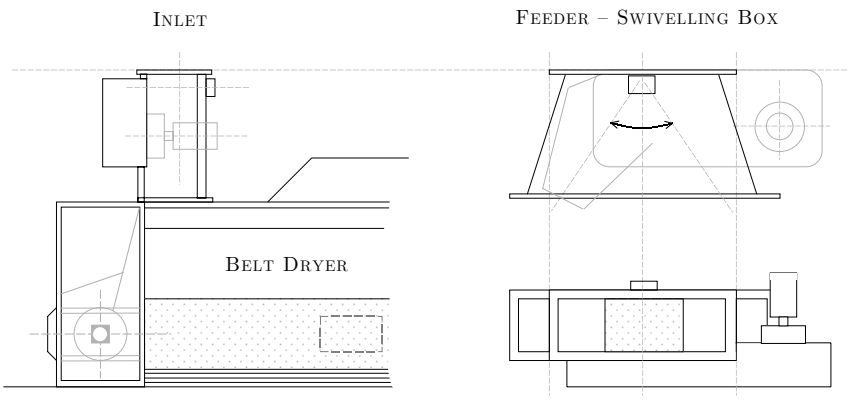

Figure 7.4: A belt dryer from Amandus Kahl GmbH & Co with a feeding device.

are available, including swivelling screw feeders and swivelling belt feeders, etc. Totally, Amandus Kahl GmbH & Co offers five types of feeding devices; see Svantesson et al. (2002). The feeder ensures that the material in the dryer is uniformly distributed on the conveyor. If this is not satisfied, air will always take the path of least resistance, flowing preferentially through the shallow parts of the material. This will result in overdried material in the shallow areas and wet material in the deep areas. Thus, it is important to choose a feeder that will work effectively with the product to be dried. The belt dryer from Amandus Kahl GmbH & Co and the selected feeding device − a swivelling box − is shown in Figure 7.4. Other components that can be added to a conveyor dryer include rotary breakers or pickers to break clumps of material and continuous cleaning equipment such as bed brushes that help keep the conveyor surfaces clean and the perforations unplugged.

The dryer, feeder and bed brushes have been purchased during the Spring of 2002 at a cost of approximately \$30 000. This price also includes the expense for the various sensors and motor drives needed to operate the dryer. However, a lump-breaker is not installed. For the belt dryer, the effective drying area is $3.3\ m^2$. This implies that if a bed-height of $0.08\ m$ is used, the volume within the dryer is 264 liters, which is approximately one batch produced in the WAH process. Hence, using a bed-height of $0.08\ m$ enables the dryer to operate in batch-mode. The applied bed height also simplifies the problem, since then it

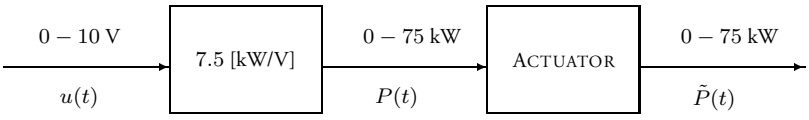

Figure 7.5: The block diagram of the actuator that generates 75 kW.

may be assumed that a *thin layer* can be considered. This means that one can assume that all particles in the layer are in the same stage of drying and the air conditions throughout the layer are the same. The batch-mode approach eliminate the influence of variation in the feed as well. However, it is crucial that the batch recently dried is not emptied until a new batch is filled to be dehydrated. This guarantees that no air will take the path of least resistance, for example, through a hole in the agglomerate bed.

7.6 Temperature Control

In this section, a control algorithm is developed that regulates the temperature of the *inlet drying air* in the agglomerate dehydration process. In Example 7.1, it is presented that an approximate value of the necessary power P required in the dehydration process is 65 kW. For that reason, an actuator delivering a maximum power of 75 kW has been installed. Since it is not recommended to conduct fast on/off switches with high powers, the operation of this actuator must be somewhat special. Therefore, a more advanced actuator has been adopted; an actuator that enables the use of a PID-controller as well.

Actuator

The actuator block diagram is depicted in Figure 7.5. To avoid fast on/off switches with high powers, the total power of 75 kW is split into smaller parts

$$\tilde{P}(t) = 4.7 + \underbrace{4.7 + 9.4 + 18.8 + 37.6}_{Q(P(t))} \text{ kW} \tag{7.4}$$

where the part $Q\left(P(t)\right)$ operates like a $4-$bit D-A converter with a time delay of 10 seconds between each transition. Thus, the input-output characteristic of

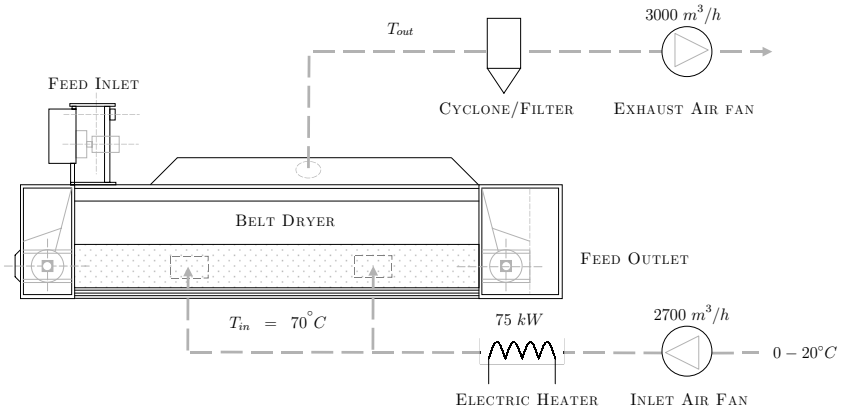

Figure 7.6: The schematics of the dryer set-up at Draken.

this quantizer is given by

$$Q\left(P(t)\right) = q \cdot \texttt{floor}\left(P(t)/q\right) \tag{7.5}$$

where $q = 4.7$ kW, and `floor(x)` rounds the elements of `x` to the nearest integers towards minus infinity. However, the first heating element of 4.7 kW, which is not included in the part $Q\left(P(t)\right)$, is controlled using a *triac* that gives pulses with an amplitude of 4.7 kW and a pulse width

$$T_{pulse}(t) = \frac{P(t) - Q\left(P(t)\right)}{q} \times T_{cycle} \tag{7.6}$$

Here, T_{cycle} is a cycle time of 6 seconds. The actual applied power $\tilde{P}(t)$ is thus a linear combination of the part $Q\left(P(t)\right)$ and the triac-controlled power of 4.7 kW. This, however, implies that the applied control signal cannot be considered to be continuous. Nevertheless, since temperature control loops generally involve processes with slow dynamics, the influence of this actuator characteristics is expected to be small. Furthermore, in Chapter 6 it is shown that the PID-controller to be implemented remains, to some extent, stable in spite of nonlinear actuator characteristics. To design this controller, however, a transfer function $G(s)$ that models the dynamics of the preheater is needed. The next section is dedicated to this issue.

A Four-Parameter Model of the Electric Heater

Consider Figures 7.5 and 7.6. The objective is to find a transfer function $G(s)$ that models the dynamics of the electric heater from the actuator input signal $u(t)$ to the temperature of the inlet drying air $T_{in}(t)$. This air is used to dehydrate the agglomerates within the dryer and here a tight control is necessary, both from an operational and economical point of view. If necessary, the exhaust air, having a temperature $T_{out}(t)$, will pass a cyclone/filter that separates the fines. This device is, however, presently not installed. It is assumed that the dynamics are reasonably well approximated by the linear transfer function

$$G(s) = \frac{T_{in}(s)}{U(s)} = \frac{K}{(1+sT_1)(1+sT_2)}e^{-sL} \tag{7.7}$$

where K is the process gain, T_1 and T_2 are the time constants and L is the dead time (Åström and Hägglund, 1995). The unit step response of the model (7.7) is given by

$$T_{in}(t) = K\left(1 + \frac{T_2 e^{-(t-L)/T_2} - T_1 e^{-(t-L)/T_1}}{T_1 - T_2}\right), \quad T_1 \neq T_2 \tag{7.8}$$

and a step response from the true physical process is shown in Figure 7.7. As seen in the figure, no dead time is present. Before any experiments were conducted the temperature was measured to be $T_{in} = 19.7$ deg C, using the input signal $u(t) = 0\%$, and when the input signal $u(t) = 80\%$ was applied the temperature was measured to be $T_{in} = 53.9$ deg C. The gain K is then determined from the steady-state values to be

$$K = \frac{53.9 - 19.7}{80.0 - 0.0} = 0.4275 \tag{7.9}$$

However, if the input signal $u(t)$ now is lowered from 80% to 0%, the temperature T_{in} decreases to about 41 deg C. Then the temperature drop seems to stop; it may thus (again) be inferred that the actuator is nonlinear. Now, finally, if the input signal $u(t)$ is increased from 0% to 80% the step response shown in Figure 7.7 is obtained. In combination with this response a graphical determination method (Åström and Hägglund, 1995) is used to determine the time constants, which gives the transfer function

$$G(s) = \frac{T_{in}(s)}{U(s)} = \frac{0.4275}{(1+50s)(1+250s)} \tag{7.10}$$

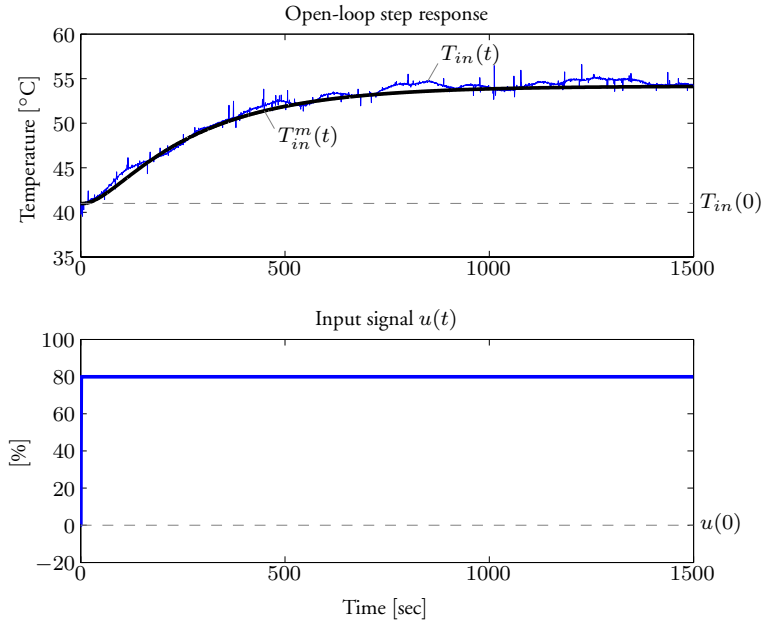

Figure 7.7: The upper plot shows the measured step response, $T_{in}(t)$ and the model output $T_{in}^m(t)$. The lower plot shows the input signal $u(t)$.

Figure 7.7 shows the obtained model response $T_{in}^m(t)$. It should be observed that this model is highly approximative: the process experiments are carried out with no product placed within the dryer. This implies that the airflow is somewhat higher than during normal operation. If it is assumed that these variations only will affect the process gain, the set of all possible plants is generated by the *structured set*

$$\mathcal{P} = \{k_p G_0(s); \quad k_p \in [k_{\min},\ k_{\max}]\} \tag{7.11}$$

where k_p is an uncertainty gain and

$$G_0(s) = \frac{1}{(1+50s)(1+250s)} \tag{7.12}$$

is a transfer function with no uncertainty. According to the retail dealers and from Example 7.1, the power of 75 kW is regarded to be sufficient to heat an airflow of 3000 m^3/hour from a temperature of 0.0 deg C into a temperature of

70.0 deg C. This implies that the largest process gain to be achieved is $k_{\max} = 0.7$. However, the operating conditions may vary due to irregular bed heights – in the previously conducted experiment no product was placed within the dryer at all, which implies an unnecessarily high airflow. Assuming that the conducted experiment express the "worst" operating condition, a lower bound on the process gain is estimated to be $k_{\min} = 0.4$; thus $k_p \in [0.4, 0.7]$. For the controller design, however, the nominal value $k_p^0 = 0.55$ has been used.

Controller Design

A controller has been designed for the electric heater using the model obtained in the previous section and the tuning method surveyed in Section 6.2. Due to the nonlinear actuator characteristics and the presented model uncertainty, the PID controller is designed for the tuning parameter $M_S = 1.3$, which yields the parameters $K = 3.52$, $T_i = 182.53$, $T_d = 0.95$, $b = 0.82$ and $T_r = 0$; see Chapter 6. The filter constant of the derivative term is chosen to $N = 10$, and the measurement signal is filtered with a first order filter given by

$$F_y(s) = \frac{1}{1 + 5s} \tag{7.13}$$

To obtain a difference equation that can be implemented on a computer, the filter derivatives are approximated using *Tustin's approximation*, see Åström and Wittenmark (1997) or Franklin et al. (1998). The corresponding discrete filter F_y^d is thus obtained as

$$F_y^d(q) = F_y\left(\frac{2}{h}\frac{q-1}{q+1}\right) \tag{7.14}$$

where h is the sampling interval and q is the forward shift operator. Tustin's approximation has the advantage that the left half-s-plane is transformed into the unit disc $D(0, 1)$. Stable continuous-time filters are therefore always transformed into stable sampled systems. The result of the design (6.18) applied to the electric heater is illustrated in Figure 7.8; all cases fulfil $\max_\omega |S(i\omega)| \leq 1.4$, which guarantees that $A_m \geq 3.5$ and $\varphi_m \geq 42°$.

Validation

A real-time experiment is conducted with no product placed within the dryer. The PID-controller is implemented with Algorithm 6.1, Section 6.3, using

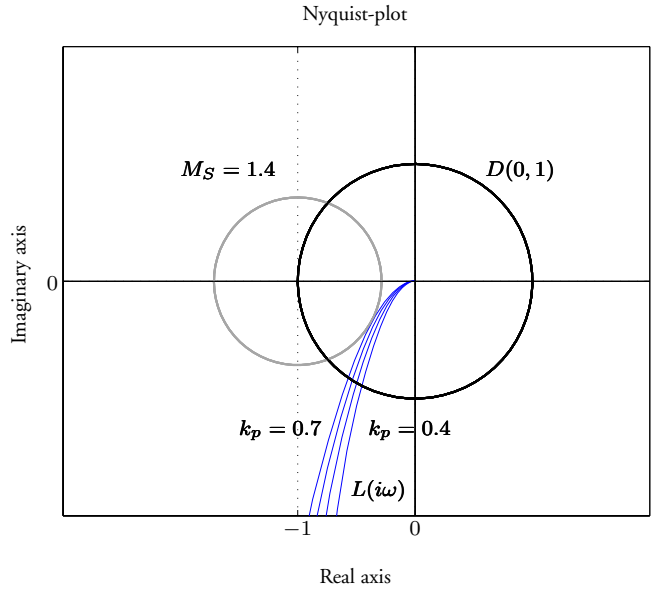

Figure 7.8: Results using the PID-design method presented in Panagopoulos (2000). The controller is designed for the nominal value $k_p^0 = 0.55$, and the closed loop system is analyzed for $k_p = \{0.4, 0.5, 0.6, 0.7\}$.

$\gamma = 1$. Since $\omega_c = 0.068$ rad/s, the sampling time is chosen to be $h = 3$ seconds, which implies that $h\omega_c \approx 0.2$. Furthermore, no extra anti-aliasing filter is utilized. The experimental result is shown in Figure 7.9. The software package `DISKREG` is used for data acquisition and a local PLC is used for control. Even though the implemented actuator is nonlinear and the model is uncertain, the performance of the closed loop system is demonstrated satisfactorily. The control signal is also observed to be smooth not imposing too much stress on the actuator.

The controller has been tested during several of drying experiments and under several of operating conditions: during both hot and cold days (load disturbances) and with a lowered airflow (affects the dynamics), which will be shown in Figure 7.11. The closed loop system has never shown any oscillatory behavior or any instabilities. Therefore, the robustness of the closed loop system is demonstrated satisfactorily.

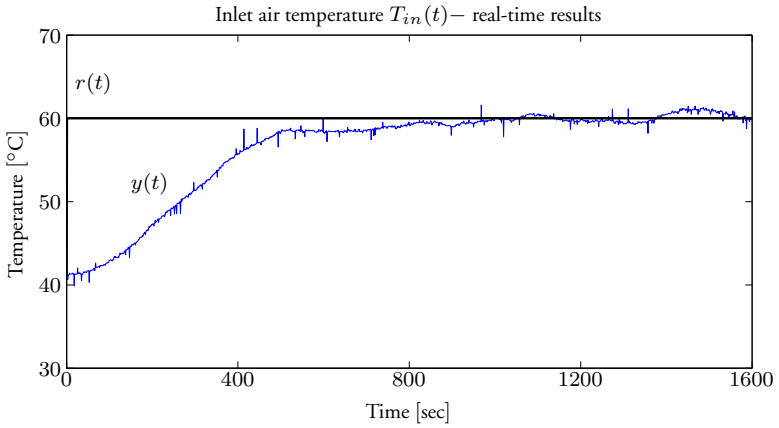

Figure 7.9: Real-time experiments with the true physical process. The plot shows a step response of the closed loop system.

7.7 Moisture Control

This section presents different measurement techniques, *direct* and *indirect*, to assess the MC of the ash agglomerates. In Courtois (1996) it is argued that *indirect* methods give open loop strategies and the use of a *direct* moisture sensor is recommended. However, the indirect moisture sensors are presented here as well since the dryer will operate in batch-mode and the information carried by the measurement signals only needs to be used as a MC indicator.

Moisture Control Based on Temperature Measurements

When a water-containing solid is being dried by passing a gas over it, a temperature difference will exist between the material and the drying gas or the ingoing and outgoing gas streams, until the vapor pressure from the water in the solid reaches equilibrium with that in the drying gas. The temperature drop is caused by the requirement of the latent heat of vaporization of the water, see Section 7.3. Normally drying is not carried on to the stage where there is no significant difference between the two temperatures. In many dryers empirical selection of a certain temperature difference can ensure good drying control, either as the end point for a batch, or to adjust the feed of material through a continuous dryer to maintain the selected temperature difference at the discharged end

of the dryer. It is a simple, inexpensive and reliable method for dryer control (Shinskey, 1968, 1969, Harbert, 1973, 1974, Köppel et al., 1995). Problems found in applying the technique include, for example, difficulties in measuring the true solid temperature − sensors to material contact may be difficult to maintain consistently − and the effect of water gradients within the particles being dried (during the falling-rate period). The latter are nearly always present in particles as they dry, and they have probably been the cause of failures in the application of the temperature difference technique. Reasons for adopting the technique are (Carr-Brion, 1986): the equipment is simple and reliable and imposes a low cost; it is reasonably easy to install. However, arguments against are: it fails with a number of materials; it is empirically calibrated when a fixed temperature difference is used and the method is sensitive to changes in feed flow and fuel flow. Nevertheless, the temperature difference method has been successfully applied to spray and fluid bed dryers in the pharmaceutical and food industries, and to the drying of textiles (Carr-Brion, 1986).

Moisture Control Based on Humidity Measurements

The previous method for moisture control is based upon an *energy balance* over the dryer

$$E^{Feed} + E^{Air}_{in} = E^{Vapor} + E^{Air}_{out} \tag{7.15}$$

where E^{Feed} is the thermal energy in the feed, E^{Air}_{in} is the thermal energy from the drying air, E^{Vapor} is the thermal energy required for vaporization of moisture and E^{Air}_{out} is the thermal energy in the exhaust air. Assuming a constant feed rate (thermal energy in feed) and temperature of the exhaust air, the energy delivered by the inlet drying air is an indicator of the moisture vaporization rate (drying rate). As an alternative the following *mass balance* can be considered

$$M^{Feed} + M^{Air}_{in} = M^{Product} + M^{Air}_{out} \tag{7.16}$$

where M^{Feed} is the moisture in the feed, M^{Air}_{in} is the inlet drying air moisture, $M^{Product}$ is the product moisture and M^{Air}_{out} is the exhaust air drying moisture. Instead of estimating the drying rate as described in the energy balance equation above, it is thus possible to evaluate it directly. This is done by measuring the *mixing ratio* (g moisture/kg air) of the exhaust air and the corresponding air flow (m^3/s). Assuming that the mixing ratio of the drying air at the dryer inlet is known, the drying rate (g/s) is computed based on these measurements. The

mixing ratio can be measured by, for example, using the HMP235 series transmitter manufactured by Vaisala. This sensor has been shown to be successful in for example the application of on-line humidity measurements in flue gases (Henriksson, 1997).

The technique is fairly inexpensive and has shown to be a reliable measurement method in various drying applications. Furthermore, a more thorough investigation showed that the method is in fact applicable for agglomerate dehydration using even the flue gases produced at the district heating plant Draken. However, twice a year the sensor needs to be calibrated using saturated salt solutions, which generate a known relative humidity in the air above them. This is considered as a significant drawback by the operating personnel.

Moisture Control Based on Capacitance Measurements

The dielectric constant of water, $\epsilon_r = 80$, is considerably higher than that of most other materials and this factor is often used to determine the moisture content of solids. If a solid is placed between two electrodes of a capacitor, the capacity will vary primarily in proportion to the solids water content. However, the dielectric constant also depends on the bulk density and chemical compositions of the solids − especially varying concentrations of ionic conductors such as salt − and for this reason the method is mainly of value with materials of roughly constant compositions. The material is allowed to flow between two metallic plates that make up the capacitor and since the wood ash agglomerates harden as they are dried, it is quite easy to obtain a uniform bulk density. The capacitance is determined in the majority of instruments by a high precision bridge technique, with built-in compensation for variations of material temperature, variations of bulk density and the effect of electrolytic conduction (Carr-Brion, 1986).

Here, the first question that arise is whether the chemical compositions of the wood ash will affect the ash agglomerates and thus the applicability of the method. In Friborg (1998) the *dielectric constant* ϵ_r and *conductivity* σ of wood ash samples obtained from the heating plant Draken are presented. The applied frequency range is 100 MHz to 3 GHz, and the amount of unburnt carbon varied in the interval $1 - 33\%$. From the measurements it is inferred that the dielectric constant ϵ_r for these samples never exceeded 25, which is well below $\epsilon_r = 80$ for water. Since carbon itself has $\epsilon_r = 5$, it seems probable that any

fluctuations will originate from the bulk density and varying concentrations of ionic conductors such as salt. The latter issue is considered to be well known and is presented in for example Eriksson (1993).

The capacitance method is relatively inexpensive, and many retail dealers are to be found in the agriculture and farming industry. To exactly predict how the chemical composition of the wood ash agglomerates – which consist of ash, dolomite and water – will affect the applicability of the method is a delicate issue. However, considering the facts presented above, it may be inferred that the method should be successful.

Moisture Control Based on Other Methods

Water strongly absorbs microwave radiation at certain frequency bands – typical two or three orders of magnitude more strongly than the base material – and this has been used to determine the moisture content of wide range of powders and granular materials (Kraszewski, 1980). Furthermore, moisture sensors for powders and granular materials based on the NIR technique are presented in the literature as well (Carr-Brion, 1986). In Sweden, the cost for a moisture sensor based on microwave radiation is approximately $\$50\ 000$, whereas the cost for a moisture sensor based on the NIR technology is about half that amount. In any case, both methods are too expensive for ash recycling processes. Furthermore, capacitance, microwave and NIR moisture sensors require that there be no moisture gradients in the solids, which reduces the applicability of the method.

Implemented Moisture Control Scheme

Based on this survey, maintenance and economical issues imply that the approach of "moisture control based on temperature measurements" is to be selected. Hence, this method does not require physical contact with the solid under test. Since the dryer will operate in batch-mode, the drying curve is assumed to be similar to the one shown in Figure 7.2, and the temperature difference $\Delta T = T_{in} - T_{out}$ can thus be used as decision variable. Furthermore, the problem of varying "fuel flow" will be eliminated by using a constant air flow combined with a tight control of the inlet temperature T_{in}. But most important of all, since the dryer operate in batch-mode the sensitivity to varying feed flow is eliminated.

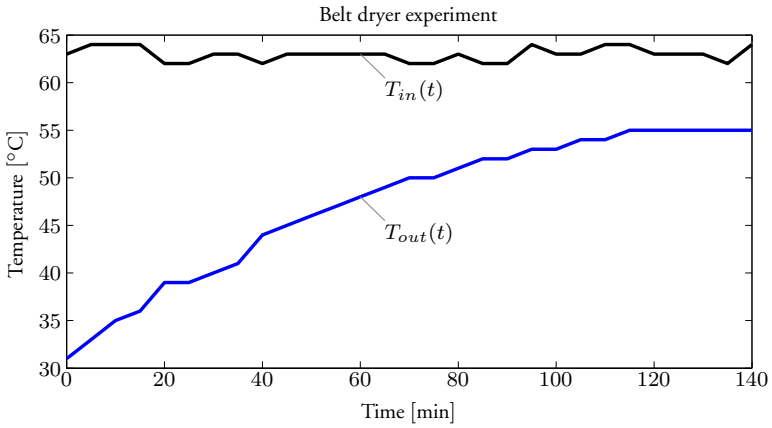

Figure 7.10: Full-scale drying test using the belt dryer from Amandus Kahl GmbH & Co. The recording of time versus the exhaust air temperature $T_{out}(t)$ is shown in the plot when the input signal $u(t) = 100\%$ is used. The uncontrolled input air temperature $T_{in}(t)$ is shown as well.

7.8 Full-Scale Drying Tests

During the first initial experiment, a batch was put into the dryer that is depicted in Figure 7.6. Using the control signal $u(t) = 100\%$, the inlet air and exhaust air temperatures, $T_{in}(t)$ and $T_{out}(t)$ respectively, were recorded. The result is shown in Figure 7.10. As expected, the temperature difference $\Delta T(t) = T_{in}(t) - T_{out}(t)$ is a good indicator of the product MC (at a constant ingoing air condition), and only one drying period is observed – a falling-rate period. By physical inspection it is also concluded that the whole batch is totally dry after approximately 2 hours; this means that at this temperature $T_{in}(t)$, the evaporation rate is approximately $20 - 25$ kg of water per hour. This should be compared to the time of one month in the old setup. From visual judgment, it is also concluded that no lump breaker is necessary to install within the belt dryer.

As one can see, the inlet air temperature never reaches the desired temperature $T_{in} = 70$ deg C, even though the applied input signal is $u(t) = 100\%$. The reason for this is, most probably, that the true air flow is greater than 3000

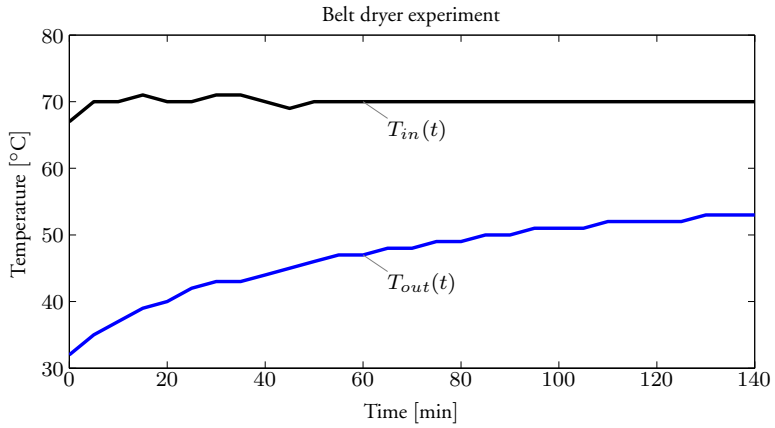

Figure 7.11: Full-scale drying test using the belt dryer from Amandus Kahl GmbH & Co and a temporarily lowered air flow. The recording of time versus the exhaust air temperature $T_{out}(t)$ is shown in the plot. The controlled input temperature $T_{in}(t)$ is shown as well.

m^3/hour, which is the air flow that the electric heater is designed for. Hence, as stated in Section 7.3, the mechanisms that operate during the falling-rate period depend mostly on the temperature of the air (an indirect influence) and the size of the product pieces; they are unaffected by the relative humidity of the air and the velocity of the air. Therefore, an additional experiment is conducted where the air flow is temporarily lowered, so that it is possible to control the inlet air temperature T_{in} to be 70 deg C. The previous experiment is now repeated, and the result is shown in Figure 7.11. Comparing Figures 7.10 and 7.11, the time constant(s) of the drying process seem to be almost unaffected. However, since the bed-height is approximately $0.08\ m$ it may be inferred that it is more efficient to use the greater air flow. Therefore, the final implementation is to use a controller reference value $r(t) = 60$ deg C.

When excluding the water, one batch of agglomerates consists of 100 kg of wood ash and 50 kg of ETEC-dolomite. Therefore, the setup installed at the central heating plant "Draken" of Kalmar has a capacity to handle approximately $0.6 - 1.2$ tons of wood ash per day; this means that approximately $0.9 - 1.8$ tons of agglomerates are produced per day. These numbers are based on the assumption that one batch takes about $2 - 4$ hours to produce; approx-

imately 95% of this time constitute the dehydration. It is believed that the difference in drying time is caused by varying wood ash carbon contents; if the ash has a low carbon content, the drying takes about 2 hours whereas if the ash has a high carbon content, the dehydration takes about 4 hours to complete. The reason for this is yet not scientifically determined, but one initial guess may be that the water is more strongly bound to the product when ash with high carbon content is used in the transformation process. Furthermore, if the ash has a low carbon content the temperature T_{out} at the equilibrium moisture content is 55 deg C using $T_{in} = 60$ deg C. However, if the ash has a high carbon content the temperature T_{out} at the equilibrium moisture content is much lower, for example $46-48$ deg C using $T_{in} = 60$. A simple solution to this problem may be to terminate the drying process when the derivative of the temperature T_{out} is close to zero. As an alternative, the temperature difference $\Delta T(t) = r(t) - T_{out}(t) \leq \chi$ can be used to terminate the drying process in combination with a maximum drying time of 4 hours. Here, χ is a threshold selected empirically.

In the full-scale drying tests it is also concluded that the agglomerates produced with high ash carbon contents have a somewhat smaller size distribution compared to the ones manufactured with a low carbon content. Furthermore, to decrease the drying time, the capacity of the transformation process may be dramatically increased by using a larger electric heater, using flue gases in the dehydration process, or using flue gases to furthermore heat the inlet drying air. These methods are, however, associated with an additional installation cost.

7.9 Summary and Concluding Remarks

In this chapter, a new method is presented for thermal drying of wood ash agglomerates. The today adopted method based on self-hardening has been outlined together with its apparent disadvantages. To enable an automated manufacture, three types of dryers are presented as the possible solution to the outlined drying problem: a vibro-fluid bed dryer, a belt dryer and a bin dyer. These techniques are briefly presented and some advantages and disadvantages of each drying method are given. A belt dryer from Amandus Kahl GmbH & Co, represented in Sweden by Roland Carlberg Processystem AB, has finally been selected as drying method. The dryer is installed with a feeder and bed brushes, and this setup was purchased during the Spring of 2002.

Four different methods for moisture control have been considered: moisture control based on temperature measurements; moisture control based on humidity measurements; moisture control based on capacitance measurements, and finally, moisture control based on other methods such as microwave radiation and sensors that utilize NIR spectroscopy. Maintenance and economical issues deduce that the approach of "moisture control based on temperature measurements" should be implemented to control the drying time. Using an electric heater, the inlet air temperature is regulated using a robust PID-controller designed with the method presented in Chapter 6. The novel method yields a fully automated drying of agglomerates, which leads to shorter processing time and a good control of the quality of the final product. In particular, the production time is reduced from 1 month to only a few hours.

Chapter 8

Co-ordination of Control

8.1 Introduction

The control system and the physical process must of course work well together. For example, a controller is normally designed for operation around one operating state. It is, however, necessary to make sure that the system will work well also during start-up and shutdown and under *emergency conditions*, such as process failures. During normal conditions it is natural to design for maximum efficiency. At a failure, it may be much more important to recover and quickly return to safe operating conditions. In any automated manufacturing system that is operational 24 hours a day the *robustness* of a control system is crucial. The discussion above implies that a *robust* and *safe* control system must be designed for the ash transformation process in order to face all possible situations that may occur.

Here, an industrial control system is suitable as a base to solve the computer real-time problem. However, the control system should not only be able to interact with the process but also with the *operator*. It is important to emphasize that the *man-machine interface* plays an essential role in these kind of applications. If the operator does not understand the information he/she is receiving, it is impossible to make the correct decision about the next step in the process. Therefore, it is important to facilitate the exchange of information between the user and the equipment to be controlled. A well designed interface not only makes work conditions more pleasant but also helps considerably to reduce errors and thus limit the extent of possible damage.

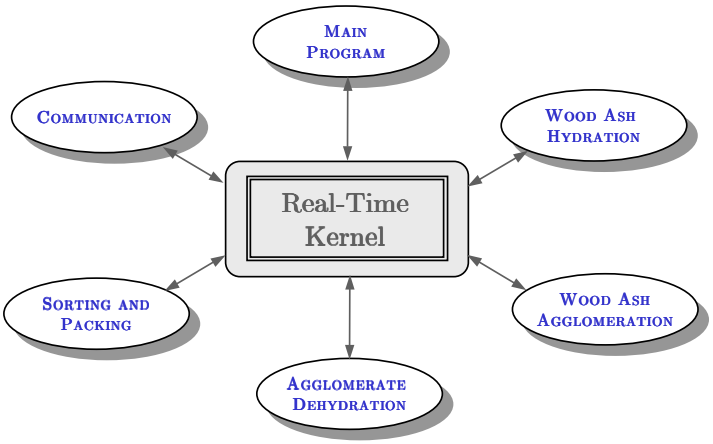

Figure 8.1: The real-time environment.

The ash transformation process consists mainly of six different tasks that will run concurrently, as depicted in Figure 8.1. Some of the processes can be divided into smaller parts, for example, the ash scheduling is included in the main program. These tasks run in parallel and need information from the ”world outside” through measurements to be able to execute the next step in the program code. This implies that many sensors must be included to convey this information. In order to physically connect the computer to the process many technologies have to be applied. Since it is impossible to become an expert in all the related fields, it is important to be aware of the different interfacing problem in order to get a functional closed-loop system. If poor measurements are obtained of the quantity that is to be controlled, it is waisted time to use any theory from automatic control. In this case, when dealing with a true physical process, we cannot ignore what is happening beyond the A-D-converters. A book that clearly remark the importance of this issue is Olsson and Piani (1992).

As mentioned previously, each process needs different kinds of sensors. Therefore, numerous digital and analog inputs-outputs must be connected to the control system.

8.2 Control System Philosophy

This section presents the general philosophy applied during the development and implementation of the control program for the ash transformation process.

Two Mode Operations

To enable flexible operation it is possible to run the ash transformation process in two different modes:

Mode1 : *Bypass operation*
Mode2 : *Ash transformation*

It is the operator that manually sets the current mode of the transformation process.

Bypass Operation Mode

In this mode, the ash will never pass through the ash transformation process and no agglomerates are thus produced. The ash will instead be transported to an ash container; see Appendix B. By having this mode, it is possible to redirect the ash transportation and shut down the transformation process if a failure occurs. Hence, running the process in mode 1 is the same solution as applied earlier: the ash is deposited as waist. In this mode no alarms are enabled from any object that is included in the ash transformation process. This is so because the staff should be able to do repairs/services on the equipment without any unmotivated alarms occurring, for example, if any safety switch is turned off during the service. Alarms are, however, still enabled to become active from the parts still in operation, for example, if the spiral-feeder for the ash transportation fails.

Ash Transformation Mode

In this mode the ash is transformed into fertilizing agglomerates in the manufacturing line. The process will run in this mode until the operator orders shut down, or if any failure occurs. If *mode 2* is active, the wood ash is transported to an ash buffer (see Appendix B) for later agglomeration, whereas if *mode 1* is active, the ash is always transported to the ash container.

Fault Detection

During operation of any manufacturing system, many predictable and unpredictable sources for system failure may occur. When dealing with a production line, as the ash transformation process, it may be fruitful to divide the total manufacturing system into several successively smaller pieces as depicted in Figure 8.1. If a failure occurs in one stage of operation, the control system must make a proper decision whether to shut down the whole production line or to keep some part of the system running.

Fault detection is to determine as quickly as possible if something in the production line has gone wrong based on knowledge of the system and observations. Based on the detection we have to make a *fault isolation*, i.e., from observations of the system we wish to determine if a fault has occurred, where it occurred, and what it is. Fault detection is done statically and dynamically. The standard for IEC1131 gives rules, which can statically (at compile time) find out semantical and syntactical errors in PLC programs. Reachability, deadlock and timing analysis of programs fall also in the static category. Dynamical (on-line) fault detection is based on two methods: analyzing signals and analyzing the execution of programs (execution monitoring methods). Signal-based fault detection is using e.g. signal allowed range intervals, statistical, fuzzy or neural network methods. An example of execution monitoring fault detection is *ontological control*, see Fodor (1998).

In our case the problem is to decide which component has failed. Components can be arbitrary items such as sensors, actuators, electric drive systems, feeders etc. Since the process can run in two different *modes,* some failures can occur in any of these two modes. If a failure occurs, the control system identifies the failure and then classifies how critical it is depending on the current mode. The failures are classified as *critical alarms* or *non-critical alarms*. The control system then gives an alarm and take proper actions depending on in which mode (Mode1/Mode2) the process is running. Hence, irrespectively of the process mode, after the failure it is always necessary for the operator to correct the source of error and acknowledge before the process again can be put in full operation. If any source of error is not corrected accurately, and the operator anyway acknowledges, it is not possible to restart the ash transformation process.

In this application two alarm-types are used. The first type is alarms caused by the hardware, called Hardware Alarms (HA) and the second type is alarms caused by the software, called Software Alarms (SA). An example of a HA may be that a safety switch is switched off to the electrical motor used in the ash spiral-feeder conveying system. On the other hand, a SA could be that the hardware does not indicate any failure, but no ash is filled into the mixer. This is monitored by the control system. Also if the execution of any of the implemented control-algorithms fails, this is regarded as a SA and the control system should take proper actions.

8.3 Distributed Control

The microprocessors have had a profound impact on the way computers have been applied to control entire production plants. It became economically feasible to develop systems consisting of several interactive microcomputers sharing the overall workload. Such systems generally consist of process stations, controlling the process; operator stations, where process operators monitor the activities; and various auxiliary stations, for example, for system configuration. All of them are interacting by means of some kind of communication network. The allure was to boost performance by facilitating parallel multi-tasking, to improve overall availability by not putting ”all the eggs in one basket” to further expandability and to reduce the amount of control cabling. The term ”distributed control” was coined. The first systems were oriented towards regulatory control, but over the years distributed control systems have adopted more and more of the capabilities of programmable (logic) controllers, making today's distributed control systems able to control all aspects of production and enabling operators to monitor and control activities from a single computer console.

Distributed control is adopted to solve the co-ordination problem of control, see Figure 8.2. The whole system contains a local Central Processing Unit (CPU) that is connected to the ash transformation process through several I/O units. This CPU (`SattCon 200`) is independent and programmed via a Personal Computer (PC), which is easily connected to the front end of the `SattCon 200` unit. The software `DOX10` is used to design the program to be downloaded. `DOX10` supports five different types of programming methods: Sequential Function Chart (SFC), Function Blocks, Ladder, Enhanced Instruc-

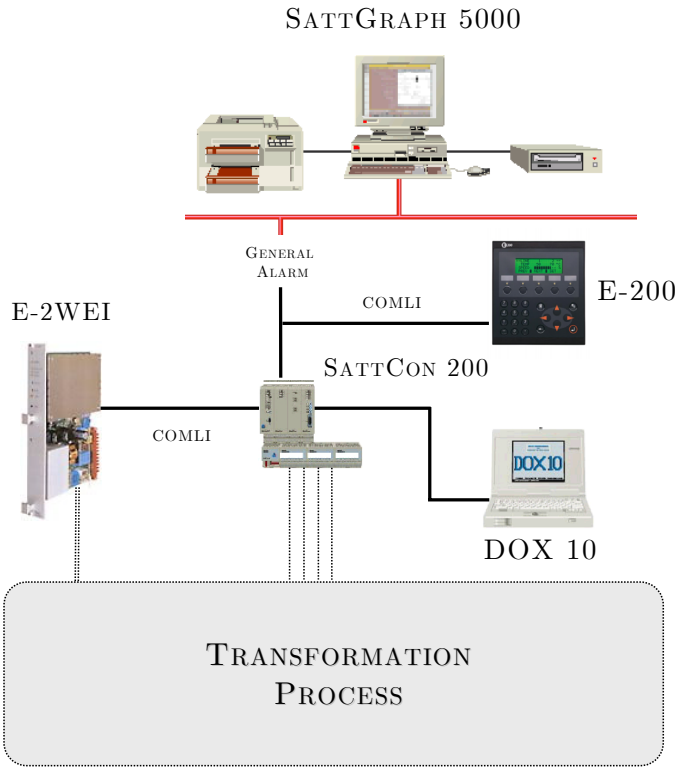

Figure 8.2: Co-ordination of control.

tion List and Structured Text, which is floating point in `SattCon 200`. If any failure occurs, the local control system `SattCon 200` triggers a general alarm in `SattGraph 5000`, which is used for supervision at the district heating plant "Draken" in Kalmar. The operator then has to walk to the transformation process and read about the cause of error, which is presented in the *operator terminal* `E-200`; the terminal presents the current step in the transformation process during normal operation as well. Furthermore, four load cells are connected to the weight transmitter E-2 WEI. The WEI unit is a slave under `SattCon 200` and is used as a transmitter between the load cells and the PLC. The data communication is carried out over an isolated RS 485 serial interface with COMmunication LInk (COMLI) used as protocol.

8.4 Used Programming Methods

In this section the used programming methods in DOX10; Grafcet and CALC-IDE are described. Function Blocks are also used but not discussed.

Grafcet

Grafcet was proposed in France in 1977 as a formal specification and realization method for logical controllers. The name Grafcet was derived from graph, since the model is graphical in nature, and AFCET (Association Francaise pour la Cybernétique Economique et Technique) – the scientific association that supported the work.

During several years, Grafcet was tested in French industries. It quickly proved to be a convenient tool for representing small and medium scale sequential systems. Grafcet was therefore introduced in the French educational programs and proposed as a standard to the French association AFNOR where it was accepted in 1982. In 1988 Grafcet, with minor changes, was also adopted by the International Electrotechnical Commission (IEC) as an international standard named IEC848 (IEC848, 1988). In this standard Grafcet goes under the name Sequential Function Chart (SFC). Seven years later, in 1995, the standard IEC1131-3, with Grafcet as essential part, arrived. The standard concerns programming languages used in Programmable Logic Controller (PLC)s. It defines four different programming language paradigms together with SFC. No matter which of the four different languages that is used, a PLC program can be structured with SFC. The two international standards, Grafcet and SFC, are today widely accepted in the industry where they are used as representation formats for sequential control logic at the local PLC level. In (Svantesson, 2000, Section 7.8) a brief overview of Grafcet is given. A more thorough presentation is to be found in David and Alla (1992).

CALC-IDE

CALC-IDE, an extension of DOX10, is utilized to implement the more advanced control algorithms. CALC-IDE is a stand alone program in Windows^{TM} that is used for arithmetic calculations in SattCon 200. Floating-point calculations for controllers, mean-value calculations, handling of arrays, statistical analyses etc. are all thus solvable with CALC-IDE. The language is based on selected

parts of the system program specification for programmable logic controllers, described in the international standard IEC1131-3 (IEC1131-3, 1993). Compared to `Structured Text`, this programming language has some prominent differences.

Variables

The following class of variables are not implemented:

VAR_ACCESS . . . END_VAR
VAR_CONSTANT . . . END_VAR

A program that follows the rules in IEC1131-3 declares the absolute variables in a `VAR . . . END_VAR` − construction. A program in `SattCon 200` uses `VAR . . . END_VAR`, `VAR_INPUT . . . END_VAR`, `VAR_IN_OUT . . . END_VAR` and/or a `VAR_OUTPUT . . . END_VAR` − constructions. The variables are further not affected directly. They are copied to a reserved memory area in a data-segment at the instance before the execution begins. The variables are then copied back to the memory or register at the end of the execution.

Datatypes

Generic datatypes, time, date and ascii-strings are not implemented. The following datatypes are missing:

BOOL	INT	REAL	STRING	TIME
SINT	LINT	USINT	UINT	UDINT
ULINT	DATE	TIME_OF_DAY	TOD	DATE_AND_TIME
DT	BYTE	WORD	DWORD	LWORD

and datatypes triggered by flanks.

8.5 Implementation

Totally, to control and monitor the ash transformation process, a numerous of three-phase asynchronous machines**,** discrete control valves and sensors are incorporated. The asynchronous machines that are sources of mechanical power, are used as movers for: spiral-feeder conveying systems, fans, high-pressure

pump operation, stirrer drive, the roll-pelletizer, conveyor belts and distributors. Some of these induction motors are speed regulated. It is possible to run each individual motor manually *or* via the PLC. Furthermore

- A power transducer is utilized to measure the normalized effective power $P_e(t)$ as discussed in Chapter 3,
- Inductive proximity sensors are applied to control the mixer outlet,
- Load cells with high resistance for lateral and longitudinal forces are used to measure the shear stress in the bars at which the mixer is placed upon. The stress is measured by straingauges in a fullbridge giving an analog output. The load cells are connected to E-2WEI shown in Figure 8.2,
- Electromechanical sensors are used for level monitoring in the buffers.

Ultrasonic Sensors

Ultrasonic sensing is applied for level monitoring at the inlet of the roll-pelletizer. Ultrasonic sensing, which is a non-contact measuring method, is well suited since the mixture of ash/dolomite/water is very sticky. This type of level sensor is based upon high-frequency sound waves that are generated by the application of an alternating current to a piezoelectric crystal. Sonic waves may undergo surface reflection. They also have a velocity of propagation which is medium dependent. If such a wave is launched into a medium towards a level interface, it will undergo reflection. The wave takes a finite time to travel a distance equal to twice the distance between the sensor and the interface. Hence, by measuring the time from launch to reception of the reflected wave, the calculation of the distance is made using the velocity of propagation of the sound wave. If a wave travels in, for example, an empty cylindrical space with a velocity v (m/s), and takes the time t (s) to travel the distance $2(h_2 - h_1)$ (m), where h_2 (m) is the length from the sensor to the bottom of the cylindrical space and h_1 (m) is the length from the sensor to the surface of the interface. Then the relevant equation for these conditions is (McGhee et al., 1998)

$$2(h_2 - h_1) = tv \tag{8.1}$$

Ultrasonic sensing is affected by several factors including the target's surface, size angle and the distance from the sensor. Environmental conditions such as

temperature, humidity, gases, and pressure may also affect the measurement. Therefore, a sensor that automatically compensates for most of these environments is selected. The measured level from the ultrasonic sensor is compared to different pre-determined levels yielding three discrete values of the inlet level: `inlet_full`, `inlet_half_empty` and `inlet_empty`.

Component Failures

If any of the components mentioned above fails, it is crucial to detect this and take proper actions. For the motors, *overcurrent relays* or *thermal overload relays* (the first operates when the current through the relay, during its operating period, is equal to or greater than its setting), *safety switches* (a manual on/off switch that ensures, in off-mode, that the motor is not started during, for example, service/repair) and *contactor failures* must be monitored in order to ensure a functional hardware. For some motors, it is crucial that the source of error is corrected before a certain time-interval has expired, i.e., some acknowledgments for hardware alarms are time constrained. This is to guarantee safe operation of the ash transformation process. Also, to further ensure safe and robust operation, several tasks have time constraints. If a task is not completed during a predetermined time-interval, an alarm becomes active. This is used to monitor:

- Mixture quality control failures,
- Failures during the ash/dolomite dosage,
- Failure of the ultrasonic sensor.

Fault detection is further applied to check:

- Superstructure in the mixer,
- Absence of water pressure,
- Failure of the dust preventing equipment.

To ensure safe (and of course a dry) operation of the *high-pressure cleaning procedure*, the gross weight of the mixer is monitored during this period.

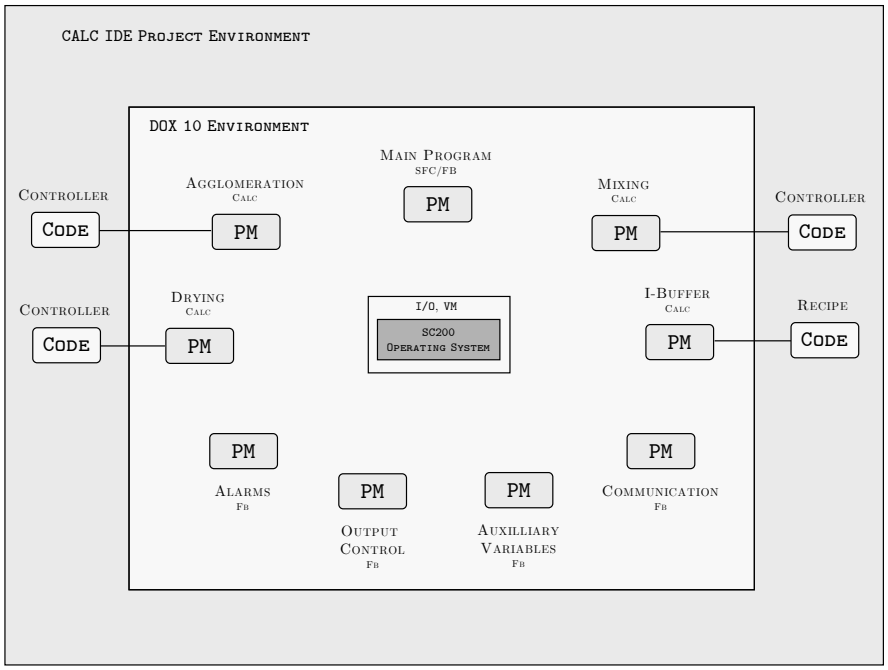

Figure 8.3: The DOX 10 program structure used when controlling the transformation process.

8.6 Program Structure

DOX 10 enables the user to structure the program (project) in Program Module (PM)s and Sub Module (SM)s. It is possible to include 255 PMs in a project, where each PM can contain up to 1000 SMs. With this feature, the user can structure the program so that each PM is controlling a specific part of the process, where each SM in the PM is controlling, for example, a specific object. Another option is to structure the program in such way that each PM is handling special events, as for example alarms. Each PM and SM can be given a name and be documented. In order to make communication between the different PMs possible, forty Variable Module (VM)s are available to the user. All user variables are located in this real-time protected area. It is possible to connect any VM to an arbitrary chosen PM, which enables flexible programming.

The selected program structure for the ash transformation process is depicted in Figure 8.3. Here nine program modules are implemented to control specific parts of the ash transformation process, c.f. Figures 8.1 and 1.4. The main program also includes the ash scheduling. The approach of having special program modules for alarm events, output control etc. is adopted. The PM for communication is handling all interactions between `SattCon 200` and the operator terminal `E-200` and this communication line uses an asynchronous serial RS232 interface and the protocol `COMLI`. Furthermore, SFC procedure steps are implemented in order to enable effective usage of the weight transmitter. However, the PMs labeled `I-buffer` and `Agglomeration` are for future use if necessary, c.f. Svantesson (2000).

All PMs are implemented in the `DOX 10` environment. Program codes, which are implemented in the `CALC IDE` project environment, are connected to the corresponding PM in the `DOX 10` environment via a real-time configuration. In this configuration, it is possible to choose if the program code should be executed periodically or if it should be triggered and executed once by a bit changing state from false to true. If the program code is set to be executed periodically, it is possible to enable/disable the periodical execution, which gives the opportunity to run, for example, a control algorithm in some special SFC step in the main program. All implemented program codes uses the program skeleton suggested in (Åström and Wittenmark, 1995, p. 491).

8.7 Summary and Concluding Remarks

In this chapter, the general philosophy applied during implementation of the control system has been presented. Also a detailed description of the used sensors, the selected program structure and programming methods are outlined. The usage of fault detection has also been presented. Furthermore, the program is now implemented and carefully tested. The academical potential of the work presented in this chapter may not be the greatest, but on the other hand, for the operator of any process controlled by computers, a well designed, robust and good structured program/operator interface is of critical value. This takes a considerable time to achieve practically, but the academical writing about it is minor. However, it increases the engineering significance of the work.

Chapter 9

Concluding Remarks

This work has discussed the control of an ash transformation process that automatically transforms wood ash produced at district heating plants into fertilizing agglomerates. This is the first of its kind in Sweden, and to the best of the authors knowledge, the first of its kind in the world. The manufactured agglomerates are recycled back to the forest grounds, as a fertilizer, or as a tool to reduce the acidification in the forest soil at the spreading area. Other areas of application are, for example, structural fill and substitute for cement in ready-mix concrete.

The issue of wood ash carbon content analysis has been targeted, and it is concluded that CIFA analyzers based on microwave methods are today too expensive for the application of wood ash transformation. However, in Samuelsson (2002) that recently was issued by the Swedish National Board of Forestry, it is stated that there are currently *no requirements* on the wood ash carbon content. This implies that the installation of a CIFA monitoring device is needless, and therefore, all wood ash is transformed into agglomerates. Nevertheless, there is still a need to optimize the burner efficiency. It is also concluded that the presence of $Ca(OH)_2$ and $CaCO_3$ do not affect the color of the wood ash, since these components are not visible to the eye. On the other hand, this may result in gross errors in the Loss-On-Ignition (LOI) tests for fly ashes. Experimental results show that the color of the wood ash varies with different fuels used at combustion. This implies that a measuring method based on machine vision would be poor.

Mixing ash/dolomite/water in order to obtain granular material is one method to stabilize wood ashes. The main problem is predicting the quantity of water to be added, since the necessary amount varies with the wood ash quality. In Sundqvist (1999) it is reported that the critical water-to-ash ratio varies between ash types and must therefore be determined for each ash. However, one possible solution is to measure the mixture viscosity and study whether this parameter can be used to control the amount of added water. In Chapter 3, the viscosity of the ash/dolomite/water mixture is estimated by measuring the normalized effective power $P_e(t)$, which represents the rate of useful work being performed by the three-phase asynchronous machine used as stirrer drive. It is shown that this measurement is well suited for control of the amount of added water to the WAH process. Methods to predict the critical water-to-ash ratio are presented in Chapter 4. The outlined implementation is based upon a simple control sequence performed in open-loop combined with a change detector that uses the one-sided CUSUM-test as stopping rule. Here it should be stressed, that if the water-to-ash ratio do not show any apparent changes over a year, which is the case at the central heating plant "Draken" of Kalmar, a foolproof approach is to use the detection algorithm only once to determine a proper ratio. The WAH procedure may then be controlled by a simple weighing-in of water.

In Chapter 5, we conclude that the roll-pelletizing method for wood ash agglomeration is the superior method in all categories. The process unit is simple, robust and no advanced automatic control is necessary for its operation. It is also verified that the produced agglomerates fulfil the quality requirements stated for a product suitable for recycling. However, even though the last of the three rollers in the roll-pelletizing equipment was redesigned during the Fall of 2001, it never worked satisfactorily. Therefore, this roller was deactivated in the agglomeration process. A similar approach was utilized in Lövgren et al. (2000). Furthermore, by means of experiments it is concluded that it is only necessary to use 50 kg of ETEC-dolomite for each batch produced in the ash transformation process; that is half the amount that was suggested in Svantesson (2000). It is also proposed that the water used to wash the mixer should be recycled in the WAH procedure of the following batch. See Appendix B for a practical solution of such an approach.

As always, it is the total effort of process & control system design and cost that is the final goal, and Chapter 5 demonstrates the kind of compromise between

process design and control system design that ought to take place more often in process control; a complex control problem can often be simplified by a change in process design. However, in numerous of process designs there is a need for several of control problems to be solved. Then controller design, analysis and implementation have to be targeted and Chapter 6 is dedicated to these issues.

In Chapter 7, a new method is presented for thermal drying of wood ash agglomerates. The today adopted method based on self-hardening has been outlined together with its apparent disadvantages. To enable an automated manufacture, three types of dryers are presented as the possible solution to the outlined drying problem: a vibro-fluid bed dryer, a belt dryer and a bin dyer. These techniques are briefly presented and some advantages and disadvantages of each drying method are given. A belt dryer from Amandus Kahl GmbH & Co, represented in Sweden by Roland Carlberg Processystem AB, has finally been selected as drying method. The dryer is installed with a feeder and bed brushes, and this setup was purchased during the Spring of 2002.

Four different methods for moisture control have been considered: moisture control based on temperature measurements; moisture control based on humidity measurements; moisture control based on capacitance measurements, and finally, moisture control based on other methods such as microwave radiation and sensors that utilize NIR spectroscopy. Maintenance and economical issues deduce that the approach of "moisture control based on temperature measurements" should be implemented to control the drying time. Using an electric heater, the inlet air temperature is regulated using a robust PID-controller designed with the method presented in Chapter 6. The novel method yields a fully automated drying of agglomerates, which leads to shorter processing time and a good control of the quality of the final product. In particular, the production time is reduced from 1 month to only a few hours.

Finally, the whole ash transformation process is controlled by an industrial control system in order to enable automatic manufacture; see Chapter 8. The academical potential of the work presented in this chapter may not be the greatest, but on the other hand, for the operator of any process controlled by computers, a well designed, robust and good structured program/operator interface is of critical value. This takes a considerable time to achieve practically, but the academical writing about it is minor.

In summary, to make the ash transformation process fully automated several of problems had to be attacked: Carbon In Fly Ash (CIFA) monitoring, estimation of viscosity, components of actuating systems, modeling & system identification, agglomeration techniques, dehydration techniques, moisture control, process design, control system design and control system implementation. However, a personal concluding remark is that the major problem of building a machine for automated manufacture is related to *process design*; it is not easy to design an apparatus that does not obtain superstructures on the mechanical parts when processing the sticky mixture of ash/dolomite/water.

Extensions and Future Work

There are a number of open problems that may be further investigated regarding automated manufacture of fertilizing agglomerates. A list for future research and development is:

- As stated in Chapter 7, the agglomerate dehydration takes much longer time to complete if the wood ash carbon content is high, as compared to the case when the used wood ash has a low carbon content. The reason for this is yet not scientifically determined, but one initial guess may be that the water is more strongly bound to the product when ash with high carbon content is used in the transformation process; how to optimize the dehydration process during these operating conditions is still an open question. Furthermore, one might suspect that the capacity of the dehydration process can be dramatically increased by using: a larger electric heater, using flue gases in the dehydration process, or using flue gases to furthermore heat the inlet drying air. These methods are, however, associated with an additional installation cost.
- More attempts need to be conducted to optimize the burner efficiency.
- The agglomerates should be packed in a container for later transportation, see Ericson et al. (1994). The packing is still not implemented, but a design is completed.

Appendix A

Mathematical Review

To increase the readability for the practitioner engineer, some basic mathematical concepts have been summarized in this appendix.

1.1 Vectors and Matrices

Definition A.1 (Definition of a Vector) Let $x_1, x_2, \ldots, x_n$ be any n real numbers and $\mathbf{x}$ an ordered set of these numbers, that is

$$\mathbf{x} = [x_1 \; x_2 \; \ldots \; x_n]^T \tag{A.1}$$

then $\mathbf{x}$ is called an *n-vector* (or simply a *vector*). Here T denotes the *transpose* (exchange of rows and columns) of the vector $\mathbf{x}$. □

Definition A.2 (Definition of a Matrix) A *matrix* is a rectangular array of real elements. The $(i,j)-$th element a_{ij} of the matrix $\mathbf{A}$ stands in the $i-$th row and $j-$th column of the array. The *order* (size) of a matrix is said to be $m \times n$ if the matrix includes m rows and n columns. For example,

$$\mathbf{A} = \{a_{ij}\} = \begin{bmatrix} a_{11} & a_{12} & \cdots & a_{1n} \\ a_{21} & \ddots & & \vdots \\ \vdots & & \ddots & \vdots \\ a_{m1} & \cdots & \cdots & a_{mn} \end{bmatrix} \tag{A.2}$$

is a $m \times n-$matrix. □

Definition A.3 (Inverses of Nonsingular Square Matrices) If $\mathbf{A}$ and $\mathbf{B}$ are square matrices of the same dimension, and such that their product

$$\mathbf{AB} = \mathbf{I} \tag{A.3}$$

where $\mathbf{I}$ is the *identity matrix,* which has ones along the main diagonal and zeros everywhere else, then $\mathbf{B}$ is the *matrix inverse* of $\mathbf{A}$ and $\mathbf{A}$ is the matrix inverse of $\mathbf{B}$. The matrix inverse of $\mathbf{A}$ is unique, if it exists, and is denoted by $\mathbf{A}^{-1}$. □

Definition A.4 (Quadratic forms) Given

$$\mathbf{x} = [x_1 \; x_2 \; \ldots \; x_n]^T \tag{A.4}$$

and the square matrix $\mathbf{A}$

$$\mathbf{A} = \begin{bmatrix} a_{11} & a_{12} & \cdots & a_{1n} \\ a_{21} & \ddots & & \vdots \\ \vdots & & \ddots & \vdots \\ a_{n1} & \cdots & \cdots & a_{nn} \end{bmatrix} \tag{A.5}$$

then

$$\mathbf{x}^T\mathbf{Ax} = \sum_{i=1}^{n}\sum_{j=1}^{n} a_{ij}x_i x_j \tag{A.6}$$

is called a *quadratic form*. □

Definition A.5 (Positive definite matrix) A square symmetric matrix $\mathbf{A}^T = \mathbf{A}$ is said to be *positive definite*, denoted by $\mathbf{A} \succ 0$ if

$$\mathbf{x}^T\mathbf{Ax} > 0 \quad \forall \mathbf{x} \neq 0 \tag{A.7}$$

□

Definition A.6 (Positive semi-definite matrix) A square symmetric matrix $\mathbf{A}^T = \mathbf{A}$ is said to be *semi-definite*, denoted by $\mathbf{A} \succeq 0$ if

$$\mathbf{x}^T\mathbf{Ax} \geq 0 \quad \forall \mathbf{x} \neq 0 \tag{A.8}$$

□

1.2 Stochastic Processes

Definition A.7 (Stochastic process) A sequence of random (stochastic) variables

$$\{y(k), \quad k = 1, 2, 3, \ldots\} \tag{A.9}$$

shorter denoted $\{y(k)\}$ is called a *discrete-time stochastic process.* □

Expectation

The statistical average value $m_y(k)$ of a random variable $y(k)$ is given by the mathematical *expectation operator* denoted E. Hence

$$m_y(k) = E\{y(k)\} \tag{A.10}$$

Assume that a number of realizations $y^{(1)}(k)$, $y^{(2)}(k), \ldots, y^{(n)}(k)$ of the random variable $y(k)$ are available. The expectation can then be considered as the average value when an infinite numbers of realizations are utilized. Thus

$$m_y(k) = E\{y(k)\} = \lim_{n\to\infty} \frac{1}{n} \sum_{i=1}^{n} y^{(i)}(k) \tag{A.11}$$

For a stochastic process $\{y(k)\}$ this means that the average value generally is a time-varying function $m_y(k)$. However, in a *stationary stochastic process* we obtain a constant function if the expectation operator is applied. The average value, m_y, for instance, then becomes

$$m_y = E\{y(k)\} = E\{y(k+i)\} \qquad i = \pm 1, \pm 2, \ldots \tag{A.12}$$

For stationary processes the average taken over a number of realizations can naturally be replaced by a time average of one single realization $\{y(k)\}_{k=1}^{N}$. In particular, this is true for the average value. Hence, (A.11) is then replaced by

$$m_y = E\{y(k)\} = \lim_{N\to\infty} \frac{1}{N} \sum_{k=1}^{N} y(k) \tag{A.13}$$

Correlation

The *auto-correlation* for a discrete-time stochastic process $\{y(k)\}$, defined as

$$r_{yy}(k,\tau) = E\left\{(y(k+\tau) - m_y(k+\tau))\,(y(k) - m_y(k))\right\} \tag{A.14}$$

describes how the process is correlated in time. For a slowly varying process, there is a strong correlation between values at different time instances, while the correlation is insignificant for a rapidly varying process except for very short time differences τ.

Assuming a stationary process, the correlation does not depend on the time k, but only on the time difference τ. Thus, we simplify the notation for the correlation to $r_{yy}(\tau)$, and experimentally it can be determined by the time average as

$$\begin{aligned} r_{yy}(\tau) &= E\left\{(y(k+\tau) - m_y)\,(y(k) - m_y)\right\} \\ &= \lim_{N\to\infty} \frac{1}{N} \sum_{k=1}^{N} (y(k+\tau) - m_y)\,(y(k) - m_y) \end{aligned} \tag{A.15}$$

If the average $m_y = 0$ we also note that the *variance* becomes

$$Var\; y(k) = E\left\{y^2(k)\right\} = r_{yy}(0) \tag{A.16}$$

It is also important to know how two different stochastic processes are related to each other. Assume that $\{y(k)\}$ and $\{u(k)\}$ are stationary stochastic processes. The dependence between these processes is then described by the *cross-correlation*

$$\begin{aligned} r_{yu}(\tau) &= E\left\{y(k+\tau)u(k)\right\} \\ &= \lim_{N\to\infty} \frac{1}{N} \sum_{k=1}^{N} (y(k+\tau) - m_y)\,(u(k) - m_u) \end{aligned} \tag{A.17}$$

Example A.1 — *White-noise*

White noise is a type of discrete-time stochastic process that often is used as a unit disturbance. It is simply defined as an uncorrelated stationary process.

Assume that the stochastic process $\{e(k)\}$ is white noise with variance r_e and the average

$$m_e = E\{e(k)\} = 0 \tag{A.18}$$

Then the auto-correlation is

$$r_{ee}(\tau) = \begin{cases} r_e & , \tau = 0 \\ 0 & , \tau \neq 0 \end{cases} \tag{A.19}$$

Spectrum

The frequency content of a signal is described by its *spectrum.* Depending on the property of a signal, different types of spectra are defined. For a stochastic process $\{y(k)\}$ the *auto-spectrum* can be considered as the expectation of the power spectrum for realizations of $y(k)$, i.e.,

$$\Phi_{yy}(\omega) = \lim_{N\to\infty} \frac{1}{Nh} E\left|Y_N(\omega)\right|^2 \tag{A.20}$$

where Y_N is given by the *Discrete Fourier Transform* (N measurements)

$$Y_N(\omega) = h\sum_{m=1}^{N} y(mh)e^{-i\omega mh} \tag{A.21}$$

The normalizing factor Nh is the real time between the first and last non-zero value of the signal. Hence, $\Phi_{yy}(\omega)$ describes the average frequency content of $\{y(k)\}$. Hence, equation (A.20) can also be written as

$$\Phi_{yy}(\omega) = \frac{1}{2\pi}\sum_{\tau=-\infty}^{\infty} r_{yy}(\tau)e^{-i\omega\tau} \tag{A.22}$$

which shows that the spectrum for a stochastic process can be considered as the Fourier transform of the correlation function $r_{yy}(\tau)$. In fact, (A.22) is the original definition of spectrum for a stochastic process.

In the same way, the *cross-spectrum* for two stochastic processes is defined as

$$\Phi_{yu}(\omega) = \frac{1}{2\pi}\sum_{\tau=-\infty}^{\infty} r_{yu}(\tau)e^{-i\omega\tau} \tag{A.23}$$

This means that the cross-spectrum for two *independent* signals is zero since $r_{yu} = 0$.

Example A.2 – *White-noise cont'd*

For white noise $e(k)$ with variance r_e, (A.19) and (A.22) imply that

$$\Phi_{ee}(\omega) = \frac{1}{2\pi} r_e \tag{A.24}$$

i.e., the spectrum is constant. This is in fact the reason for the designation *white noise,* since the white color has an equal mix of all colors (frequencies).

1.3 Discrete-Time Markov Chains

A simple random walk is one example of a sequence of random variables that evolve in some random but predescribed manner. Such collections are called *random processes.* A typical random process X is a family $\{X_t : t \in T\}$ of random variables indexed by some set T. If for example $T = \{0, 1, 2, \ldots\}$ we call the process a discrete-time process; in other important examples $T = \mathrm{R}$ or $T = [0, \infty)$ and we then call it a continuous-time process. In this section we are interested in discrete-time processes and we let $\{X_0, X_1, \ldots\}$ be a sequence of random variables that take values in some countable set $\mathcal{S}$. In a *discrete-time Markov chain* the state changes at certain discrete time instants, indexed by an integer variable n. At each time step n, the Markov chain has a *state*, denoted by X_n, which belongs to a set $\mathcal{S}$ of possible states, called the *state space*. Here, we will assume that $\mathcal{S}$ is finite, $\mathcal{S} = \{1, \ldots, m\}$ for some positive integer m. Such a Markov chain is called a finite Markov chain. The Markov chain is described in terms of its transition probabilities p_{ij} : whenever the state happens to be i, there is a conditioned probability p_{ij} that the next state is equal to j. Mathematically, for *homogeneous* transition probabilities, this is

$$\begin{aligned} p_{ij} &= \Pr\left[\text{going to } j \mid \text{in } i\right] \\ &= \Pr\left[X_{n+1} = j \mid X_n = i\right], \quad i, j \in \mathcal{S} \end{aligned} \tag{A.25}$$

The key assumption underlying Markov processes is that the transition probabilities p_{ij} apply whenever state i is visited, no matter what happened in the past, and no matter how state i was reached.

Definition A.8 (Markov Chain) The process X is a *Markov Chain* if it satisfies the *Markov condition:*

$$\begin{aligned}\Pr\left[X_n = j \mid X_0 = i_0,\ X_1 = i_1, \ldots,\ X_{n-1} = i\right] \\ = \Pr\left[X_n = j \mid X_{n-1} = i\right] = p_{ij}\end{aligned} \tag{A.26}$$

for all times n, all states i, $j \in \mathcal{S}$, and all possible sequences $i_0, \ldots, i$ of earlier states. □

All of the elements of a Markov chain model can be encoded in a transition probability matrix, which is simply a two-dimensional array whose element at the $i-$th row and $j-$ th column is p_{ij}, thus

$$\mathbf{P} = \{p_{ij}\} = \begin{bmatrix} p_{11} & p_{12} & \cdots & p_{1m} \\ p_{21} & \ddots & & \vdots \\ \vdots & & \ddots & \vdots \\ p_{m1} & \cdots & \cdots & p_{mm} \end{bmatrix} \tag{A.27}$$

and we have the following theorem.

Theorem A.1. The *transition probability matrix* $\mathbf{P}$ is a stochastic matrix, which is to say that $\mathbf{P}$ has non-negative entries, or $p_{ij} \geq 0$ for all i, $j \in \mathcal{S}$ and $\mathbf{P}$ has row sums equal to one, or $\sum_j p_{ij} = 1$.

Proof. An easy exercise. ■

One of the main objectives of Markov chain analysis is the determination of probabilities of finding the chain at various states at specific time instants. Therefore, the *state probabilities* are defined as

$$p_i(n) \stackrel{\text{def}}{=} \Pr\left[X_n = i\right] \tag{A.28}$$

Accordingly, we define the *state probability vector*

$$\mathbf{p}(n) = \begin{bmatrix} p_1(n) & p_2(n) & \cdots & p_m(n) \end{bmatrix} \tag{A.29}$$

This is a row vector whose dimension is specified by the dimension of the state space of the chain. Note, that each component in the vector $\mathbf{p}(n)$ is a probability, thus attains a value between zero and one. Furthermore, the sum of the

components in $\mathbf{p}$ is equal to one, since the system has to be in *some* state. A discrete-time Markov chain model is completely specified if, in addition to the state space $\mathcal{S}$ and the transition probability matrix $\mathbf{P}$, we also specify an initial state probability vector

$$\mathbf{p}(0)=\left[\begin{array}{cccc} p_1(0) & p_2(0) & \cdots & p_m(0) \end{array}\right] \tag{A.30}$$

which provides the probability distribution of the initial state, X_0, of the chain.

Once a model is specified through $\mathcal{S}$, $\mathbf{P}$ and $\mathbf{p}(0)$, we can start addressing questions such as: what is the probability of moving from state i to state j in n steps? Or: What is the probability of finding the chain at state i at time k? In answering such questions, we limit ourselves to given finite numbers of steps over which the chain is analyzed. This is what we refer to as *transient* analysis and we must therefore derive a difference equation that relates the states to each other. The state j at time $n+1$ can be reached from any other state i at the time n. From each one of the states there is a transition probability from that state to state j. This can formally be expressed as

$$p_j(n+1) = p_1(n)p_{1j}+p_2(n)p_{2j}+\cdots+p_j(n)p_{jj}+\cdots+p_m(n)p_{mj} \tag{A.31}$$

Using equations (A.27) and (A.29), the difference equation for all the states can be written on the form

$$\mathbf{p}(n+1) = \mathbf{p}(n)\mathbf{P} \quad , n = 0, 1, 2, \ldots \tag{A.32}$$

By using (A.32), it is possible to obtain an expression for $\mathbf{p}(n)$ in terms of a given initial state probability vector $\mathbf{p}(0)$ and the transition probability matrix $\mathbf{P}$. Specifically, for $n = 0$, (A.32) becomes

$$\mathbf{p}(1) = \mathbf{p}(0)\mathbf{P} \tag{A.33}$$

Then for $n = 1$, we get

$$\mathbf{p}(2) = \mathbf{p}(1)\mathbf{P} = \mathbf{p}(0)\mathbf{P}^2 \tag{A.34}$$

and continuing in the same fashion (or using a formal induction argument) we obtain

$$\mathbf{p}(n) = \mathbf{p}(0)\mathbf{P}^n \quad , n = 0, 1, 2, \ldots \tag{A.35}$$

It is thus possible to completely study the transient behavior of homogenous discrete-time Markov chains.

Classification of States

We will now provide several definitions in order to classify the states of a Markov chain in ways that turn out to be particularly convenient for the study of steady state behavior.

Definition A.9. A state j is said to be *reachable* from a state i if $p_{ij}^n > 0$ for some $n = 1, 2, \ldots$ □

Definition A.10. A subset $\bar{\mathcal{S}}$ of the state space $\mathcal{S}$ is said to be *closed* if $p_{ij} = 0$ for any $i \in \bar{\mathcal{S}}$, $j \notin \bar{\mathcal{S}}$. □

Definition A.11. A state i is said to be *absorbing* if it forms a single-element closed set. □

Definition A.12. A state i is called *persistent* (or *recurrent*) if

$$\Pr\left[X_n = i \text{ for some } n \geq 1 \mid X_0 = i\right] = 1 \tag{A.36}$$

which is to say that the probability of eventual return to state i, having started from state i, is 1. If this probability is strictly less than 1, the state i is called *transient*. □

Appendix B

Magnificus Apparatus

"Rome was not built in one day"

John Heyward (1497-1589).
Proverbs, Part I, Chapter XI.

Fejmert Mixer
Belt Dryer
Dolomite buffer
Ash buffer

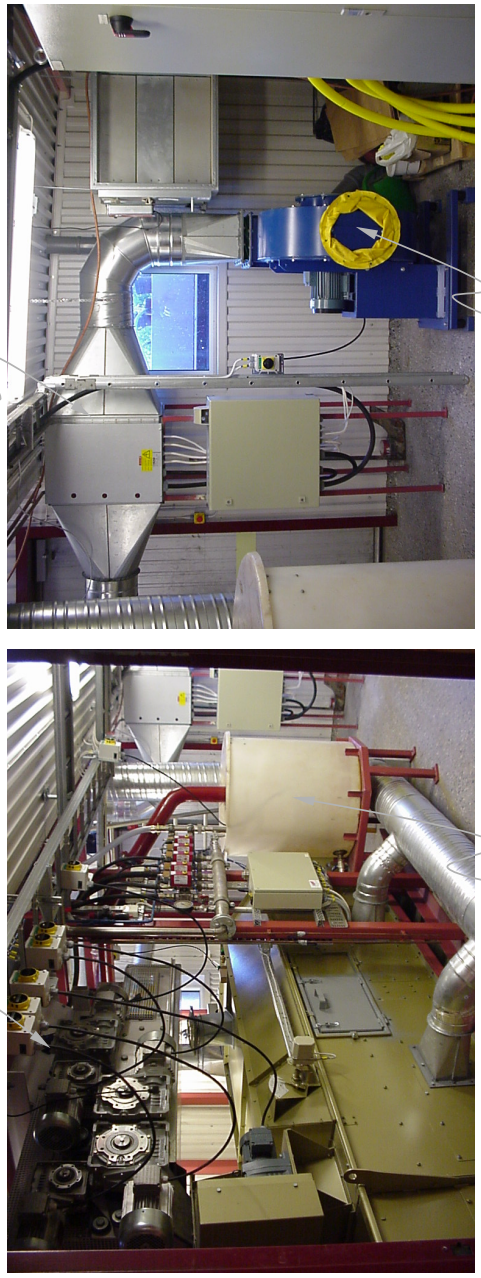
Electric Heater
Inlet Air Fan
Roll-Pelletizer
Recycling of washing water

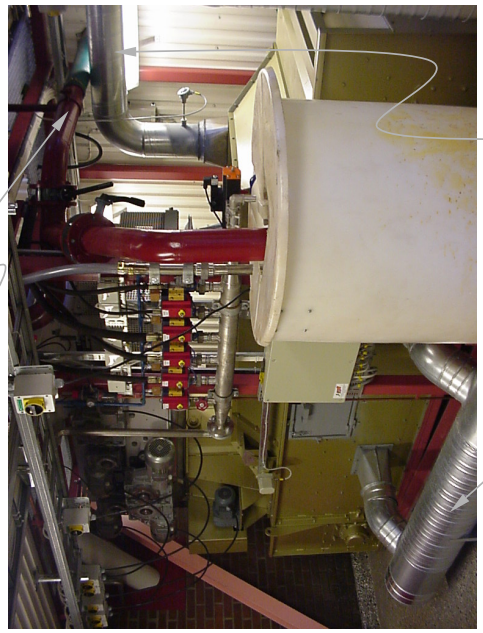
If Mixture control fails
Exhaust Air
Inlet Air

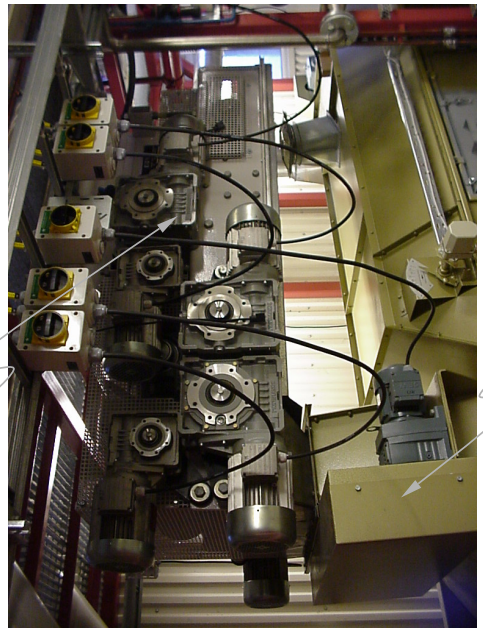
Roll-Pelletizer
Feeder

Operator interface

Manual control

Dust preventer

Ash container

Index

Bibliography

Abouzeid, A.-Z. M., Seddik, A. A. and El-Sinbawy, H. A. (1979). Pelletization kinetics of an earthy iron ore and the physical properties of the pellets produced, *Powder Technology* **24**(2): 229–236.

Adetayo, A. A., Litster, J. D. and Cameron, I. T. (1995). Steady state modelling and simulation of a fertilizer granulation circuit, *Computers Chem. Engng* **19**(4): 383–393.

Adetayo, A. A., Litster, J. D. and Desai, M. (1993). The effect of process parameters on drum granulation of fertilizers with broad size distributions, *Chemical Engineering Science* **48**(23): 3951–3961.

Adetayo, A. A., Litster, J. D., Pratsinis, S. E. and Ennis, B. J. (1995). Population balance modelling of drum granulation of materials with wide size distribution, *Powder Technology* **82**: 37–49.

Åström, K. J. and Hägglund, T. (1995). *PID Controllers: Theory, Design, and Tuning*, 2nd edn, Instrument Society of America.

Åström, K. J. and Wittenmark, B. (1995). *Adaptive Control*, 2nd edn, Addison Wesley.

Åström, K. J. and Wittenmark, B. (1997). *Computer-Controlled Systems: Theory and Design*, 3rd edn, Prentice Hall Inc.

Babb, A. T. S. and Casson, C. B. (1970). An in-line consistency meter for dough-like materials, *Measurement and Control* **3**(11): 173–180.

Baker, C. J. (ed.) (1997). *Industrial Drying of Foods*, Chapman & Hall, London, UK.

Ban, H., Schaefer, J. L. and Stencel, J. M. (1995). Electrostatic separation of powdered materials: Beneficiation of coal and fly ash, *Energeia* **6**(4).

Banks, J. and Carson, J. S. (1984). *Discrete-Event System Simulation*, Prentice-Hall International Inc., London.

Basseville, M. and Nikiforov, I. V. (1993). *Detection of abrupt changes: theory and application*, Prentice Hall, Englewood Cliffs, NJ.

Benson, I. B. (1995). The characteristics and scope of continuous on-line near infrared measurement, *Spectroscopy Europe* **7**(6): 18–24.

Bertelsen, F. (1998). *Ashes and particulate emissions of biomass combustion. Formation characterization, evaluation, treatment*, 1st edn, Dbv-Verlag für die Technische Universität Graz, Austria, chapter Importance of ash recirculation for economy, ecology and for meeting the Danish renewable energy policy goals.

Berthold, E. (2000). On-line analyzer for the measurement of carbon of fly-ash in power stations (Webpage, October 23, 2002). `http://berthold.com.au/ industrial_pages/fly%20ash.html`.

Bierman, G. J. (1977). *Factorization Methods for Discrete Sequential Estimations*, Academic Press, New York.

Blomqvist, D. and Forsberg, B. (1998). Modeling of a drum granulator unit, *Report*, Dept. of Technology, University College of Kalmar, Sweden.

Bonazzi, C., Courtois, F., Geneste, C., Pons, B., Lahon, M. C. and Bimbenet, J. J. (1994). Experimental study on the quality of rough rice related to drying conditions, *9th Internation Drying Symposium (IDS '94)*, Gold Coast, Australia, pp. 1031–1036.

Boscolo, A., Mangiavacchi, C. and Tuzzi, O. (1993). Fuzzy sensor data fusion for quality monitoring in concrete mixing plant, *Proceedings of the Instrumentation and Measurement Technology Conference*, pp. 671–675.

Brown, R. C. and Dykstra, J. R. (1995). Systematic-errors in the use of loss-on-ignition to measure unburned carbon in fly-ash, *FUEL* **7**(4): 570–574.

Brunzell, H. (1998). *Signal Processing Techniques for Detection of Buried Landmines using GPR*, Ph.D. thesis, Department of Signals and Systems, Chalmers University of Technology, Sweden.

Carr-Brion, K. (1986). *Moisture Sensors in Process Control*, Elsevier, London.

Chadwick, P. and Bridgwater, J. (1997). Solids flow in dish granulators, *Chemical Engineering Science* **52**(15): 2497–2509.

Champ, C. W. and Rigdon, S. E. (1991). A comparison of the Markov chain and the integral equation approaches for evaluating the run length distribution of quality control charts, *Communications in Statistics: Simulation and Computation* **20**(1): 191–204.

Chen, J. and Patton, R. J. (1999). *Robust Model-Based Fault Diagnosis for Dynamic Systems*, Kluwer Academic.

Clarke, D. W. and Gawthrop, P. J. (1979). Self-tuning control, *IEE Proceedings, Part D*, Vol. 126, pp. 663–640.

Courtois, F. (1995). Computer aided design of corn dryers with quality prediction, *Drying Technology* **13**(1): 147–164.

Courtois, F. (1996). *Computerized Control Systems in the Food Industry*, Mittal ed., chapter Automatic Control of Drying Processes, pp. 295–316.

Courtois, F., Lebert, A., Duquenoy, A., Lasseran, J. C. and Bimbenet, J. J. (1991). Modelling of drying in order to improve processing quality of maize, *Drying Technology* **9**(4): 927–945.

Courtois, F., Nouafo, J. L. and Trystram, G. (1995). Control strategies for corn mixed-flow dryers, *Drying Technology* **13**(5): 1153–1165.

Courtois, F. and Trystram, G. (1994). *Study and control of the dynamics of drying processes*, Amsterdam, Elsevier, chapter Automatic Control of Food and Biological Processes, pp. 289–296.

Crowder, S. V. (1987). A simple method for studying run-length distributions of exponentially weighted moving average charts, *Technometrics* **29**(4): 401–407.

Crowley, T. J., Meadows, E. S., Kostoulas, E. and Doyle, F. J. (2000). Control of particle size distribution described by a population balance model of semibatch emulsion polymerization, *Journal of Process Control* **10**(5): 419–432.

David, R. and Alla, H. (1992). *Petri Nets and Grafcet: Tools for modelling discrete events systems*, Prentice-Hall International UK Ltd.

de Bruyn, C. S. (1968). *Cumulative sum tests: theory and practice*, Hafner, New York.

Donskoi, D. M., Mironov, I. S. and Leskin, V. N. (1979). Research on a filter to forecast the optimal system for automatically controlling the mixing of dough, *Izvestiya Vysshikh Uchebnykh Zavedenii Pishchevaya Tekhnologiya* **5**: 80–83. In Russian.

Douglas, P. L., Jones, J. A. T. and Mallick, S. K. (1994a). Modelling and simulation of crossflow grain dryers: Part I - model development., *Transactions of the Institution of Chemical Engineers, Part A,* **72**: 325–331.

Douglas, P. L., Jones, J. A. T. and Mallick, S. K. (1994b). Modelling and simulation of crossflow grain dryers: Part II - design modification., *Transactions of the Institution of Chemical Engineers, Part A,* **72**: 332–340.

Douglas, P. L., Jones, J. A. T. and Mallick, S. K. (1994c). Modelling and simulation of crossflow grain dryers: Part III - optimization., *Transactions of the Institution of Chemical Engineers, Part A,* **72**: 341–349.

Douglas, P. L., Kwade, A., Lee, P. L. and Mallick, S. K. (1993). Simulation of a rotary dryer for sugar crystalline, *Drying Technology* **11**(1): 129–155.

Dutta, D. K., Bordoloi, D. and Borthakur, P. C. (1997). Investigation on reduction of cement binder in cold bonded pelletization of iron ore fines, *International Journal of Mineral Processing* **49**(1-2): 97–105.

Dykstra, J. R. and Brown, R. C. (1995). Comparison of optically and microwave excited photoacoustic detection of unburned carbon in entrained fly-ash, *FUEL* **74**(3): 368–373.

Efron, B. and Tibshirani, R. (1993). *An Introduction to the Bootstrap*, Chapman and Hall.

ELFI (1999). Load measurement – EL-FI G3 Power meter, Emotron AB (Webpage, October 23, 2002). `http://www.emotron.com/`.

Elmqvist, H., Mattsson, S. E. and Olsson, G. (1981). Datorer i reglersystem, *Report*, Inst. för Reglerteknik, Tekniska Högskolan i Lund. In Swedish.

Ericson, S.-O., Lundborg, A. and Oskarsson, R. (1994). Wood ash in the forest - collected experiences and knowledge from the project skogskraft, *Report*, Södra, Vattenfall. In Swedish.

Eriksson, H. (1999). Återföring av granulerad vedaska – effekter på avrinningsvatten, markvatten och markkemi, *Report*, The Research Programme for Recycling of Wood Ash, NUTEK, Vattenfall and Sydkraft. In Swedish, summary in English.

Eriksson, H. M. (1998). Short-term effects of granulated wood ash on forest soil chemistry in SW and NE sweden, *Scand. J. For. Res.* **2**: 43–55.

Eriksson, J. (1993). Characterization of wood-ash with respect to contents and solubility of plant nutrients and heavy metals, *Report*, Vattenfall Research, Bioenergy. In Swedish.

Eriksson, J. (1996). Härdade vedaskors upplösning i skogsjord, *Report*, The Research Programme for Recycling of Wood Ash, NUTEK, Vattenfall and Sydkraft. In Swedish, summary in English.

Farkas, I., Mészaros, C. and Seres, I. (1998). New algorithm for modelling the decoupled heat and mass transfer in a solar crop dryer, *IFAC international workshop on control applications in post-harvest and processing technology*, Budapest, Hungary, pp. 169–172.

Farkas, I., Remenyi, P. and Biro, A. (1998a). Modelling of alfalfa drying using neural network, *Proceedings of the 11th international drying symposium*, Vol. A, pp. 168–175.

Farkas, I., Remenyi, P. and Biro, A. (1998b). Modelling of thin-layer drying using neural network, *IFAC international workshop on artificial intelligence in agriculture*, Makuhari, Japan, pp. 100–103.

Fellows, P. J. (2000). *Food processing technology - principles and practice*, 2nd edn, Woodhead Publishing and Limited and CRC Press LLC.

Fodor, G. A. (1998). *Ontologically Controlled Autonomous Systems: Principles, Operations and Architecture*, Kluwer Academic Publishers, Boston/Dordrecht/London.

Fowler, E. R. (2000). New techniques for commercial bread dough mixing, *IEEE Instrumentation & Measurement Magazine* **33**(1): 21–25.

Franklin, G. F., Powell, J. D. and Workman, M. L. (1998). *Digital Control of Dynamic System*, 3rd edn, Addison Wesley Longman, Inc.

Friborg, J. (1998). Mätning av dielektrisk konstant och konduktivitet för träaskor med olika förbränningsgrad. Malå GeoScience AB.

Fritze, H., Perkiömäki, J., Saarela, U., Katainen, R., Tikka, P., Yrjälä, K., Karp, M., Haimi, J. and Romantschuck, M. (2000). Effect of Cd-containing wood ash on the micro flora of coniferous forest humus, *FEMS Microbiology Ecology* **32**: 43–51.

Gauss, C. F. (1963). *Theory of Motion of the Heavenly Bodies*, New York, Dover. Reprints from 1809.

Gustafsson, F. (2000). *Adaptive filtering and change detection*, John Wiley & Sons, Ltd.

Gustafsson, F. (2001). *Adaptive Filtering and Change Detection Toolbox*, Department of Electrical Engineering, Linköping University, Linköping, Sweden. User's Manual.

Gyllin, M. and Kruuse, A. (1996). Effekter på floran efter tillförsel av ved och blandaska, *Report*, The Research Programme for Recycling of Wood Ash, NUTEK, Vattenfall and Sydkraft. In Swedish, summary in English.

Hägglund, T. (1983). The problem of forgetting old data in recursive estimation, *Prepr. IFAC Workshop Adaptive System Control, Signal Processing*, number SAC-6, San Francisco, USA.

Hall, C. W. (1980). *Drying and storage of agricultural products*, Avi, Westport.

Hall, P. (1988). Theoretical comparison of bootstrap confidence intervals, *The Annals of Statistics* **16**: 927–953.

Hallström, A. (1985). *Drying of porous granular materials*, Ph.D. thesis, Department of Chemical Engineering, Lund University, Lund, Sweden.

Harayama, M. and Uesugi, M. (1992). On-line measurement of average pellet size with spatial frequency analysis, *Proceedings of the 1992 International Conference on Industrial Electronics, Control, Instrumentation, and Automation*, Vol. 3, pp. 1613–1618. San Diego, CA, USA.

Harbert, F. C. (1973). Control of dryers by the temperature difference technique, *Instruments and Control Systems* **46**(9): 71–72.

Harbert, F. C. (1974). Automatic control of drying processes moisture measurement and control by the temperature difference method, *Chemical Engineering Science* **29**(3): 888–890.

Harnby, N. (2000). An engineering view of pharmaceutical powder mixing, *Pharmaceutical Science & Technology Today* **3**(9): 303–309.

Henriksson, H. (1997). Fältförsök med kapacitiv fuktgivare i rökgas, *Anläggningsteknik 615*, Värmeforsk. In Swedish.

Holmberg, S. (2000). *Chemical and Mineralogical Characterization of Granulated Wood Ash*, Licentiate thesis, Department of Geology, Gothenburg University, Gothenburg, Sweden.

Holmberg, S. (2002). Limestone and dolomite powder as binders during wood ash agglomeration. Manuscript, Department of Biology and Environmental Science, University College of Kalmar.

Holmberg, S., Claesson, T., Abul-Milh, M. and Steenari, B.-M. (2001). Drying of granulated wood ash by flue gas from saw dust and natural gas combustion. Manuscript, Department of Biology and Environmental Science, University College of Kalmar.

Holzner, H. (1998). *Ashes and particulate emissions of biomass combustion. Formation characterization, evaluation, treatment*, 1st edn, Dbv-Verlag für die Technische Universität Graz, Austria, chapter Ecological and economic evaluation of biomass ash utilization – the Austrian approach.

Hoornaert, F., Wauters, P. A., Meesters, G. M., Pratsinis, S. E. and Scarlett, B. (1998). Agglomeration behaviour of powders in a Lödige mixer granulator, *Powder Technology* **96**(2): 116–128.

Horowitz, I. M. (1963). *Synthesis of Feedback Systems*, Academic Press, New York.

IEC1131-3 (1993). Programmable controllers - part 3: Programming languages. International Electrotechnical Commission, Technical Report.

IEC848 (1988). Preparation of function charts for control systems. International Electrotechnical Commission, Technical Report.

Johansson, R. (1993). *System Modeling & Identification*, Prentice Hall Inc.

Kapur, P. C., Arora, S. C. D. and Subbarao, S. V. B. (1973). Water-bentonite interaction in balling of iron ores, *Powder Technology* **28**(8): 1535–1540.

Karlsson, L. G. (1997). Beräkning av kemisk stabilitet hos biobränsleaskor, *Report*, The Research Programme for Recycling of Wood Ash, NUTEK, Vattenfall and Sydkraft. In Swedish, summary in English.

Kendall, M. G. and Stuart, A. (1967). *The Advanced Theory of Statistics*, Charles Griffin & Company Ltd.

Keningley, S. T., Knight, P. C. and Marson, A. D. (1997). An investigation into the effects of binder viscosity on agglomerate behaviour, *Powder Technology* **91**(2): 95–103.

Khalil, H. K. (1992). *Nonlinear Systems*, 2 edn, Macmillan Publishing Company, New York.

Kiranoudis, C. T. (1998). Design and operational performance of conveyor-belt drying structures, *Chemical Engineering Journal* **69**: 27–38.

Kiranoudis, C. T. and Markatos, N. C. (2000). Pareto design of conveyor-belt dryers, *Journal of Food Engineering* **46**: 145–155.

Knight, P. C. (2001). Structuring agglomerated products for improved performance, *Powder Technology* **119**(1): 14–25.

Köppel, V., Segal, M., Remer, M., Lopano, M. and Tonneguzzo, N. (1995). Inferential determination of moisture in solids in drying processes, *Proceedings of the IFAC conference on low cost automation*, pp. 81–86. Buenos Aires, Argentina.

Kraszewski, A. (1980). *Journal of Microwave Power* **15**(4): 209–220.

Kristiansson, B. (2000). *Evaluating and Tuning of PID Controllers*, Licentiate thesis, Chalmers University of Technology, Sweden.

Larrimore, C. L. and Sorge, J. (1997). Evaluation of on-line carbon-in-ash measurement technologies, *Third Annual Conference on Unburned Carbon on Utility Fly Ash*, FETC Publications.

Lennartson, B. (2001). *Reglerteknikens Grunder*, Studentlitteratur, Lund, Sweden.

Leuenberger, H. (2001a). New trends in the production of pharmaceutical granules: batch versus continuous processing, *Journal of Pharmaceutics and Biopharmaceutics* **52**(3): 289–296.

Leuenberger, H. (2001b). New trends in the production of pharmaceutical granules: the classical batch concept and the problem of scale-up, *Journal of Pharmaceutics and Biopharmaceutics* **52**(3): 279–288.

Lewis, M. J. (1990). *Physical Properties of Foods and Food Processing Systems*, Woodhead Publishing, Cambridge, UK.

Lindahl, M. and Claesson, T. (1996). Recycling of ashes. granules made of wood ash, etec-dolomite and water, *Report*, University College of Kalmar, Kalmar Energi & Miljö, Kalmar, Sweden. In Swedish.

Litster, J. D. and Waters, A. G. (1990). Kinetics of iron ore sinter feed granulation, *Powder Technology* **62**: 125–134.

Ljung, L. (1987). *System Identification: Theory for the User*, Prentice-Hall, Englewood Cliffs, N.J. USA.

Ljung, L. (1999). Model validation and model error modeling, *Technical Report LiTH-ISY-R-2125*, Department of Electrical Engineering, Linköping University, S-581 83 Linköping, Sweden.

Ljung, L. and Söderström, T. (1983). *Theory and Practice of Recursive Identification*, The MIT Press Cambridge, Massachusetts, London, England.

Ljung, S. and Ljung, L. (1985). Error propagating properties of recursive least-squares adaptive algorithms, *Automatica* **21**(2): 157–167.

Lövgren, L., Lundmark, J.-E. and Jansson, C. (2000). Kretsloppsanpassning av bioaskor. Utvärdering av ny teknik för pelletering av bioaska med avseende på dels driftegenskaper, dels miljöeffekter i skogen av askåterföring, *Rapport Etapp 1 Projekt P11647-1*, Statens Energimyndighet, Sweden. In Swedish.

Lucas, J. M. and Saccucci, M. S. (1990). Exponentially weighted moving average control schemes: Properties and enhancements, *Technometrics* **32**(1): 1–29.

Lundborg, A. (1997). Ash recycling, *BIOENERGI* **6**. In Swedish.

Manoukian, E. B. (1986). *Modern Concepts and Theorems of Mathematical Statistics*, Springer Verlag.

MathWorks (1998). *SIMULINK: Writing S-Functions*, The MathWorks, Inc. Version 3.

McGhee, J., Henderson, I., Kulesza, W. and Korczynski, J. (1998). *Measurement Science for Engineering*, Lodart.

Mészaros, C., Farkas, I. and Balint, A. (1999). Stochastic modelling of drying processes using percolation theory, *Second European Congress of Chemical Engineering*.

Mikulic, D. and Krstic, V. (1995). Knowledge supported mix design of concrete, *Proceedings of the 17th International Conference on Information Technology Interfaces*, Zagreb, Croatia.

Morris, K. R., Nail, S. L., Peck, G. E., Byrn, S. R., Griesser, U. J., Stowell, J. G., Hwang, S.-J. and Park, K. (1998). Advances in pharmaceutical materials and processing, *Pharmaceutical Science & Technology Today* **1**(6): 235–245.

Nilsson, A. (1993). Techniques for wood ash processing, *Report 1993:42*, NUTEK, Stockholm, Sweden. In Swedish.

Nilsson, T. and Eriksson, H. M. (1997). Vedaska och kalk – effekter på kvävemineralisering och nitrifikation i en skogsjord, *Report*, The Research Programme for Recycling of Wood Ash, NUTEK, Vattenfall and Sydkraft. In Swedish, summary in English.

Nilsson, T. and Eriksson, H. M. (1998). Vedaska och kalk – effekter på upptag av näringsämnen och tungmetaller i blåbär, *Report*, The Research Programme for Recycling of Wood Ash, NUTEK, Vattenfall and Sydkraft. In Swedish, summary in English.

Nordenberg, F. (1996). *Granulation with stirrer technique*, B.Sc. thesis, Inst. för Energiteknik, Mälardalens Högskola, Sweden. In Swedish.

Nybrant, T. (1986). *Modelling and control of agricultural driers*, Ph.D. thesis, Department of Systems and Control, Uppsala University, Sweden.

Olsson, G. and Piani, G. (1992). *Computer Systems for Automation and Control*, Prentice Hall Inc.

OptiSizer (2002). OptiSizer PSDA Analysis Technique, (Webpage, October 23, 2002). `http://www.micromeritics.com/`.

Osborne, B. G., Fearn, F. and Hindle, P. H. (1993). *Practical NIR Spectroscopy with applications in food and beverage analysis*, 2nd edn, Longman Group UK Limited.

Panagopoulos, H. (2000). *PID Control: Design, Extension, Application*, Ph.D. thesis, Department of Automatic Control, Lund University, Sweden.

Patton, R. J., Frank, P. M. and Clark, R. N. (2000). *Issues of Fault Diagnosis for Dynamic Systems*, Springer-Verlag.

Peetz-Schou, J. (1998). Economics of on-line ash, coal and unburned carbon monitors in coal-fired power plants, *Conference on Unburned Carbon on Utility Fly Ash*, FETC Publications.

Platt, D., Rumsay, T. R. and Palazoglu, A. (1992). Dynamics and control of cross-flow grain dryers, a feedforward-feedback control strategy, *Drying Technology* **10**(2): 333–363.

Pottmann, M., Ogunnaike, B. A., Adetayo, A. A. and Ennis, B. J. (2000). Model-based control of a granulation system, *Powder Technology* **108**(2-3): 192–201.

Quiang, L. and Bakker-Arkema, F. W. (2001). A model-predictive controller for grain drying, *Journal of Food Engineering* **49**: 321–326.

Quirijns, E. J., van Willigenburg, L. G., van Boxtel, A. J. B. and van Straten, G. (2000). The significance of modelling spatial distributions of quality in optimal control of drying processes, *Benelux Quarterly Journal on Automatic Control*, Vol. 41, pp. 56–64. Special issue Modelling and Control in Bioprocesses. Invited paper.

Ramaker, J. S. (2001). *Fundamentals of the high-shear pelletization process*, Ph.D. thesis, University of Groningen, The Netherlands.

Rantanen, J., Lehtola, S., Rämet, P., Mannermaa, J.-P. and Yliruusi, J. (1998). On-line monitoring of moisture content in an instrumented fluidized bed granulator with a multi-channel NIR moisture sensor, *Powder Technology* **99**(2): 163–170.

Rantanen, J., Räsänen, E., Antikainen, O., Mannermaa, J.-P. and Yliruusi, J. (2001). In-line moisture measurement during granulation with a four-wavelength near-infrared sensor: an evaluation of process-related variables and a development of non-linear calibration model, *Chemometrics and Intelligent Laboratory Systems* **56**(1): 51–58.

Rantanen, J., Räsänen, E., Tenhunen, J., Känsäkoski, M., Mannermaa, J.-P. and Yliruusi, J. (2000). In-line moisture measurement during granulation with a four-wavelength near infrared sensor: an evaluation of particle size and binder effects, *European Journal of Pharmaceutics and Biopharmaceutics* **50**(2): 271–276.

Ripke, S. J. and Kawatra, S. K. (2000). Can fly-ash extend bentonite binder for iron ore agglomeration?, *International Journal of Mineral Processing* **60**(3-4): 181–198.

Roberts, S. W. (1959). Control charts based on geometric moving averages, *Technometrics* **8**: 411–430.

Rodriguez, G., Vasseur, J. and Courtois, F. (1996a). Design and control of drum dryers for the food industry. Part 1, set-up of a moisture sensor and inductive heater., *Journal of Food Engineering* **28**: 271–282.

Rodriguez, G., Vasseur, J. and Courtois, F. (1996b). Design and control of drum dryers for the food industry. Part 2, automatic control., *Journal of Food Engineering* **30**: 171–183.

Rosen, K., Eriksson, H., Clarholm, M., Lundkvist, H. and Rudebeck, A. (1993). Granulerad vedaska till skog på fastmark – ekologiska effekter, *Report*, The Research Programme for Recycling of Wood Ash, NUTEK, Vattenfall and Sydkraft. In Swedish.

Rudling, L. (2000). NOx-reduktion med stegvis lufttillförsel och tillsats av ammoniak vid stökiometri nära 1.0, vid förbränning av träpulver, *Miljö och förbränningsteknik 676*, Värmeforsk. In Swedish.

Rühling, Å. (1996). Upptag av tungmetaller i svamp och bär samt förändring i florans sammansättning efter tillförsel av aska till skogsmark, *Report*, The

Research Programme for Recycling of Wood Ash, NUTEK, Vattenfall and Sydkraft. In Swedish, summary in English.

Samuelsson, H. (2002). Recommendations for the extraction of forest fuel and compensation fertilising. Swedish National Board of Forestry, Issue 3.

Sander, B. (1997). Properties of Danish biofuels and the requirements for power production, *Biomass and Bioenergy* **12**(3): 177–183.

Savaresi, S. M., Bitmead, R. R. and Peirce, R. (2001). On modelling and control of a rotary sugar dryer, *Control Engineering Practice* **9**(3): 249–266.

Sfiris, G., Johansson, A., Valmari, E., Kauppinen, J., Pyykkönen, J. and Lyyränen, J. (1999). Askans partikelfraktionsfördelning och metallernas beteende vid eldning av Salix i en CFB panna, *Report*, The Research Programme for Recycling of Wood Ash, NUTEK, Vattenfall and Sydkraft. In Swedish, summary in English.

Shahhosseini, S., Cameron, I. T. and Wang, F. Y. (2001). A dynamic model with on-line identification for rotary sugar drying, *Drying Technology* **19**(9): 2103–2129.

Shannon, C. E. (1949). Communication in presence of noise, *Proceedings of IRE*, Vol. 37, pp. 10–21.

Shinskey, F. G. (1968). How to control product dryness without measuring it, *Proceedings of the 1968 Joint Automatic Control Conference*, American Automatic Control Council.

Shinskey, F. G. (1969). How to control product dryness - a new system, *Mineral processing* pp. 10–14.

Siegmund, D. (1985a). Corrected diffusion approximations in certain random walk, *Proceedings of the Berkeley conference in Honor of Jerzy Neyman and Jack Kifer*, Vol. 2, pp. 559–617. L. Le Cam and R.A. Olshen, eds.

Siegmund, D. (1985b). *Sequential Analysis - Tests and Confidence Intervals*, Series in Statistics, Springer, New York.

Siettos, C. I., Kiranoudis, C. T. and Bafas, G. V. (1999). Advanced control strategies for fluidized bed dryers, *Drying Technology* **17**(10): 2271–2292.

Skogestad, S. and Postlethwaite, I. (1996). *Multivariable Feedback Control - Analyis and Design*, John Wiley & Sons.

Snowdon, B. (1998). Sekam on-line carbon-in-ash monitor, application examples and operating experience, *Conference on Unburned Carbon on Utility Fly Ash*, FETC Publications.

Söderström, T. and Stoica, P. (1989). *System Identification*, Prentice Hall Inc.

Steenari, B.-M. (1996). Biobränsleaskors innehåll och härdningsegenskaper, *Report*, The Research Programme for Recycling of Wood Ash, NUTEK, Vattenfall and Sydkraft. In Swedish, summary in English.

Steenari, B.-M. and Lindqvist, O. (1997). Stabilisation of biofuel ashes for recycling to forest soil, *Biomass and Bioenergy* **13**(1-2): 39–50.

Sundqvist, T. (1999). *A High Temperature Granulation Process for Ecological Ash Recirculation*, Licentiate thesis, Luleå University of Technology, Sweden.

Svantesson, T. (1997). Real-time implementation of adaptive algorithms in dspace/simulink, *Technical Report LiTH-ISY-EX-1958*, Department of Electrical Engineering, Linköping University, Linköping, Sweden.

Svantesson, T. (2000). *Automated Manufacture of Fertilizing Granules from Burnt Wood Ash*, Licentiate thesis, Department of Industrial Electrical Engineering and Automation, Lund University, Lund, Sweden.

Svantesson, T. and Hultgren, A. (2002). Teaching automatic control using the parallel-cart process, *Preprints of the Swedish National Conference on Automatic Control, Reglermöte 2002*, Linköping, Sweden, pp. 19–24.

Svantesson, T., Hultgren, A. and Johansson, B. (1998). Diskreta PID algoritmer, *Report*, Dept. of Technology, University College of Kalmar, Sweden. In Swedish.

Svantesson, T., Lauber, A. and Olsson, G. (1998). Automated manufacture of granules from burnt wood ash, *Proceedings of Fifth National Science-Technical Conference. Macro-Levelling and Reclamation of Areas with use of By Products Combustion*, Swinoujscie, Poland.

Svantesson, T., Lauber, A. and Olsson, G. (2000). Viscosity model uncertainties in an ash stabilization batch mixing process, *Proceedings of 17th IEEE Instrumentation and Measurement Technology Conference, IMTC 2000*, Vol. 2, Baltimore Maryland, USA, pp. 909–914.

Svantesson, T. and Olsson, G. (2000). Optimal adaptive control of an ash stabilization batch mixing process using change detection, *Proceedings of IEEE International Conference on Control Applications, CCA 2000*, Vol. 1, Anchorage, Alaska, USA, pp. 109–114.

Svantesson, T. and Olsson, G. (2002). Wood ash agglomeration – have we reached an automatic solution yet?, *Technical Report TEIE-7187*, Department of Industrial Electrical Engineering and Automation, Lund University, Sweden.

Svantesson, T., Petersson, T. and Jedfelt, D. (2001). Utvärdering av försök med valspelleteringsmetod, *Report*, Dept. of Technology, University College of Kalmar, Sweden. In Swedish.

Svantesson, T., Quirijns, E. J. and Olsson, G. (2002). Wood ash agglomerate moisture control – hardware, sensors and control algorithms, *Technical Report TEIE-7188*, Department of Industrial Electrical Engineering and Automation, Lund University, Sweden.

Swedish Standard: SS 02 81 13 (1981). Determination of dry matter and ignition residue in water, sludge and sediment.

Tanihara, N., Sonode, K., Hamazaki, M. and Takata, S. (1996). Preparing granular foods without water addition, *Trends in Food Science & Technology* **7**(8): 273.

Taylor, J. D. (1995). *Introduction to UWB Radar Systems*, CRC Press.

Temple, S. J., Tambala, S. T. and van Boxtel, A. J. B. (2000). Monitoring and control of fluid-bed drying of tea, *Control Engineering Practice* **8**(2): 165–173.

Temple, S. J. and van Boxtel, A. J. B. (1999). Modelling of fluidized-bed drying of black tea, *Journal of Agriculture Engineering Research* **74**: 203–212.

Temple, S. J. and van Boxtel, A. J. B. (2000a). Control of fluid bed tea dryers: control in the context of design and operation conditions, *Computers and Electronics in Agriculture* **29**(3): 209–216.

Temple, S. J. and van Boxtel, A. J. B. (2000b). Control of fluid bed tea dryers: controller design and tuning, *Computers and Electronics in Agriculture* **26**(2): 159–170.

Temple, S. J., van Boxtel, A. J. B. and van Straten, G. (2000). Control of fluid bed tea dryers: controller performance under varying operating conditions, *Computers and Electronics in Agriculture* **29**(3): 217–231.

Thies, R. and Kleinebudde, P. (1999). Melt pelletisation of a hygroscopic drug in a high shear mixer; Part 1. Influence of process variables, *International Journal of Pharmaceutics* **188**(2): 131–143.

Thornton, C. L. and Bierman, G. J. (1980). $\mathbf{UDU}^T$ *covariance factorization for Kalman filtering*, Control and Dynamic Systems 16, Academic Press, New York.

Toyoda, K. (1989). Study on intermittent drying of rough rice in a recirculation dryer, *Drying '89*, pp. 289–296.

Toyoda, K. (1992). Study on drying characteristics of rough rice by two-tank model, *Drying '92*, pp. 1426–1435.

Toyoda, K., Farkas, I. and Kojima, H. (1995). Estimation of moisture content of grain during drying in a recirculation dryer, *International symposium on automation and robotics in bioproduction and processing*, Vol. 2, pp. 229–236.

Toyoda, K., Kojima, H., Miyomoto, S. and Takeuchi, R. (1997). Measurement and analysis of moisture changes in agricultural products using FFT noise impedance spectroscopy, *Drying Technology* **15**: 2025–2035.

Trelea, I. C., Trystram, G. and Courtois, F. (1997). Optimal constrained non-linear control of batch processes: application to corn drying, *Journal of Food Engineering* **31**: 403–421.

Trerice, D. N., DiGioia, A. M. and Reid, J. B. (1998). Experience with microwave-based systems for measurement of LOI, *Conference on Unburned Carbon on Utility Fly Ash*, FETC Publications.

Ulriksen, P. (1982). *Application of impulse radar to civil engineering*, Ph.D. thesis, Department of Engineering Geology, Lund University, Sweden.

van Boxtel, A. J. B. and Knol, L. (1996). A preliminary study on strategies for optimal fluid-bed drying, *Drying Technology* **14**: 481–500.

Voundi, J. C., Demeyer, A. and Verloo, M. G. (1998). Chemical effects of wood ash on plant growth in tropical acid soils, *Bioresource Technology* **63**: 251–260.

Wald, A. (1947). *Sequential Analysis*, Wiley, New York.

Walker, G. M., Holland, C. R., Ahmad, M. N., Fox, J. N. and Kells, A. G. (2000). Drum granulation of NPK fertilizers, *Powder Technology* **107**(3): 282–288.

Watano, S. (2001). Direct control of wet granulation processes by image processing system, *Powder Technology* **117**(1-2): 163–172.

Watano, S. and Miyanami, K. (1999). Control of granulation process by fuzzy logic, *Proceedings of the 18th International Conference of the North American Fuzzy Information Processing Society*, pp. 905–908. New York, NY, USA.

Wauters, P. A. L. (2001). *Modelling and Mechanisms of Granulation*, Ph.D. thesis, Delft University of Technology, The Netherlands.

Wide, P. (1999). The human decision making in the dough mixing process estimated in an artificial sensor system, *The International Journal of Food Engineering* **39**(1): 39–46.

Wieringa, J. E. (1999). *Statistical process control for serially correlated data*, Ph.D. thesis, Department of Econometrics, University of Groningen, The Netherlands.

Williams, T. M. (1988). Obtaining water quality permits for land application of biomass boiler ash, *Biomass and Bioenergy* **13**(4-5): 279–287.

Willsky, A. S. (1976). A survey of design methods for failure detection in dynamic systems, *Automatica* **12**: 601–611.

Windelhed, K. (1998a). Askåterföring – typlösning omfattande befuktningsanläggning och valspelletering, *Anläggningsteknik 645*, Värmeforsk. In Swedish.

Windelhed, K. (1998b). Mekanisk bearbetning av bioaskor, *Technical Report ER 12:1998*, The Swedish National Energy Administration, Stockholm, Sweden. In Swedish.

Windelhed, K. (2000). Valspelletering. Utvärdering och uppföljning av pilotprojekt omfattande ny teknik för framställning av pellets för återföring av bioaska till skogsmark, *Anläggningsteknik 695*, Värmeforsk. In Swedish.

Wunderli, S., Zennegg, M., Dolezal, I. S., Gujer, E., Moser, U., Wolfensberger, M., Hasler, P., Noger, D., Studer, C. and Karlaganis, G. (2000). Determination of polychlorinated dibenzo–p–dioxins and dibenzo–furans in solid residues from wood combustion by HRGC/HRMS, *Chemosphere* **40**: 641–649.

Yamamoto, S. and Hashimoto, I. (1991). Present status and future needs: The view from Japanese industry, *Proceedings of the Fourth International Conference on Chemical Process Control*. Texas, USA.

Yokoi, N., Aizu, Y. and Mishina, H. (1999). Novel phase doppler method for particle size measurements using a single directional polarized detection, *Proceedings of the 16th IEEE Instrumentation and Measurement Technology Conference, 1999. IMTC/99*, Vol. 3, pp. 1352–1357. Venice, Italy.

Zhang, J., Litster, J. D., Wang, F. Y. and Cameron, I. T. (2000). Evaluation of control strategies for fertiliser granulation circuits using dynamic simulation, *Powder Technology* **108**(2-3): 122–129.

Zhang, Q. and Litchfield, J. B. (1993). Fuzzy logic control for a continuous cross-flow grain dryer, *Journal of Food Process Engineering* **16**: 59–77.

Zoubir, A. M. (1993). Bootstrap: Theory and applications, *Proceedings of the SPIE 1993 Conference on Advanced Signal Processing Algorithms, Architectures and Implementations*, San Diego, pp. 216–235.

Zoubir, A. M. and Boashash, B. (1988). The bootstrap and its application in signal processing, *IEEE Signal Processing Magazine* **15**(1): 55–76.

Zoubir, A. M. and Iskander, D. R. (1998). *Bootstrap MATLAB Toolbox*, Queensland University, Brisbane, Australia. Version 2.0 (May 1998).